بسم الله الرحمن الرحيم

Sudan University of Science and Technology

Collage of Graduate Studies

Usage of Optical Chaos for Diode Laser Networks

(a Computer Simulation)

إستخدام الشواش الضوئي لشبكات الليزرات الثنائية(محاكاة بالحاسوب)

A Thesis Submitted in Fulfillment of the Requirements for the
Degree of Doctor of Philosophy in Laser Application in Electronics Engineering

By:

Babekir Abdelrahman Osman Elsayed

Supervisor:

Kais Al Naimee

Co-Supervisor:

Abdelmoneim Mohammed Awadelgied

February 2016

الاية

قال تعالى:

بسم الله الرحمن الرحيم

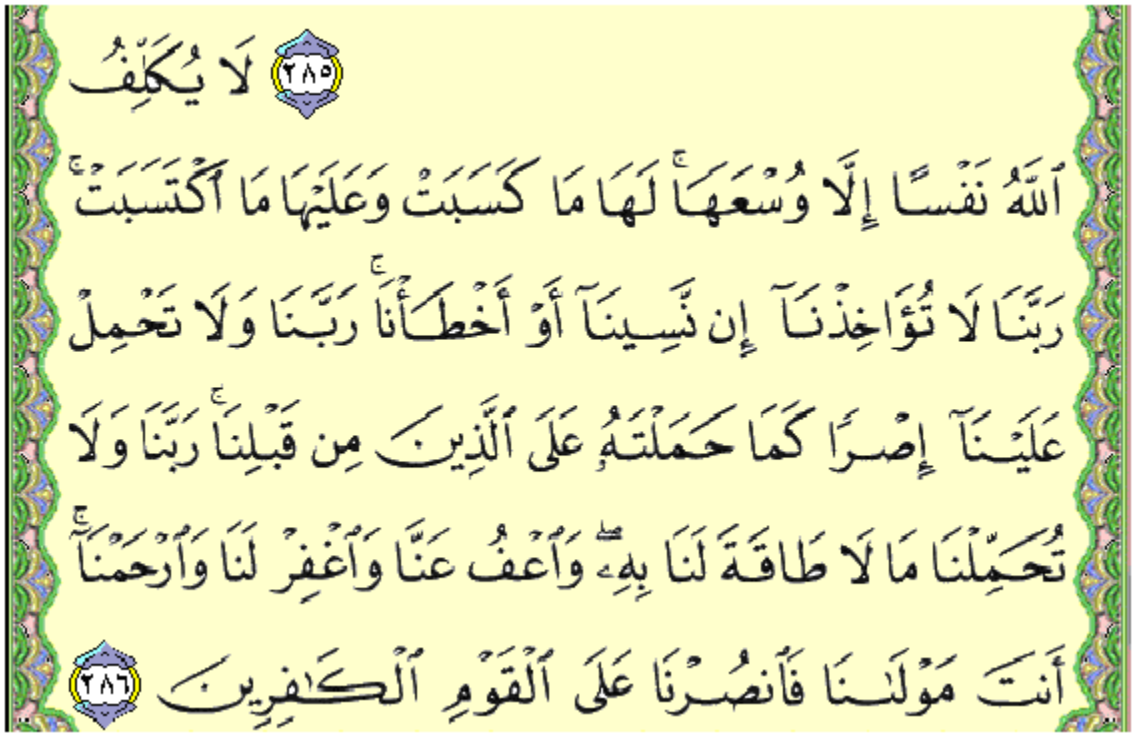

صدق الله العظيم

الآية (286) من سورة البقرة

Dedication

My Father……

My Mother……

My family ……..

Acknowledgement

I would like to express my sincere appreciation to my research

Supervisor:

Professor*:* Kais Al Naimee

For giving me the major steps to go on to explore the subject, for welcoming me in his research group, for his continuous help and guidance, for so many fruitful discussions and sharing his ideas.

Also I would like to great thank my co-supervisor:

D. Abdelmoneim Mohammed Awadelgied

For his available advice, encouragement and his supervision support and confidence in me.

It would have been impossible to carry out this work without the assistance and support of administrative and technical staff of the Institute of Laser at SUST, special thanks to D.Sora F.Abdalah , Instituted Nazionale di Ottica, Largo E.Fermi 6, and 50125 Firenze, Italy for good support and all assistances in this works.

Finally 1 would like to thank all the individuals who have assisted in one way or other in the accomplishment of this work

Abstract

Chaotic Optical Communication (COC) system is a novel communication scheme that utilizes an optical chaotic waveform as carrier of information, in secure communication applications.

In this work, we have studied an implemented AC-couple Optoelectronic Feedback Semiconductor Laser (OEFSL). This work has been expanded to configure 2^8 laser oscillators network.

The physical model of such chaotic system has been demonstrated by means of physical parameters, the time scales of each parameter are different. To solve this problem, a dimensionless transformation has been made.

We have started from the creation of the chaotic simulation system, study the properties and determine the control parameters that lead to regular behavior. Chaotic behavior has been generated by selecting the experimental initial conditions for the OEFSL under appropriate conditions. We have a lot consider effectively analyze the behavior of a dynamical system under the influence control parameters. This step has been done by modeling and programming the system above using MATLAB packages.

In order to achieve the synchronization condition between master and slave oscillators, a unidirectional coupling configuration is implemented, in this configuration, the coupling between master and slave enables the master oscillator to fully driving and controlling the slave.

The master-slave configuration is expanded to implement Optoelectronic Feedback Semiconductor Laser Network (OEFSLN) by means of Simulink environment in

MATLAB package to implement 256 chaotic oscillators. The synchronization condition among the all network oscillators has been achieved by means of coupling factor. We consider this approach is very fruitful step to build OEFSLN.

المستخلص

أنظمة اتصالات الشواش الضوئي (COC) هي أنظمة الاتصالات التي تستخدم موجة الشواش الضوئي كناقل للمعلومات. في تطبيقات الاتصالات الآمنة.

في هذا العمل، تم تمثيل نموذج حقن التيار لشبه الموصل الليزري ذو التغذيه العكسيه الكهروضوئيه (OEFSL). وقد تم توسيع هذا العمل لتكوين شبكة من 2^8 مذبذبات ليزريه .

تم شرح النموذج الفيزيائي من هذا النظام الشواشي عن طريق المتغيرات الفيزيائيه، وبتدريج زمني مختلف لكل متغير مختلف. لحل هذه المشكلة، تم استخدام التحويل الرياضي لمعادلات النظام غير المعتمده علي الوحدات.

بدأنا من إنشاء نظام محاكاة الشواش ، ودراسة خصائص وتحديد معالم السيطرة التي تؤدي إلى السلوك العادي. تم إنشاء السلوك الفوضوي عن طريق تحديد الشروط الأولية التجريبية للـ OEFSL في ظل ظروف مناسبة اولينا الكثير من الاهتمام بشكل فعال بتحليل سلوك ديناميكيه النظام تحت متغيرات السيطرة. وقد تم ذلك بنمذجة وبرمجة النظام أعلاه باستخدام حزم برنامج الـ MATLAB.

من أجل تحقيق شرط التزامن بين المتحكم والتابع ، تم تنفيذ تكوين اقتران أحادي الاتجاه، في هذا التكوين، تم الربط والاقتران بين المتحكم والتابع تمكن المذبذب الرئيسي لقيادة التابع والسيطرة عليه بالكامل .

تم توسيع تكوين المتحكم والتابع لتنفيذ شبكه ليزرات شبه الموصل ذو التغزيه العكسيه الكهروضوئيه (OEFSLN) عن طريق بيئة الـ SIMULINK في حزمة الـ MATLAB لتنفيذ 256 مذبذب شواس . وقد تحقق شرط التزامن بين جميع مذبذبات الشبكة عن طريق عامل اقتران.

ونحن نعتبر هذا النهج هو خطوة مثمرة للغاية لبناء شبكه من شبه الموصل الليزري ذو التغذيه العكسيه الكهروضوئيه OEFSLN

Table of Contents

Table of Contents

List of Tables

List of Figures

List of Abbreviations

(COC) Chaotic Optical Communication

(SL) Semiconductor lasers

(SLs) Semiconductor lasers

(OEFSL) Optoelectronic Feedback Semiconductor Laser Optoelectronic Feedback

(OEFSLN) Semiconductor Laser Network

(OEFB) Optoelectronics feedback Inter-Spike Interval (ISI)

(CS) Complete Synchronization

(GS) Generalized Synchronization

(UCC) Unidirectional Coupling Configuration

(FRM) Free Running Mode

(CRM) Coupling Running Mode

1 Chapter one: Introduction and Literature Review

1.1 Introduction

Nonlinear dynamics of semiconductor lasers (SL) have been widely investigated due to their useful applications in nonlinear optics, laser spectrometry, optical communications and optical chaos communications especially. As an important aspect of the nonlinear dynamics, multi stability in a SL with feedback or optical injection has been investigated experimentally and theoretically. In recent years, the SLs with the optoelectronics feedback (OEFB) have received considerable attention due to their application in optical chaos communication (Sivaprakasam and Shore, 1999). SL rate equations are used to model the dynamics of a SL with OEFB.

Chaos is an inherent feature of many nonlinear systems. In particular, the transition from order to disorder occurs with universality, irrespective of physical properties of the systems. Chaos occurs in optics, both in lasers and in nonlinear optical devices. Such systems, which are fundamentally simple both in construction and in the mathematics that describe them, provide excellent opportunities for investigating these nonlinear phenomena as well as for technological innovation (Tricker, 2002). An early pioneer of the theory was Edward Lorenz whose interest in chaos came about accidentally through his work on weather prediction in (Lorenz and N., 1993). The CO_2 laser was described by six rate equations model given by (Pisarchik et al., 2001)**.** The semiconductor laser subjected to the feedback injection is suitable way to produce a chaotic dynamic. These chaotic systems using semiconductor lasers can be described by three dynamic rate equations (Al Naimee et al., 2009).

In order to understand these complex dynamics, frequently observed in biological environments, and to provide controllable and reproducible experiments, considerable efforts have been devoted to the search of analogous phenomena in nonlinear optical systems, and HC has been found in CO_2 laser with feedback (Pisarchik et al., 2001).

1.2 Chaos Signal:

Chaos is a paradigmatic name used to describe deterministic dynamical systems whose behavior is complex, unpredictable and extremely sensitive to initial conditions. Chaos is theoretically and experimentally encountered in almost all types of lasers (solid-state, gas, semiconductor, etc...). Methods to lead lasers to chaos are numerous and based on two necessary conditions: nonlinearity and threefold dimensionality. Hence, when the nonlinearity of the laser (system) is not strong enough, an external nonlinear element can be introduced. Along the same line, when the dimensionality of the laser system is not high enough, it can be increased by parameter modulation or by feedback loops (Chembo Kouomou, 2006).

There are three basic dynamical properties that collectively characterize chaotic behavior. First, it exhibits an essentially continuous and possibly banded frequency spectrum that resembles random noise. Second, it is sensitive to initial conditions—that is, nearby orbits in the phase space (a geometrical perspective in which the dynamical states are plotted against each other so that time becomes implicit) diverge rapidly. Third, it contains an ergodicity and mixing of the dynamic orbits, which in essence implies the wholesale visit of the entire phase

space by the chaotic behavior and a loss of information because of the loss of predictability (Silva, 2011).

1.3 Chaotic Application:

Chaotic systems are used in various applications due to their ability to generate highly complicated signals by a simple recursive procedure (Silva, 2011). Chaotic sequences are attractive candidates for use in signal analysis, signal synthesis, practical engineering, and communications applications.

Chaotic systems are used as models for a wide range of signal processing applications as well as for practical engineering systems like analog-to digital converters and power converters. Chaotic systems have the potential to give rise to good joint source–channel codes due to their ability to separate orbits of nearby initial states while maintaining global boundless, thus conforming to energy and peak amplitude constraints (Tricker, 2002).

1.4 Chaos Generation:

Ideal components to generate optical chaotic signal are semiconductor lasers which can act as carrier transmitters and receivers in optical communication systems. Different control parameters play crucial roles in generating a chaotic behavior of the laser output. These parameters are laser power, injection current of the laser diode and the amplifier gain (Soucek, 1992).

1.5 Optical Communication with Chaotic:

Semiconductor lasers are the most important light sources for optical communications because of their compact size, efficiency, high speed, and

semiconductor laser has the ability to be electrically pumped and current modulated (Liu et al., 2001).

Single-mode semiconductor lasers, such as the distributed-feedback lasers and the vertical-cavity surface emitting lasers, are particularly important for high bit- rate optical communication systems. For these reasons, single-mode semiconductor lasers are used as transmitters and receivers for chaotic optical communications (Liu et al., 2001). Figure 1.1 shows the operating principle of a chaos-based optical communication system. In this system, a data message encoded on a deterministically chaotic carrier is recovered by using a receive incorporating a similar deterministically chaotic oscillator (Syvridis and Bogris, 2006).

The transmitter consists of a chaotic oscillator forced by external feedback to operate in the chaotic regime, producing a chaotic carrier that use to carry information by encoded on this chaotic carrier using different techniques. In a chaotic optical communication system, a nonlinear dynamical system is used to generate the chaotic signal for message transmission. Messages are embedded through chaos signal then Message recovery process is achieved by comparing the received signal with a reproduced chaotic signal which synchronizes with the transmitter chaotic signal (Syvridis and Bogris, 2006).

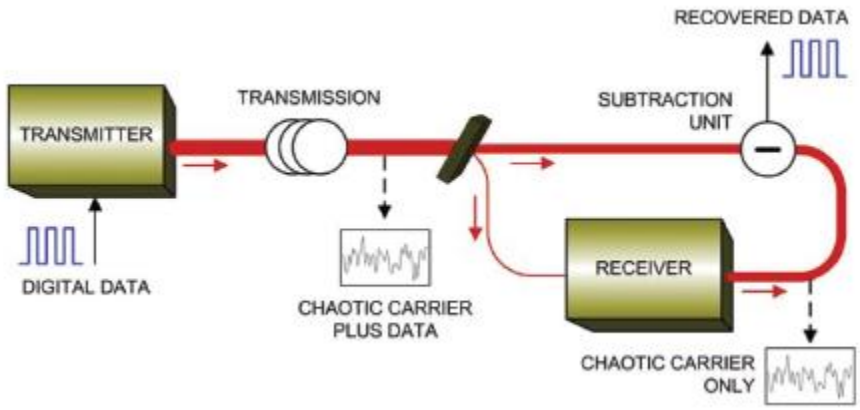

Figure 1-1 Chaos-based optical communication systems(Liu et al., 2001)

1.6 Chaos Synchronization:

Since the early 1990s researchers have realized that chaotic systems can be synchronized. The recognized potential for communications systems has driven this phenomenon to become a distinct subfield of nonlinear dynamics, with the need to understand the phenomenon in its most fundamental form viewed as being essential. All forms of identical synchronization, where two or more dynamical system execute the same behavior at the same time, are really manifestations of dynamical behavior restricted to a flat hyper plane in the phase space (Ding and Ott, 1994).

Synchronization of chaos is a phenomenon that may occur when two, or more, chaotic oscillators are coupled, or when a chaotic oscillator drives another chaotic oscillator. Because of the butterfly effect, which causes the exponential divergence of the trajectories of two identical chaotic system started with nearly the same initial conditions, having two chaotic system evolving in synchrony might appear quite surprising. However, synchronization of coupled or driven chaotic oscillators

is a phenomenon well established experimentally and reasonably understood theoretically (Fischer et al., 2000).

Chaos synchronization in discrete-time has been extensively studied, due to its potential applications for secure communication. Different types and various powerful methods and techniques of chaos synchronization have been reported to investigate chaos synchronization in discrete dynamical systems(Ouannas, 2014)

1.7 The aim of the Work:

The aim of this work is to implement and investigate the chaotic optoelectronics network based on AC-coupled optoelectronic feedback semiconductor lasers.

In addition: network synchronization among 256 chaotic oscillators would be investigated in this study.

1.8 Thesis Layout:

This thesis contains four chapters summarized as follows:

Chapter One:

Presents an introduction and literature review

Chapter Two:

Discuss and explain the Chaos concept and chaos generation techniques.

Nonlinear dynamics of semiconductor lasers (SLs), a SL with OEFB as chaos generator, chaos signal, chaos synchronization and chaos application in secure optical communication.

Chapter Three:

Discuss Implementation Techniques including:

- Describe the implementation and design of the proposed model.
- Providing a detailed explanation for designing each part of the system.
- Netware block oscillators design.

Chapter Four:

Results and Discussion which includes:

- The free running operation results.
- Generation of chaos signal results.
- Coupling system synchronization chaos.
- System responds and effects to the variable.
- Results due to the Feedback injection current **(δ_0)** and feedback strength **(ε)** variation**.**
- Conclusions.
- Future work.
- Recommendations.

1.9 Literature review:

(Fischer et al., 2000) presented experimental evidence for the synchronization of two semiconductor lasers exhibiting chaotic emission on sub nanosecond time scales. The transmitter system consists of a semiconductor laser with weak to moderate coherent optical feedback and therefore exhibits chaotic oscillations.

The receiver system is realized by a solitary semiconductor laser in which a fraction of the transmitter signal is coherently injected.

(Chen and Liu, 2000)generated a chaotic carrier waveform from different chaotic state in transient rather than from a fixed chaotic state in static.

The discrete distribution of homoclinic orbits has been investigated numerically and experimentally in a CO2 laser with feedback. The narrow chaotic ranges appear consequently when a laser parameter (bias voltage or feedback gain) changes exponentially. Up to six consecutive chaotic windows have been observed in the numerical simulation as well as in the experiments. Every subsequent increase in the number of loops in the upward spiral around the saddle focus is accompanied by the appearance of the corresponding chaotic window(Pisarchik et al., 2001)

(Sivaprakasam et al., 2001) used an optical coupling to affect synchronization between two diode lasers in a master-slave configuration. The effect of frequency detuning between the master and slave lasers on the character of the observed synchronization has been studied. Experimental conditions are found under which the synchronization plot (formed by plotting the output power of the slave laser against that of the master at each instant in time) makes a transition from a positive gradient to a negative gradient. (Wieczorek et al., 2001) has been studied sudden changes in the chaotic output of an optically injected semiconductor laser. Bifurcations that cause abrupt changes between different chaotic outputs, or even sudden jumps between chaotic and periodic output are identified. These sudden chaotic transitions involve attractors that exist for large regions in parameter space. They have used modern tools from bifurcation theory that is facilitated

experimental exploration of these transitions. The authors in (Al Naimee et al., 2009) have been demonstrated experimentally and theoretically the existence of slow chaotic spiking sequences in the dynamics of a SL with ac-coupled OEFB. The time scale of these dynamics is fully determined by the high-pass filter in the feedback loop and their erratic, though deterministic, nature is evidenced by means of inter-spike interval (ISI) probability distribution.

They showed that this regime is the result of an incomplete homoclinic scenario to a saddle focus, where an exact homoclinic connection does not occur (Tricker, 2002). (Al Naimee et al., 2010) have studied experimentally and theoretically the dynamics of a SL with ac-coupled nonlinear OEFB.

A period doubling sequence of small periodic and chaotic attractors was observed, each of them displaying excitable features. These results extend the fixed point based excitability concept also to the case of higher-dimensional attractors. The transitions between chaotic and periodic mixed mode oscillation, experimentally observed (Tricker, 2002). We report on experimental evidence of generation and control of low spiking events in a semiconductor laser. (Abdalah et al., 2010) have studied experimentally and theoretically an experiment has been carried on a semiconductor laser with an electro-optic feedback, set in a parameter range where chaos occurs. The feedback is modulated by 1 kHz and 10 kHz, frequencies, 50mV amplitudes. The dependence of the injected current on the feedback fraction is observed. (Abdalah et al., 2010) experiments and modeling chaotic spiking behavior has been recently reported in semiconductor lasers with optoelectronic feedback showing strict similarities with homoclinic chaos.

The same dynamics can be explored in LEDs with the same feedback configuration. (Abdalah et al., 2011) has been presented the experimental results for the synchronization of chaotic optical network, Experimental configurations for particular cases of asymmetric coupling in the case of three and six coupled oscillators. Also reported and characterize synchronization phenomena in such optoelectronic networks. This approach allows controlling the parameter mismatch between the coupled units, what usually occurs in the experimental setups.

2 Chapter – Two: Theoretical concepts

2.1 Chaotic Theory:

Chaos Theory studies the behavior of dynamical systems that are highly sensitive to initial conditions; an effect which is popularly referred to as the butterfly effect. Small differences in initial conditions yield widely diverging outcomes for chaotic systems, rendering long-term prediction impossible in general (Argyris et al., 2005). This happens even though these systems are deterministic, meaning that their future behavior is fully determined by their initial conditions, with no random elements involved. In other words, the deterministic nature of these systems does not make them predictable. This behavior is known as deterministic chaos, or simply chaos (DeCusatis, 2002). Chaotic behavior can be observed in many natural systems, such as the weather. Explanation of such behavior may be sought through analysis of a chaotic mathematical model, or through analytical techniques such as recurrence plots (Werndl, 2009).

2.1.1 Chaotic dynamics:

In common usage, "chaos" means "a state of disorder", but the adjective "chaotic" is defined more precisely in chaos theory (Danforth, 2013). Although there is no universally accepted mathematical definition of chaos, a commonly used definition says that, for a dynamical system to be classified as chaotic, it must have the following properties:

- **i.** It must be sensitive to initial conditions;
- **ii.** It must be topologically mixing; and
- **iii.** Its periodic orbits must be dense.

The requirement for sensitive dependence on initial conditions implies that there is a set of initial conditions of positive measure which do not converge to a cycle of any length (Danforth, 2013).

2.1.2 Sensitivity to initial conditions:

Sensitivity to initial conditions means that each point in such a system is arbitrarily closely approximated by other points with significantly different future trajectories. Thus, an arbitrarily small perturbation of the current trajectory may lead to significantly different future behavior (Medio and Lines, 2001). Sensitivity to initial conditions is popularly known as the "effect", as show in figure 2.1 so called due to Edward Lorenz in 1972 to the American Association for the Advancement of Science in Washington, D.C. entitled Predictability: Does the Flap of a Butterfly's Wings in Brazil set off a Tornado in Texas. The flapping wing represents a small change in the initial condition of the system, which causes a chain of events leading to large-scale phenomena. Had the butterfly not flapped its wings, the trajectory of the system might have been vastly different (Medio and Lines, 2001).

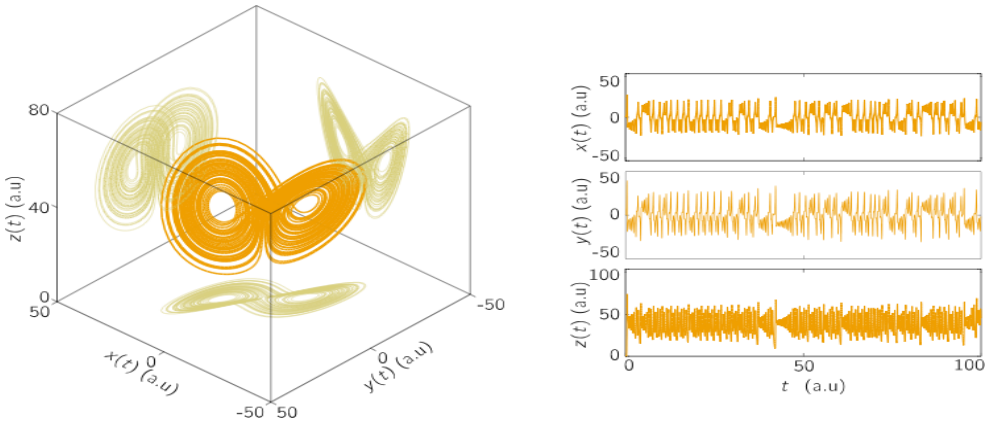

Figure 2-1 butterfly effect in Lorenz model(Lorenz and N., 1993)

2.1.3 Strange attractors:

The states variable representations in phase space describe the chaotic states so evolution of the state can be represented as one dimension (1D) time series (fig2.2), also the evolution of the state variable can be represented simultaneously in a (n) dimension (nD) phase space(fig2.3). When the system is chaotic, the trajectory is called a ‘‘strange attractor’’. The Lorenz attractor displays chaotic behavior. These two plots demonstrate sensitive dependence on initial conditions within the region of phase space occupied by the attractor.

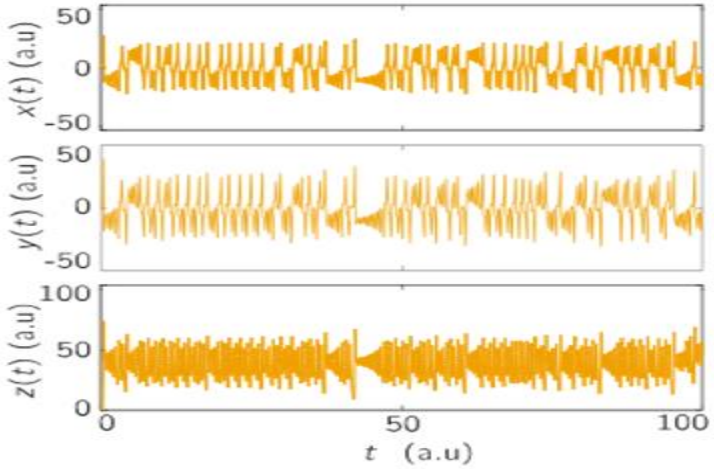

Figure 2-2 Figure 2.2 the time series Lorenz model(Lorenz and N., 1993)

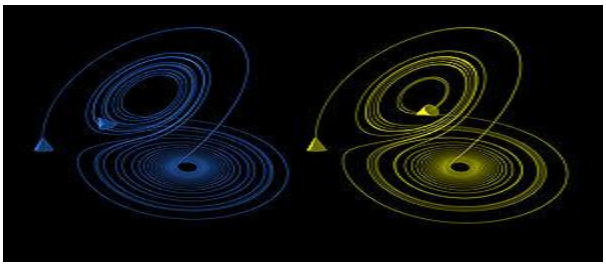

Figure 2-3 the strange attractor Lorenz model(Lorenz and N., 1993)

2.1.4 Research Directions for Engineering Applications with Chaotic Lasers:

The research directions with chaotic lasers for engineering applications are summarized in Figure 2.4. There are three main research directions treated in this book, related to the concepts of how to harness chaos. For chaos communication applications, the characteristics of chaos are used in a straightforward way, that is,

The determinism of chaos results in synchronization ability of chaos, and the middle degrees of complexity are suitable to hide a message signal. By contrast, for the applications of random number generation, the randomness of chaos needs to be maximized and determinism of chaos needs to be eliminated by converting analog chaos signals to binary signals. The important technique is how to extract and distill the randomness from deterministic chaos for this application. The research on random number generation requires a new engineering approach of chaos for maximizing the randomness of chaos (Argyris et al., 2005). By contrast, control and stabilization of chaos is a technique to completely avoid Complexity and instability of chaos. To design and establish ultra stable lasers, chaos control techniques may be useful for the suppression of chaotic instabilities. The features of deterministic chaos including unstable periodic orbits can be utilized for controlling chaos. The research on controlling chaos is the opposite direction of the research on random number generation, depending on minimizing or maximizing the complexity of chaos, respectively (Argyris et al., 2005).

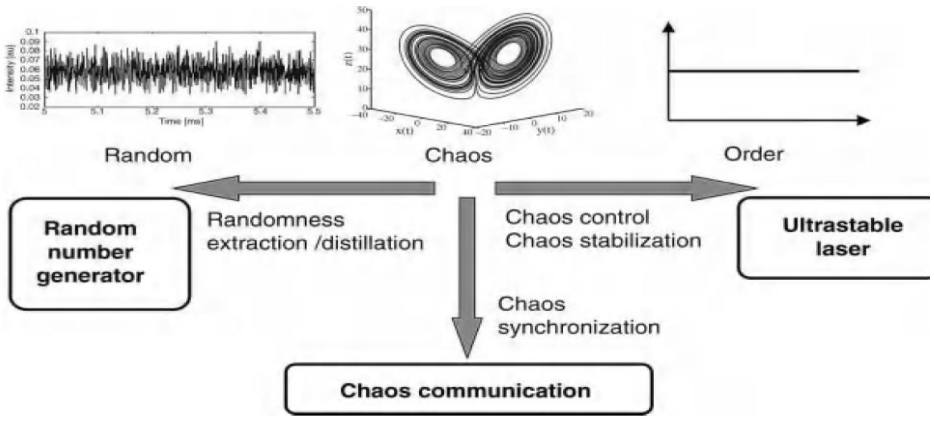

Figure 2-4 Three research directions for chaotic lasers engineering applications (Argyris et al., 2005).

2.2 Classification of Generation Techniques of Chaos in Lasers:

For commercially available lasers (e.g., class B lasers including SL and SSl). The dynamics of the electric field and the population inversion are treated, and the time scale for exchanging the energy between these two physical variables is characterized by the "relaxation oscillation frequency", which determined by a combination of three parameters (Baker and Gollub, 1996):

i. The photon life time.
ii. The population inversion life time.
iii. The pumping rate above threshold.

Class B lasers provide stable laser intensity in most situations, since there are only two variables of the electric field and the population inversion that are not satisfied with the condition for generating deterministic chaos. At least one more degree of freedom (i.e., one variable) is required for the generation of chaos (Strogatz, 1994) (Baker and Gollub, 1996).

The techniques for generating chaos with additional degrees of freedom can be classified into the following types:

- **i.** Optical feedback (with or without time delay);
- **ii.** Optical coupling and injection;
- **iii.** External modulation (for pump or loss);
- **iv.** Insertion of nonlinear devices.

2.2.1 Optical Feedback:

The dynamics of semiconductor lasers with time-delayed optical feedback is a typical example of feedback-induced chaos in lasers. An external mirror is placed in front of the laser cavity, and the laser light is reflected back from the external mirror and re injected into the laser cavity, as shown in (Figure 2.5a) the optical self-feedback signal may disturb the balance of the carrier–photon interaction in the laser medium and induce the instability of laser intensity. In this situation, the temporal dynamics is determined by the two dominant frequency components: the relaxation oscillation frequency and the external cavity frequency (Uchida, 2012).

The relaxation oscillation frequency is proportional to the square root of the normalized pump power divided by the carrier lifetime and the photon lifetime, as shown in Equation (2.1), so it is determined by the characteristics of the semiconductor medium. The typical value of the relaxation oscillation frequency of semiconductor lasers is a few GHz. On the other hand, the external cavity frequency (f_{ext}) depends on the distance between the facet of the laser cavity and the external mirror (i.e., the external cavity length) as,

$$f_{ext} = \frac{c}{2nL_{ext}} \ldots\ldots\ldots\ldots (2.1)$$

Where ($\mathbf{L_{ext}}$) is the external cavity length (one-way), (**n**) is the refractive index in the external cavity, and (**c**) is the speed of light. The nonlinear interaction between the relaxation oscillation frequency and the external cavity frequency results in the quasi periodicity route to chaos as the feedback strength increases (Uchida, 2012).

2.2.2 Optical Coupling and Injection

The unidirectional or mutual optical coupling from one laser to another laser can generate chaotic instability of laser output, as shown in Figure (Figure 2.5b).

It is worth noting that the laser intensity has two dominant frequency components one is the optical-carrier frequency ($\boldsymbol{f_c}$) determined by the optical wavelength ($\boldsymbol{\lambda}$) and the speed of light(C) as:

$$\boldsymbol{f_c = \frac{c}{\lambda}} \quad \ldots\ldots (\mathbf{2.2})$$

When the detuning of the optical carrier frequencies between an injection and injected lasers is set to the order of the relaxation oscillation frequency, the nonlinear interaction between the optical-carrier frequency detuning and the relaxation oscillation frequency can occur and chaotic fluctuation may appear. The control of the detuning of the optical-carrier frequency, as well as the coupling strength, is crucial for chaos generation in this method (Uchida, 2012).

2.2.3 External Modulation

When an external modulation is added to the pumping of a laser system as shown in (Figure 2.5c) (i.e., pump modulation), chaotic instability of laser intensity may appear. The external modulation frequency needs to be set around the relaxation

oscillation Frequency of the laser, so that the nonlinear interaction between the external modulation frequency and the relaxation oscillation frequency may result in the generation of chaos (Uchida, 2012).

The external modulation can also be applied to the loss of the laser cavity, which is referred to as loss modulation. Chaotic dynamics is typically observed through the quasi periodicity route to chaos as the external modulation strength is increased (Uchida, 2012).

2.2.4 Insertion of Nonlinear Element

The insertion of a nonlinear element may cause chaotic dynamics, as shown in (Figure 2.5d). For example, chaotic intensity fluctuation is observed in a solid-state laser system with a nonlinear crystal for second-harmonic generation (SHG).

The mode–mode interaction between the fundamental wavelength and the SHG wavelength occurs in a nonlinear fashion, and chaotic dynamics may be observed. Also, when a saturable absorber is inserted in a gas-laser system, complex chaotic dynamics may be observed.

An additional degree of freedom enhances the nonlinear atom–photon interaction in the laser medium and leads to chaotic intensity fluctuations (Uchida, 2012).

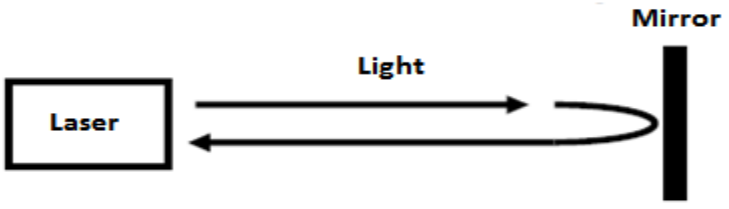

(a) Optical feedback

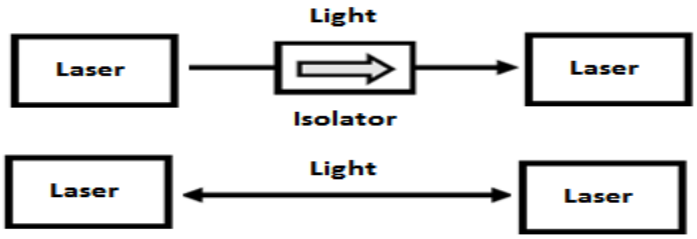

(b) Optical injection and coupling:

(Upper: unidirectional coupling, lower: mutual coupling)

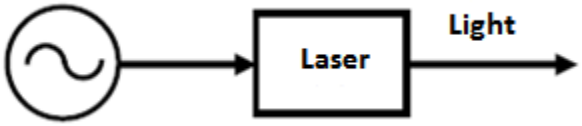

(c) External modulation

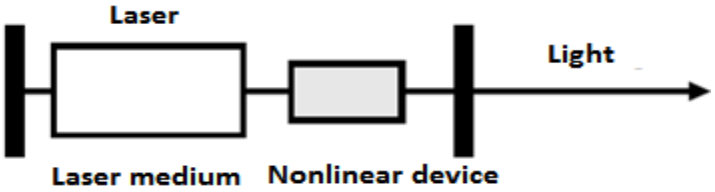

(d) Insertion of optical device

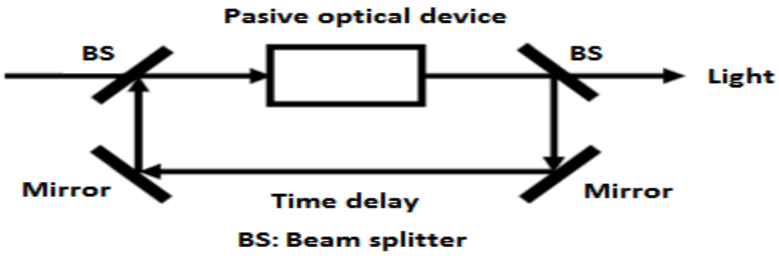

(e) Configuration of Ikeda chaos

Figure 2-5(a,b,c,d,e) Chaos Generation techniques(Uchida, 2012).

2.2.5 Semiconductor Laser with Optoelectronic Feedback

In optoelectronic feedback signal can be used for generation of chaos in semiconductor lasers. The laser output is detected by a photo detector and is converted into an electronic signal. The electronic signal is fed back to the injection current for pumping to induce instability of laser output. The feedback signal of the laser intensity only interacts with the dynamics of the carrier density, but not the electric field of the laser, thus it is considered as incoherent optical feedback (Ohtsubo, 2013). The light emitted from a semiconductor laser is detected by a photo detector and the detected photocurrent is fed back to the injection current through a bias circuit.

2.2.6 Recurrence Formula

In this section, the basic concept of deterministic chaos and related terminologies are introduced and described. First, a basic mathematical formula is introduced for the observation of deterministic chaos in discrete time system (Uchida, 2012). A discrete sequence is considered as:

$$\boldsymbol{x_0 \rhd x_1 \rhd x_2 \rhd \cdots . \rhd x_N} \quad \ldots\ldots . (\mathbf{2.3})$$

A recurrence formula (also referred to a "map".) can be defined by a function (f***)*** that relates ($x_{n+1)}$ with ($x_{n)}$ for all n, that is

$$\boldsymbol{x_{n+1} = f(x_n)} \ldots\ldots\ldots\ldots . . (\mathbf{2.4})$$

First, (x_1) can be obtained from (x_0) by using equation (2.6) when (x_0) is given as an initial condition. Then, (x_2) is obtained from (x_1), and (x_3) is obtained from (x_2), and finally all x_n (n =1, 2,…N) Value can be calculated directly from the initial

condition as shown in Equation (2.3). In this sense, the map is completely deterministic by using the rule of equation (2.6) and the initial condition (x_0) (Uchida, 2012). One of the simplest models to exhibit chaos is the Logistic map. The Logistic map is written as:

$$\boldsymbol{x_{n+1} = a x_n (1 - x_n) \ldots\ldots (2.5)}$$

Where:

$$\boldsymbol{0 \leq x_n \leq 1 and\ 0 \leq a \leq 4 \ldots\ldots (2.6)}$$

Where (a) is a parameter for the map. To observe chaos we can select (a) equal to 4.

2.2.7 Chaotic Sequence:

A sequence of the discrete variable ($\mathbf{x_n}$) in the Logistic map (**a=4**) is shown in Figure 2.5a. It is surprising that the time sequence shows an irregular behavior even though Eq. (2.5) is quite simple and completely deterministic. The deterministic rule of Eq. (2.5) can be depicted as a quadratic relationship between xn and xnþ1, as shown in Figure 2.5b. This simple recurrence formula can produce an exotic irregular behavior without external noise term in Eq. (2.6). It may seem that the irregular sequence shown in Figure 2.6a is predictable because the sequence is derived from the deterministic rule if the rule and the initial condition are known, this is true, however, the initial condition with infinite. Precision is necessary for the prediction. In real chaotic dynamical systems, it is impossible to identify the initial conditions with infinite precision. In addition, there is an important characteristic of deterministic chaos, known as sensitive dependence on

initial conditions, which describe in Figure 2.6 (a). Therefore, a tiny error of the initial conditions makes a chaotic irregular sequence Unpredictable. This fact indicates chaos can be unpredictable for long-term duration, Even though the deterministic rule exists and only short-term prediction is attainable (Uchida, 2012).

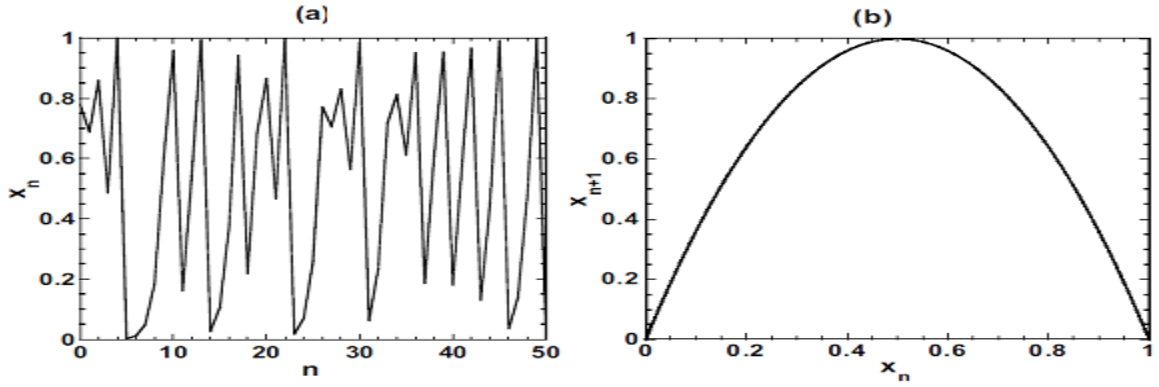

Figure 2-6 (a) Sequence of discrete variable (xn) and (b).

Quadratic relationship between (xn) and (xn+1) in logistical map (a=4). (Uchida, 2012).

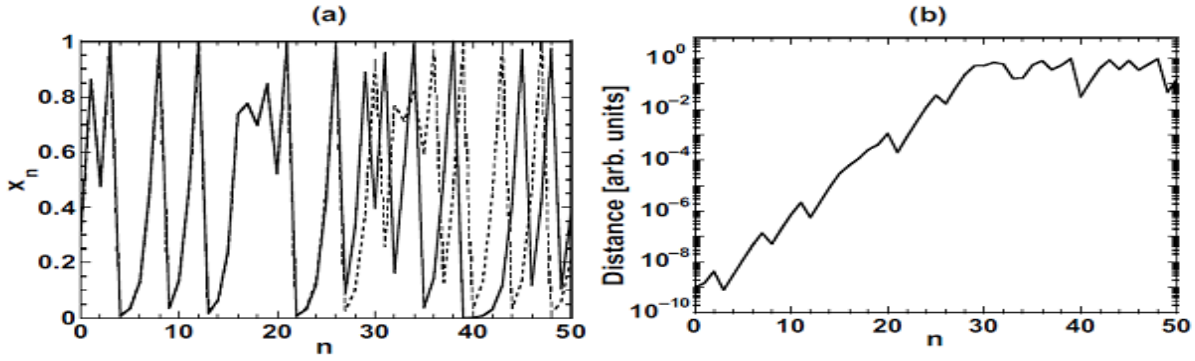

Figure 2-7 Show the sensitive dependance on initial conditions

in the logistical map(a=4) (Uchida, 2012).

(a) Two sequences of (x_n) starting from slightly different initial condition

(b) The destance of the two sequences in the semilogarithmic scale

2.2.8 Bifurcation Diagram and Two-Dimensional Dynamical Map

Another important characteristic of chaos is a transition among different dynamical States such as:

- **i.** Steady state.
- **ii.** Periodic state.
- **iii.** Chaotic sequences.

Is referred to as bifurcation in the logistic map, so when the parameter value (a) is changed, different states of sequences can be obtained as shown in Figure 2.9 shows the sequences of different values of (a) (Uchida, 2012).

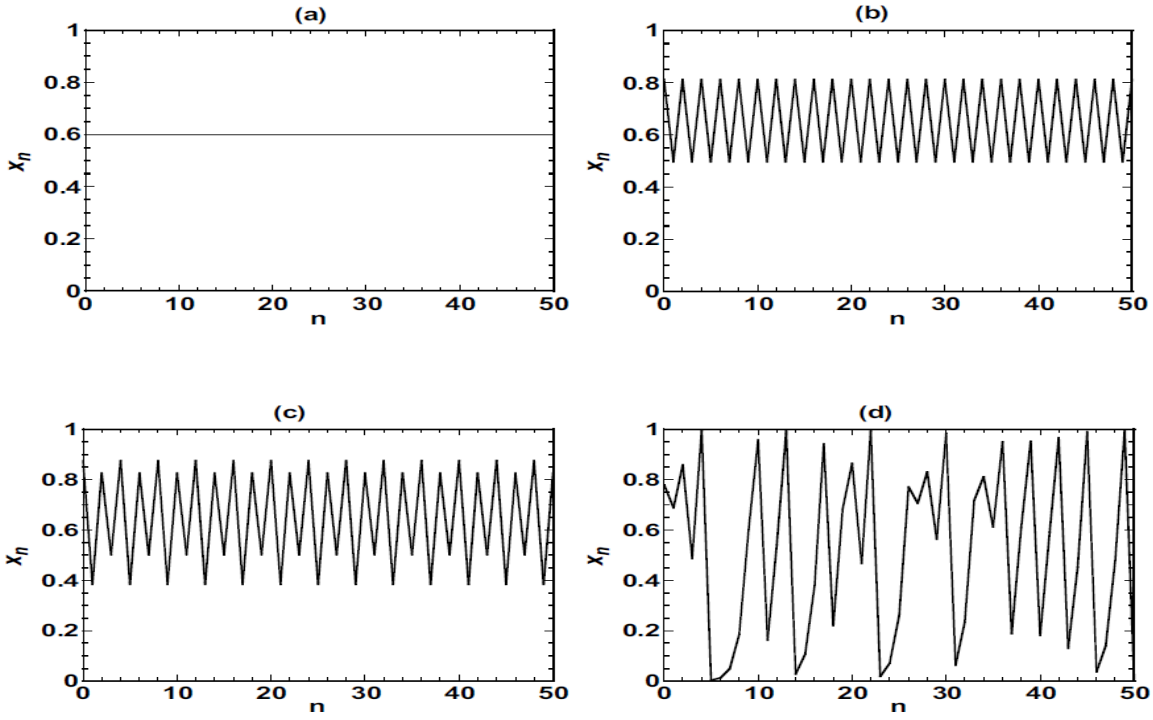

Figure 2-8 sequence of (xn) at different value of (a) in logistic map(Uchida, 2012).

(a) Periodic-1 (b) periodic-2 (c) periodic-4 (d) chaos

Also When one of the laser parameter values is changed (e.g., the optical feedback strength is increased in a semiconductor laser), the transition is found from a period-1 oscillation (Figure 2.9 a) and a quasi periodic oscillation (Figure 2.9 b) before a chaotic oscillation is observed, the bifurcation is known as the quasi periodicity route to chaos, and this result strongly indicates the existence of deterministic chaos, since bifurcation can be observed only in deterministic systems, but not in stochastic systems. The observation of bifurcation is thus one of the most convincing pieces of evidence of deterministic chaos if one of the laser parameters is accessible and changeable, particularly for experimental data (Uchida, 2012).

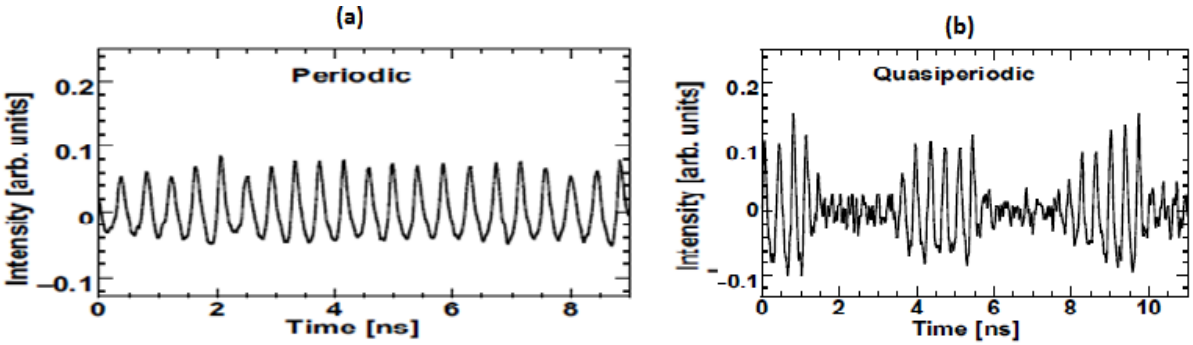

Figure 2-9 Experimental results as bifurcation diagram as function of the feedback strength

Periodic (b) Quasi periodic(Uchida, 2012).

2.3 Chaos Synchronization Concepts:

Synchronization of chaos is a phenomenon that may occur when two, or more, chaotic oscillators are coupled, or when a chaotic oscillator drives another chaotic oscillator.

Synchronization occurs when oscillatory (or repetitive) systems via some kind of interaction adjust their behaviors relative to one another so as to attain a state where they work in unison.(Mosekilde et al., 2002)

Also chaos synchronization refers to a procedure where two chaotic oscillators (either identical or non identical) adjust a given property of their motion to a common behavior (Argyris et al., 2005). Interacting chaotic oscillators are of interest in many areas of physics, biology, and engineering. In the biological sciences, for instance, one of the challenging problems is to understand how a group of cells or functional units, each displaying complicated nonlinear dynamic phenomena, can interact with one another to produce a coherent response on a higher organizational level (DeCusatis, 2002). Synchronization comes from the Greek words **syn** (with) and **chronos** (time) occurring at the same time. Synchronization refers to an adjustment of rhythms of oscillators due to weak interactions:

Oscillator: (self-sustained): active system with internal source of energy mathematically described by an autonomous system (ODE, map).

Rhythms: frequency or period of oscillations.

Coupling: interaction or transmission of information between system: unidirectional (forcing) or bidirectional (mutual interaction) (Werndl, 2009).

Chaos synchronization in discrete-time has been extensively studied, due to its potential applications for secure communication. Different types and various powerful methods and techniques of chaos synchronization have been reported to investigate chaos synchronization in discrete dynamical systems (Danforth, 2013).

2.3.1 Complete Synchronization (CS):

Existence of a type of synchronization for both amplitude and phase, and more generally for all state variables x_i of a dynamical system (Medio and Lines, 2001):

$$\sum_1 : \dot{x}_1 = F_1\left(x_1, K_1(x_1, x_2)\right) \dots\dots\dots (3.1)$$

$$\sum_2 : \dot{x}_2 = F_2\left(x_2, K_2(x_1, x_2)\right) \dots\dots\dots (3.2)$$

Then: (X_1=X_2) Asymptotically

2.3.2 Generalized synchronization (GS):

Existence of functional relationship between state variables of systems 1 and 2

$$X_1 = \psi(X_2) \dots\dots\dots (3.3)$$

Depending on the smoothness of ψ we distinguish weak or strong GS. Because of the butterfly effect, which causes the exponential divergence of the trajectories of two identical chaotic system started with nearly the same initial conditions, having two chaotic system evolving in synchrony might appear quite surprising (Medio and Lines, 2001).

2.3.3 Identical synchronization:

This is a straight forward form of synchronization that may occur when two identical chaotic oscillators are mutually coupled, or when one of them drives the other. If (x_1,x_2,,...,x_n) and (x'_1, x'_2,...,x'_n) denote the set of dynamical variables that

describe the state of the first and second oscillator, respectively, it is said that identical synchronization occurs when there is a set of initial conditions :

$$[x_1(0), x_2(0),...,x_n(0)], [x'_1(0), x'_2(0),...,x'_n(0)]$$

Such that, denoting the time by:

$$t, |x'_i(t)-x_i((t)|\rightarrow 0, \text{ for } i=1,2,...,n, \text{ when } t\rightarrow\infty$$

That means that for time large enough the dynamics of the two oscillators verifies

$$\mathbf{x'_i(t)=x_i(t), \text{ for } i=1,2,...,n,}$$

In a good approximation, this is called the synchronized state in the sense of identical synchronization (Medio and Lines, 2001). Most of the synchronization techniques belong to the master-slave (drive-response) system configurations in which the two chaotic systems are coupled in such a manner that the performance of the second (slave /response) system is influenced by the first (drive/master) system and the first system is not disturbed by the exertion of the second (slave / response) system. (Medio and Lines, 2001).

2.3.4 Generalized synchronization:

This type of synchronization occurs mainly when the coupled chaotic oscillators are different, although it has also been reported between identical oscillators. Given the dynamical variables:

$$(x_1,x_2,,...,x_n) \text{ and } (y_1,y_2,,...,y_m)$$

That determine the state of the oscillators, generalized synchronization occurs when there is a functional, Φ, such that, after a transitory evolution from appropriate initial conditions, it is:

$$[y_1(t), y_2(t),...,y_m(t)]=\Phi[x_1(t), x_2(t),...,x_n(t)]$$

This means that the dynamical state of one of the oscillators is completely determined by the state of the other. When the oscillators are mutually coupled this functional has to be invertible, if there is a drive-response configuration the drive determines the evolution of the response, and Φ does not need to be invertible. Identical synchronization is the particular case of generalized synchronization when Φ is the identity [5]. Among all types of synchronization, generalization synchronization (GS) has been extensively considers. In (GS), two chaotic systems are said to be synchronized if there exists of fundamental relationship between the states the drive and response chaotic system (Baker and Gollub, 1996).

2.3.5 Phase synchronization:

The phase of oscillations may be locked by periodic external force; another situation is the locking of the phases of two interacting oscillators.

phase synchronization of chaotic system define as, ‘appearance of a certain relation between the phases of interacting systems or between the phase of a system and that of an external force, while the amplitudes can remain chaotic and are, in general, non-correlated (Uchida, 2012). This form of synchronization, which occurs when the oscillators coupled are not identical, is partial in the sense that, in the synchronized state, the amplitudes of the oscillator remain unsynchronized, and only their phases evolve in synchrony.

The characterize phenomenon in phases synchronization analysis, while the amplitudes vary chaotically and are practically uncorrelated. Coupling a chaotic oscillator with a hyper chaotic one, we observe another new type of synchronization, where the frequencies are entrained, while the phase difference is unbounded.(Rosenblum et al., 1996)

Observation of phase synchronization requires a previous definition of the phase of a chaotic oscillator. In many practical cases, it is possible to find a plane in phase space in which the projection of the trajectories of the oscillator follows a rotation around a well-defined center, so if:

$$\varphi 1\ (t) \text{ and } \varphi 2\ (t)$$

Denote the phases of the two coupled oscillators; synchronization of the phase is given by the relation:

$$n\varphi_1\ (t) = m\varphi_2\ (t)$$

with (m) and (n) whole numbers (Uchida, 2012).

2.3.6 Anticipated and lag synchronization:

In these cases the synchronized state is characterized by a time interval (**τ**) such that the dynamical variables of the oscillators:

$$(x1, x2,,..., xn) \text{ and } (x'_1, x'_2,...,x'_n)$$

Are related by:

$$x'_i(t)=x_i(t+\tau)$$

This means that the dynamics of one of the oscillators follows, or anticipates, the dynamics of the other. Anticipated synchronization may occur between chaotic oscillators whose dynamics is described by delay differential equations, coupled in a drive-response configuration. In this case, the response anticipates the dynamics of the drive. Lag synchronization may occur when the strength of the coupling between phase-synchronized oscillators is increased (Medio and Lines, 2001).

2.3.7 Amplitude envelope synchronization:

This is a mild form of synchronization that may appear between two weakly coupled chaotic oscillators. In this case, there is no correlation between phases nor amplitudes; instead, the oscillations of the two systems develop a periodic envelope that has the same frequency in the two systems. This has the same order of magnitude than the difference between the average frequencies of oscillation of the two chaotic oscillators (Medio and Lines, 2001). Often, amplitude envelope synchronization precedes phase synchronization in the sense that when the strength of the coupling between two amplitude envelope synchronized oscillators is increased, phase synchronization develops. All these forms of synchronization share the property of asymptotic stability. This means that once the synchronized state has been reached, the effect of a small perturbation that destroys synchronization is rapidly damped, and synchronization is recovered again. Mathematically, asymptotic stability is characterized by a positive Lyapunov exponent of the system composed of the two oscillators, which becomes negative when chaotic synchronization is achieved. Some chaotic systems allow even stronger control of chaos. Both synchronization of chaos and control of chaos constitute parts of cybernetic Physics (Ohtsubo, 2013).

2.4 Coupling Schemes and Synchronization Types:

To synchronize chaotic temporal waveforms, laser systems need to be coupled to each other. Coupling schemes are very important to consider synchronization of chaos. The coupling schemes can be mainly classified into two types:

i. Unidirectional Coupling (one way).
ii. Bidirectional Coupling a mutual (two-way) couplings.

2.4.1 The unidirectional coupling:

The unidirectional coupling is treated mainly for engineering applications purpose specifically optical communications. Unidirectional is the one of the simplest coupling schemes for chaos synchronization made by a unidirectional Injection from one laser (referred to as a drive laser) to another laser (referred to as a response laser). The output of the drive laser is directly injected into the response laser. The subtraction of the outputs between the drive and response lasers can be used as an injection signal to the response laser as a coupling factor that control the state of coupling to successive synchronization between driver and response laser systems (Medio and Lines, 2001). The synchronization between coupled chaotic circuits has attracted the interest of the research community because there are rich and multi-disciplinary phenomena with broad range applications, such as in broadband communication systems, in secure communications and in cryptography. For this reason many coupling schemes between identical nonlinear circuits with chaotic behavior have been presented. However, the basic drawback of the majority of these schemes is the request the coupled circuits to be identical.

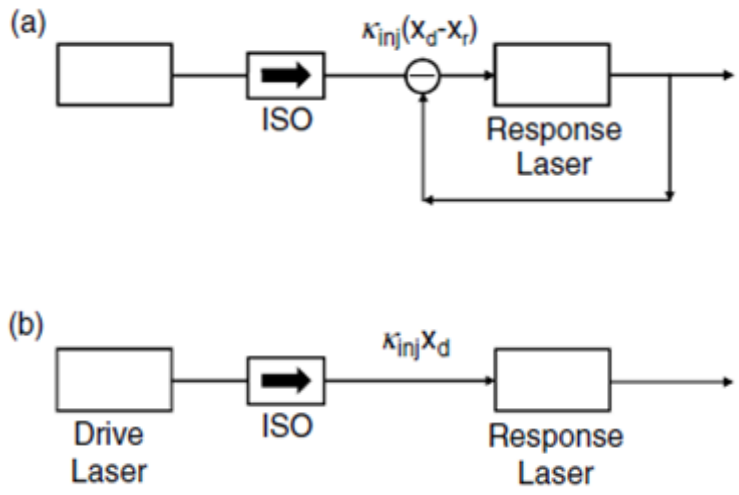

Figure 2-10 Block diagram of the schemes of the chaos synchronization(Medio and Lines, 2001).

(a) Diffusive coupling (b) Simple injection

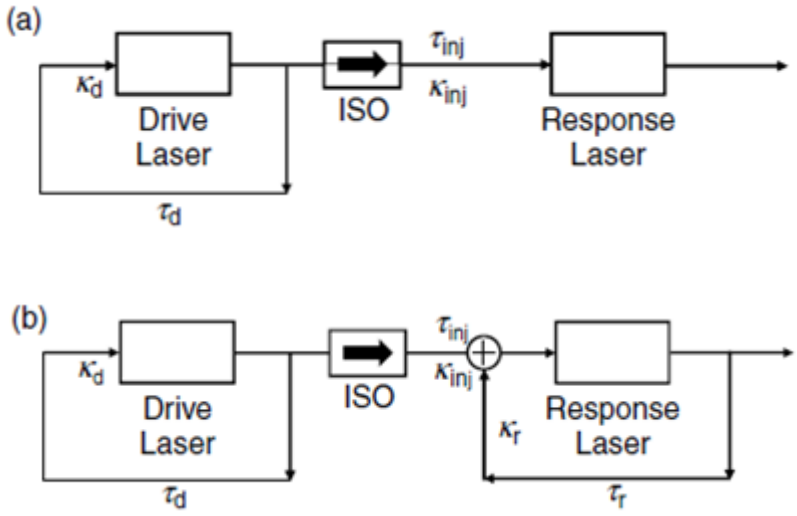

Figure 2-11 Block diagram of the schemes of the chaos synchronization with feedback in the drive laser (Medio and Lines, 2001).

(a) Open loop (b) Closed loop

2.4.2 Synchronization of Chaos for Communication Applications

The idea of synchronization of chaos leads to a possible application for communication. The application of synchronization of chaos to secret communication systems was suggested in early work, it was discovered that a chaotic transmitter could consist of an electronic circuit that generated nonlinear dynamics and chaos. A message to be concealed with small amplitude is added to the chaotic fluctuations of one of the dynamical variables and transmitted to a receiver, while another chaotic variable was separately transmitted. The receiver consisted of a subsystem of the circuits in the transmitter that generated the dynamics of the transmitter and was driven by the separately transmitted signal. The receiver synchronized to the chaos of the transmitter for the given operating parameters, and one could recover the message from the chaos through a subtraction at the receiver. An elegant variation of the method was introduced above that did not require the separate transmission of a driving signal to the receiver(Cuomo and Oppenheim, 1993). It was shown that the receiver could actually synchronize to the chaotic dynamics of the transmitter even when a message was added to the chaotic driving signal from the transmitter. The synchronized output from the receiver was then used to subtract out the information from the transmitted signal. The synchronization was not perfect, and the message, treated as a perturbation of the chaotic signal, had to be small compared to the chaos (Medio and Lines, 2001).

Synchronization of chaos is a phenomenon that may occur when two, or more, chaotic oscillators are coupled, or when a chaotic oscillator drives another chaotic oscillator. (Israr Ahmed, December 2015)

3 Chapter Three: Laser Model Design and Implementation

3.1 Introduction

Semiconductor laser (SL) with optoelectronic feedback system may be expressed mathematically by a set of differential equations that represents (OEFSL). this set reduces and converting the physical mathematical description to dimensionless equations by (Al Naimee et al., 2009). In this work we have modified the previous model (system) to new dimensionless equations as ***Al Naimee, 2016***. By this new modification, the implementing and programming of the optoelectronic feedback system has been achieved by MATLAB package and Simulink.

Due to simulation, the considered system of chaotic oscillator has been modeled by selecting experimental parameters (Sora et al., 2010). The existences of slow chaotic spiking sequences appear in the dynamics of the simulating model results. The behavior and characteristic of the simulated model is described according to the following parameters:

- **i.** System parameters setting.
- **ii.** Initial condition value.
- **iii.** Time interval responds.

3.2 Mathematical Model:

The dynamics of the photon density S and carrier density N can be described by the usual single-mode SL rate equations, SL rate equations are used to model the dynamics of a SL with OEFB. Due to the theoretical concepts the numerical simulating outputs of the model fully describe dynamics of a SL according to

model parameters and conditions. So in specifics state chaos been generating as model output(Chan and Liu, 2005)

single-mode SL rate equations appropriately modified in order to include the ac-coupled feedback loop:

$$\dot{S}= [g(N -Nt) -\gamma_0]S\ldots\ldots\ldots\ldots\ldots\ldots\ldots\ldots(i)$$

$$\dot{N}= \{I_0+ f_F(I)\}/eV-\gamma_c N-g(N -N_t)S\ldots\ldots\ldots(ii)$$

$$\dot{I}= -\gamma_f I + k\,\dot{S}\ldots\ldots\ldots\ldots\ldots\ldots\ldots\ldots\ldots(iii)$$

Where I is the high-pass filtered feedback current (before the nonlinear amplifier), f_F (I) ≡ AI/(1+s'I) is the feedback amplifier function, I_0 is the bias current, e the electron charge, V is the active layer volume, g is the differential gain, Ntis the carrier density at transparency,γ_0 and γ_c are the photon damping and population relaxation rate, respectively, γ_f is the cutoff frequency and k is a coefficient proportional to the photo detector responsively. For numerical and analytical purposes, it is useful to rewrite equations (i,ii,iii),in dimensionless form, we introduce the new variables:

x= (g/γc)S, y = g/γo(N-Nt) ,w = (g/kγc) I-x, and the time scale t`=γot.

Then the rate equations become as the following form:

The first rate equation is:

$$\mathbf{\dot{S}= [g(N -Nt) –\gamma o]S\ldots\ldots\ldots..(i)}$$

Using: $x= (g/\gamma c)S$,$S=x\gamma c/g$

$y= (g/\gamma_o)(N-N_t)$,$N-N_t=y\gamma_o/g$

$t`= \gamma_o t, d t`=\gamma_o dt$,$dt=d t`/\gamma_0$ ,$1/dt=\gamma_0/ d t`$

Substitute in (1):

$d/dt(x\gamma_c/g)=[g(y\gamma_o/g)-\gamma_0]x\gamma_c/g$

$dx/dt(\gamma_c/g)=xy\gamma_0\gamma c/g-x\gamma_0\gamma_c/g$

$\gamma_0 dx/ d t`=xy\gamma_0-x\gamma_0$,dividing by (γ_0):

$\dot{x} =xy-x$,

$$\boxed{\dot{x}(t`)=x(y-1)} \quad \cdots\cdots\cdots (a)$$

The second rate equation is:

$$\dot{N}= [(I_o +f_F (I))/eV] - \gamma_c N - g(N-N_t)S \ldots\ldots.(ii)$$

Since $N-N_t=y\gamma_0/g$,$N= y\gamma_0/g+N_t$

Then $d/dt(y\gamma_0/g)= [(I_0+f_F(I))/eV] - \gamma_c(y\gamma_0/g+N_t) - g[(y\gamma_0/g)(x\gamma_c/g)]$

And Since: $f_F(I)=AI/(1+\acute{S}I)$

Then $(\gamma_0/g)dy/dt= [(I_0+AI/1+\acute{s}I)/eV]-\gamma_c(y\gamma_0/g +N_t) –(xy\gamma_0\gamma_c/g)$,

Dividing by (γ_0/g),

$dy/dt=g/\gamma_0[(I_0+AI/1+\acute{S}I)/eV] - [g\gamma_c/\gamma_0(y\gamma_0/g+N_t)] -xy\gamma_c$

$\gamma_0(dy/ d t`) =g/\gamma_0[(I_0+AI/1+ŚI)/eV] - [g\gamma_c/\gamma_0(y\gamma_0/g +N_t)] -xy\gamma_c$

$\dot{y}(t`)=g/\gamma_0 2[(I_0+AI/1+ŚI)/eV] - [g\gamma_c/\gamma_0 2(y\gamma_0/g+N_t)] - (xy\gamma_c/\gamma_0)$

$\dot{y}= (gI_0/\gamma_0 2eV) + g/\gamma_0 2[(AI/eV(1+ŚI)] - (y\gamma_c/\gamma o) - (g\gamma_c/\gamma_0 2)N_t- (xy\gamma_c/\gamma_0)$

Since $\alpha=Ak/eV\gamma_0$, $A=eV\gamma_0\alpha/k$

Then $\dot{y}=gI_0/\gamma_0 2eV +g/\gamma_0 2[(eV\gamma_0\alpha I/k)/ eV(1+śI)]– (y\gamma_c/\gamma_0)- (g\gamma_c/\gamma_0 2)N_t-xy\gamma_c/\gamma_0$

Since $\gamma=\gamma_c/\gamma_0$,

Then $\dot{y}=gI_0/\gamma_0 2eV+ [g\alpha I/k\gamma_0(1+śI)]-y\gamma – (\gamma gN_t/\gamma_0) - xy\gamma$

Since $W= (g / k\gamma_c)I-x$, $w+x=gI/k\gamma_c$,$gI=k\gamma_c(w+x)$

Then $\dot{y}=gI_0/\gamma_o^2eV+ [\alpha k\gamma_c(w+x)/k\gamma_0(1+śI)] –(\gamma gN_t/\gamma_0) - y\gamma - xy\gamma$

$\dot{y}= (gI_0/\gamma_0^2eV) + \alpha\gamma[(w+x) /(1+śI)] –(\gamma gN_t/\gamma_0) - y\gamma - xy\gamma$

Since $S=\gamma_c śk/g$, $Sg=\gamma_c śk$ $ś=Sg/k\gamma_c$

Then $\dot{y}=gI_0/\gamma_0^2eV + \alpha\gamma[(w+x)/1+S(gI/k\gamma_c)] –(\gamma gN_t/\gamma_0) - y\gamma - xy\gamma$

Since $gI / k\gamma_c = (w+x)$,

Then $\dot{y}=gI_0/\gamma_0^2eVv + \alpha\gamma[(w+x)/1+s(w+x)]–(\gamma gN_t/\gamma_0) - y\gamma -xy\gamma$

And since $f(w+x) = \alpha[(w+x)/1+S(w+x)]$,

Then $\dot{y}=gI_0/\gamma_0^2eV + \gamma_f(w+x) - \gamma gN_t/\gamma_0 - y\gamma – xy\gamma$,

$\dot{y}=gI_0/\gamma_0^2eV -\gamma gN_t/\gamma_0 + \gamma_f(w+x) - y\gamma – xy\gamma$,

$\dot{y}=g/\gamma_0^2(I_0/eV-\gamma_c N_t) + \gamma_f(w+x) - y\gamma - xy\gamma,$

$\dot{y}=\gamma g/\gamma_0\gamma_c(I_0/eV -\gamma_c N_t) + \gamma_f(w+x) - y\gamma - xy\gamma,$

$\dot{y}=\gamma\{g / \gamma_0\gamma_c[(I_0-eV\gamma_c N_t)/eV] + f(w+x) - y - xy\},$

Since $I_{th}=eV\gamma_c(\gamma_0/g + N_t)$, $I_{th} =eV\gamma_c\gamma_0/g + eV\gamma_c N_t,$

Then $\delta =(I_0 - I_t)/(I_{th} - I_t),$

$$\boxed{\dot{y}= \gamma[\delta_0 -y+f(w+x) - xy]} \quad \text{..... (b)}$$

And the third rate equation is:

$$\dot{I} = -\gamma f I + k\dot{S} \text{……(iii)}$$

Since $w= (g/k\gamma_c)I-x$, $I= (k\gamma c/g)(w+x),$

Then $d/dt[k\gamma_c/g(w+x)] =-\gamma_f I+k\dot{S}$

$(\gamma_0 k\gamma_c/g)(\dot{w}+\dot{x})(t`)=-\gamma_f I+k\dot{S}$

Since $\dot{S}=[g(N-N_t)-\gamma_0]S=[g(y\gamma_0/g) - \gamma_0]\gamma_c x/g,$

$\dot{S}=[y\gamma_0-\gamma_0](\gamma_c x/g)$, $\dot{S}=(\gamma_c\gamma_0 X/g)(y-1)$

Then $(\gamma_0 k\gamma_c/g)(\dot{w}+\dot{x}) = (-\gamma_f k\gamma_c/g)(w+x) +(k\gamma_c\gamma_0 x/g)(y-1),$

Dividing by$(\gamma_0 k\gamma_c/g),$

$\dot{w}+\dot{x} = (-\gamma_f/\gamma_0)(w+x) + x(y-1),$

$\dot{w} = (-\gamma_f/\gamma_0)(w+x) + x(y-1) -\dot{x},$

Since $\dot{x}= x(y-1)$,

Then $\dot{w} = (-\gamma_f/\gamma_0)(w+x)$,

Let: $\varepsilon=\gamma_f/\gamma_0$,

$\dot{w}$ becomes = $-\varepsilon(w+x)$ ……..(c)

The results of these modifications can be written as following:

$$\dot{x}(t`)=x(y-1)…….(a)$$

$$\dot{y}= \gamma[\delta_0-y+f(w+x) - xy]…….(b)$$

$$\dot{w} = -\varepsilon(w+x)……...…..(c)$$

Where δ_0 is the bias current and ε is the feedback strength, γ is the population inversion relaxation rate. These are rate equations of SL in dimensionless form in order to compute and for numerical and analytical purpose.

These equations representing the non linear dynamical system which produced HC in SL with OEFB. The first equation represents the photon density or the intensity for output laser ray, the second equation represents the population inversion, while the third equation represents the feedback which is necessary to produce chaos this feedback consist from the intensity of laser output and the current bias(Al Naimee et al., 2009).

(Al Naimee et al., 2009) Laser diode with optoelectronic feedback model mathematically describes by above dimensionless differential equations as follow:

$$\dot{x} = x(y-1) \qquad (3.1)$$

$$\dot{y} = \gamma(\delta_0 - y + f(w + x) - xy) \qquad (3.2)$$

$$\dot{w} = -\varepsilon (w + x) \qquad (3.3)$$

Based on AL Naimee System, 2009 In this work we provide new generation of AL Naimee System AL Naimee System, 2016 Laser diode with optoelectronic feedback model mathematically describes by three models dimensionless differential equations as follow:

$$\dot{x} = x(y-1) \qquad (3.4)$$

$$\dot{y} = \gamma(\delta_0 - y + \frac{w}{(1+sw)} - xy) \qquad (3.5)$$

$$\dot{w} = -\varepsilon (w + x) \qquad (3.6)$$

Where $\boldsymbol{\delta_0}$ is the bias current and $\boldsymbol{\varepsilon}$ is the feedback strength, $\boldsymbol{\gamma}$ is the population inversion relaxation rate. These are rate equations of SL in dimensionless form in order to compute model simulation and analytical purpose in my work.

3.3 System model Implementation:

The semiconductor laser with optoelectronic AC-coupled feedback physical model (Eqs.3.1-3.3) has different time scale (Photon density, carrier density, feedback

strength current) Due to the mathematical model dimensionless, three differential equations Chaos generator model been implemented.

Then according to these equations SL with OEFB model simulation structure consists of three sub system describe as follow:

- X –Equation part.
- Y –Equation part.
- W –Equation part.

Using Matlab Simulink to modeling (x-equation) as shown in (fig3.1)

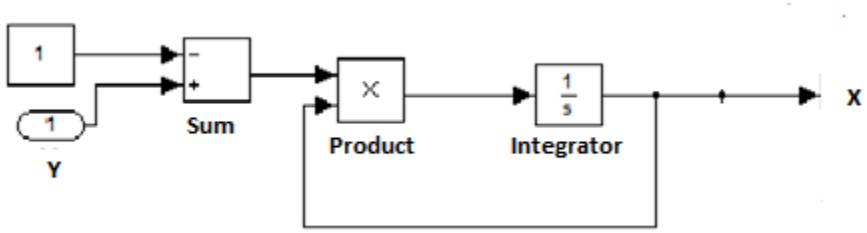

Figure 3-1 X-Equation Part

This figure describes Matlab Simulink implementation of equation (3.4) ($\dot{x} = x(y-1)$) in the OEFSL simulation model.

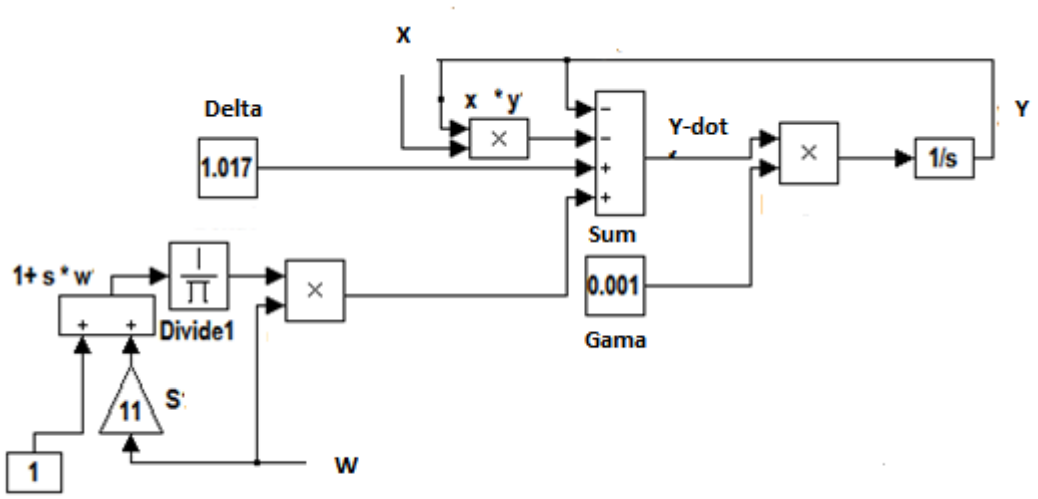

Figure 3-2 Y-Equation Part

Figure (3.2) describe Matlab Simulink implementation of equation (3.5)

($\dot{y} = \gamma(\delta_0 - y + \frac{w}{(1+sw)}$ - xy) in the OEFSL simulation model.

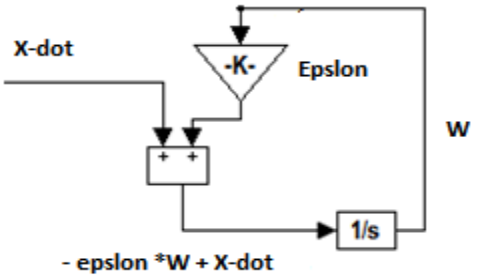

Figure 3-3 W-Equation Part

Figure (3.3) describe Matlab Simulink implementation of equation (3.6)

$\dot{w}$= -ε (w + x) in the OEFSL simulation model.

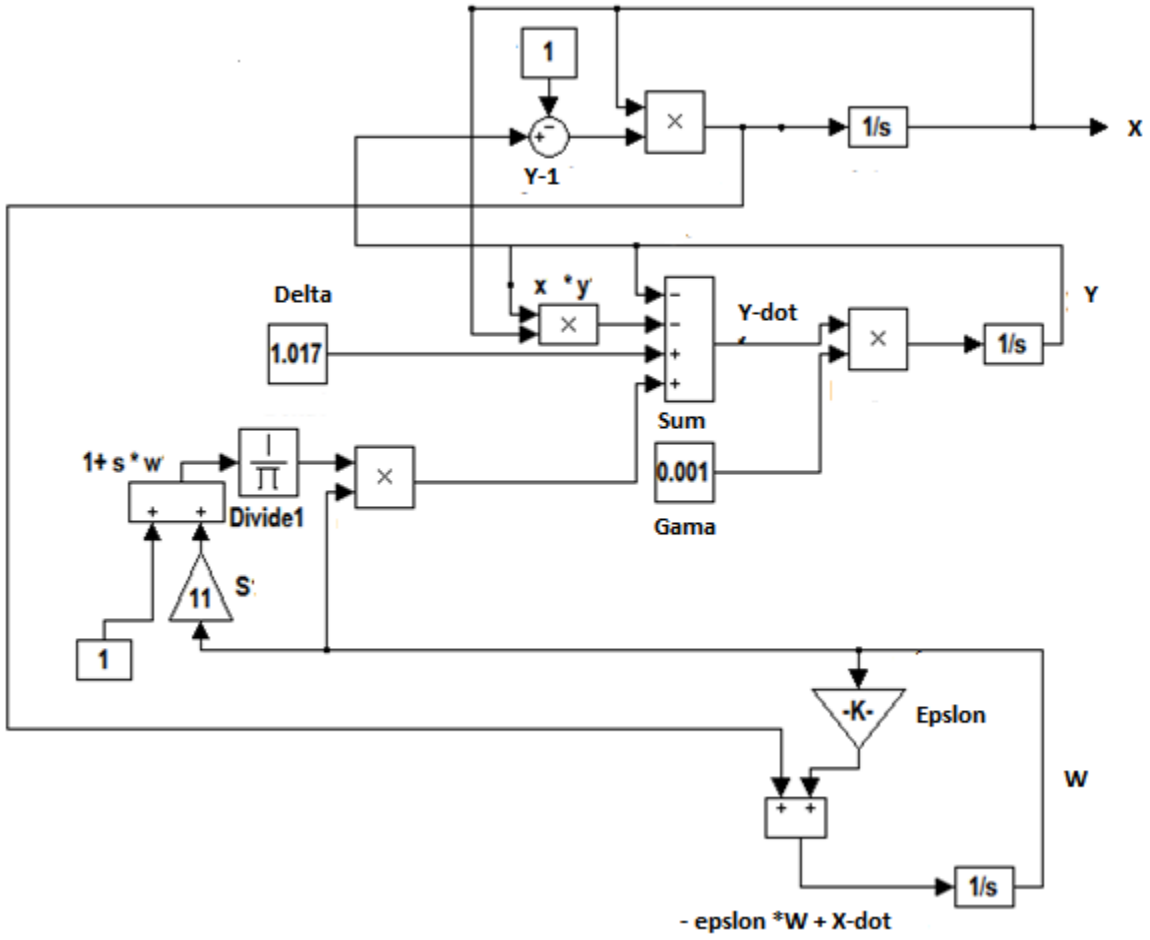

Figure 3-4 Integrated Single Oscillator Model (X, Y and W Equation)

Figure (3-4) describe the implementation of the OEFSL simulation model that consists of the three equations parts connected configuration to be works as the single laser oscillator

This oscillator simulates the behavior of OEFB physical model and generates chaos signal under specifics setting parameters and other operation values.

The dynamics of this oscillator based on the variation of the operation parameters values such as pumping current (δ0) and feedback strength (ε).

The single laser oscillator (fig3.4) model is duplicates with the same structure components and different operations value that mention in (table 3.1) to be use in coupling mode as:

- **i.** Master laser oscillator.
- **ii.** Slave laser oscillator.

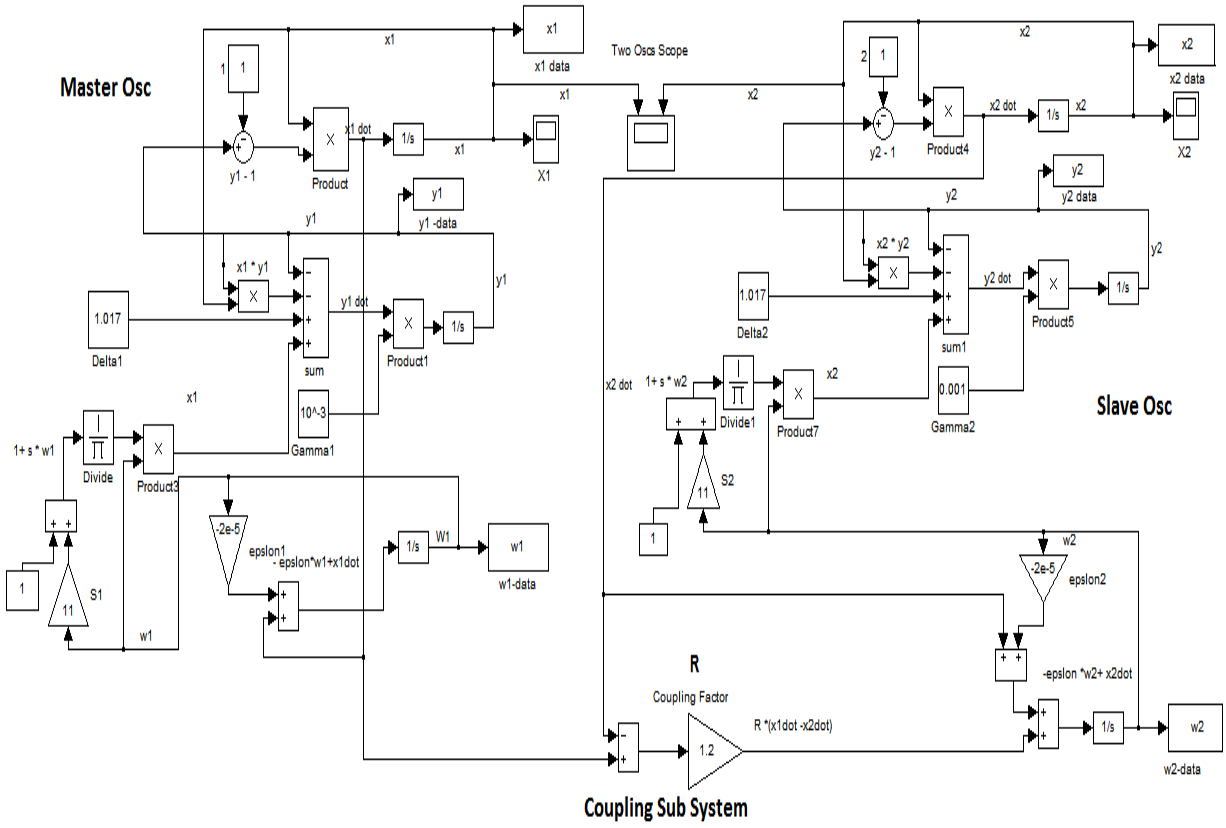

Figure 3-5 Master-Slave Osc Coupling Structure Details Components

Figure(3-5) describe the implementation of the OEFSL simulation model consists of two laser system representing master - slave laser system configuration with Unidirectional coupling configuration depend on master laser and couple factor(R).

The mater oscillator drives slave oscillator through the coupling sub system that describes in (fig 3.9) as unidirectional coupling configuration that mention in Chapter (3) section (3.3.1).

3.4 Coupling Configuration:

In order to achieve synchronization state between master and slave oscillator Unidirectional coupling configuration is implemented according to theoretical concepts that mention in (ch.3).

The coupling sub system enables the master oscillator to fully driving and controlling slave oscillator as appear in system results.

Unidirectional mathematically expression based on:

- **i.** Master oscillator feedback strength.
- **ii.** Slave oscillator
- **iii.** Coupling Factor

So unidirectional coupling configuration (UCC) mathematically express as follow:

$$\mathbf{UCC \rightarrow R *(x1dot - x2dot)\ldots\ldots\ldots\ (3.4)}$$

Coupling system implemented due to the coupling equation as follow:

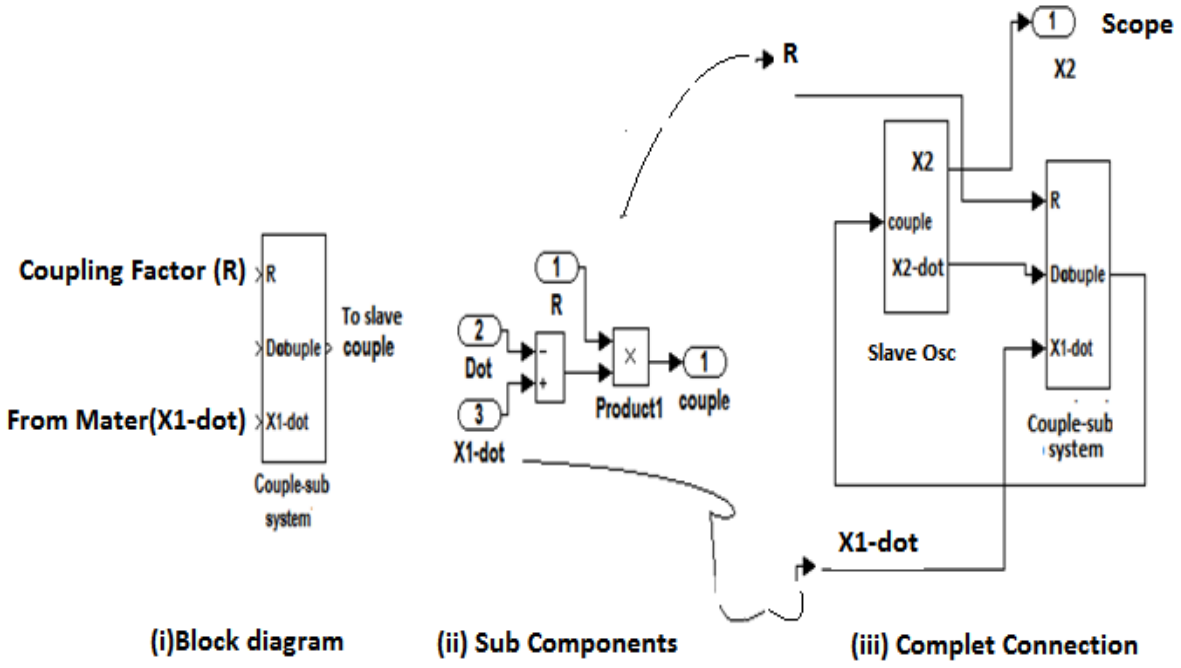

Figure 3-6 Unidirectional Coupling Configuration sub system

Figure (3-6) describe the implementation of the unidirectional coupling configuration based on the equation (3.4) this sub system consists of three parameters ,coupling factor(R),master laser components(x1-dot) and the slave laser component(x2-dot).

3.5 System Parameters and Configuration Value:

The oscillator model dynamic behaviors and characteristics describe according to the system results that obtain from system Simulink model running. The model results take respectively according to the following parameters:

- Model parameters setting.
- Initial condition value.

- Time interval responds.

Different results values obtain from different model running and setup values such as initial condition, feedback strength and injected bias current. The selected values and tune parameters enable the models to simulate the physical behaviors and dynamics of OEFSL simulation model such as the transition from steady state to periodic and chaotic state that clearly appear in system results.

3.6 Running and operation:

As mention in chapter (2), the theoretical concepts of OEFSL chaos generation is achieved and effects of bias current and feedback strength have been demonstrated. Matlab Software package used to analyze the time series generated in the chaos regime. The analysis concerns the study of the system attractors and the time series as form of model results due to the following running mode types.

i. Free Running Mode (FRM).

ii. Coupling Running Mode (CRM).

3.6.1 Free Running Mode:

In this mode of operation the coupling factor enables the master and slave laser to work identically as there is no coupling between them so the generated signal (X_1) at the master laser and (X_2) at the slave laser describe this running mode (FRM).

The operation and setting parameters for each oscillator are selecting to be different in each one so the master oscillator differs from the slave oscillator resulting different time series in (FRM).

To control the operation mode and toggle between free mode and coupling mode the coupling sub system enable easily the switching between (FRM) and (CRM) through the selection value of the coupling factor (R) as follow:

Table (3.1) Running mode as function of (R)

Coupling factor Value(R)	Operation Mode
Zero	Free Mode
None zero	Coupling Mode

Also the condition of the coupling sub system and the value of (R) determine the synchronization state.

3.6.2 Coupling Running Mode:

In this mode of operation the master oscillator control and driving slave oscillator through the coupling sub system based unidirectional coupling configuration theoretical concepts and techniques. Coupling running mode depends on:

i. Setting parameters for each oscillator.

ii. Appropriate selection of coupling factor (R).

So the coupling factor (R) value changes to enable master oscillator to change slave oscillator state in each of the following cases:

i. Free running identical state in both oscillators when (R=0).

ii. Coupling running A synchronize state between oscillators when (R > 1).

iii. Coupling running full synchronization between oscillators when (R=0.0.2).

3.7 Dynamics model:

The dynamics of Semiconductor laser with optoelectronic feedback simulation model behavior is studied according to the oscillators time series output signal (X_n) and simulation time interval so model behavior and dynamics be explain in each of the following states with respects to the setting parameters and operation values so the simulation model results describe the transition among the following states:

i. Steady state.

ii. Periodic state.

OEFSL simulation model transition from steady state to periodic state and chaotic state as the dc-pumping current was varied as explained in system results and discussion.

3.8 Netware oscillators: OEFSL

The master-slave configuration is expanded to implement Optoelectronic Feedback Semiconductor Laser Network (OEFSLN) by means of Simulink environment in MATLAB package to implement 256 oscillators. The synchronization condition among the all network oscillators has been achieved by means of coupling factor.

So Netware oscillators design to support chaos application and sciences such as secure chaos communication and neural network. The OEFSLN modeling design based on the:

i. Master oscillator base model as in figure (3.4).

ii. Slave oscillator base model as in figure (3.8).

iii. Unidirectional coupling configuration base model (3.9).

Netware oscillator model organize as driver sub system (one master oscillator) and number of slave oscillators (255 oscillators) work as (response) sub system as seen in figure (3.13). So number of slave arranged in block of oscillator as in figure (3.13) that fully control and driving by master oscillator through the coupling sub system.

The OEFSLN consist of (32) blocks each one contain (8) laser then the overall number of laser system are (256) deferent laser systems.

The design model aim to:

i. Implementing Netware chaotic oscillator model.

ii. Implementing and apply unidirectional coupling configuration.

iii. Increasing number of oscillator.

iv. Study the Netware dynamics.

v. Approve the full state synchronization between all oscillators.

3.8.1 Netware Structure sub systems:

The Netware oscillators implementing according to the following sub system:

i. Use single master oscillator as driver for all slaves' oscillators.

ii. Slave model changes initial condition to provide number of different master oscillators.

iii. Modified coupling sub system as block sub system to support the connection and coupling to all slaves oscillator blocks.

iv. Tuned scope components to be able to view the generated chaotic of each block of oscillators, (8) display channel in each scope.

3.8.2 Block structure:

Network consists of (32) block (block 1) up to (block 32). As in figure (3.13) each block consists of (8) oscillators as show in (fig3.14). (Block-1) contain (master oscillator) and (6) slave oscillators, so this block works as master driving block for all other block (2 up to 32). Each block accepts coupling factor(R) as the first input and (x1) as the second input from driving master (block-1),then produce (8) output as the chaotic signal from each of the (8) slave oscillators such as (block-2) in figure(3.10).

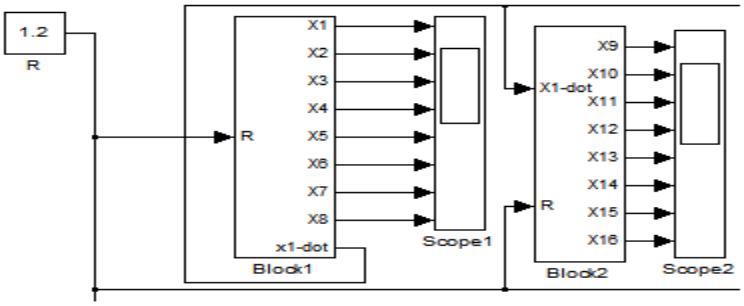

Figure 3-7 master block1 and other blocks interconnection

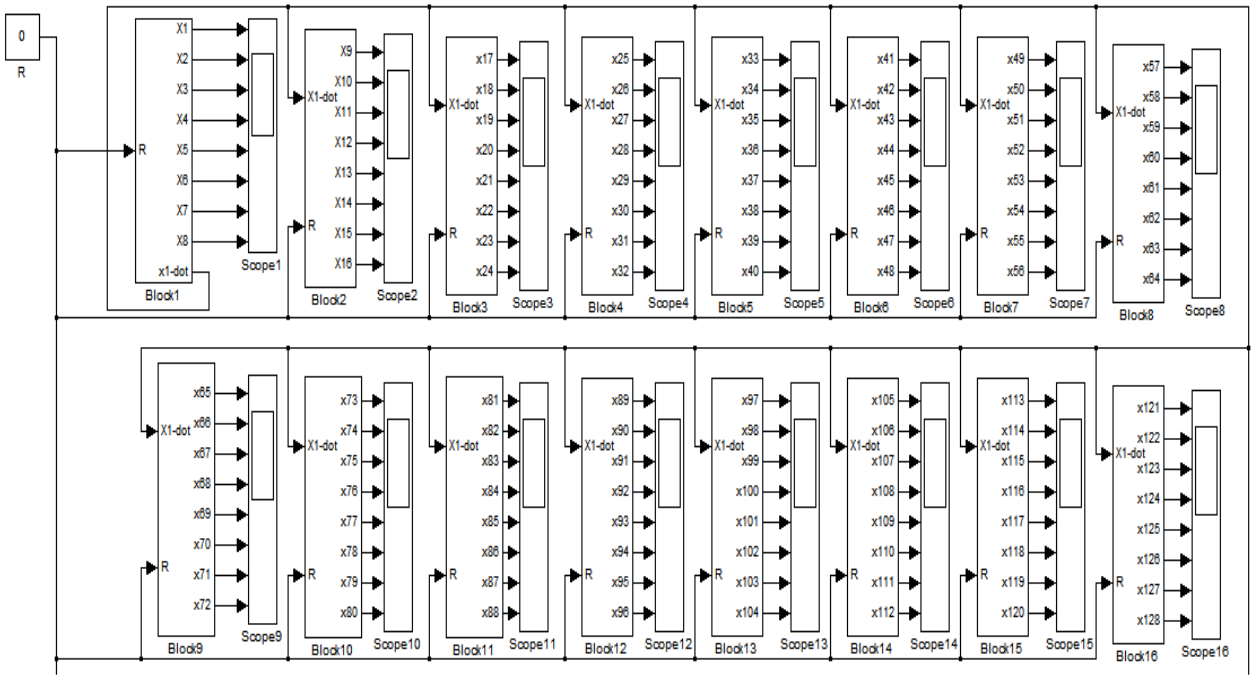

Figure 3-8 Netware Oscillator block 1-16

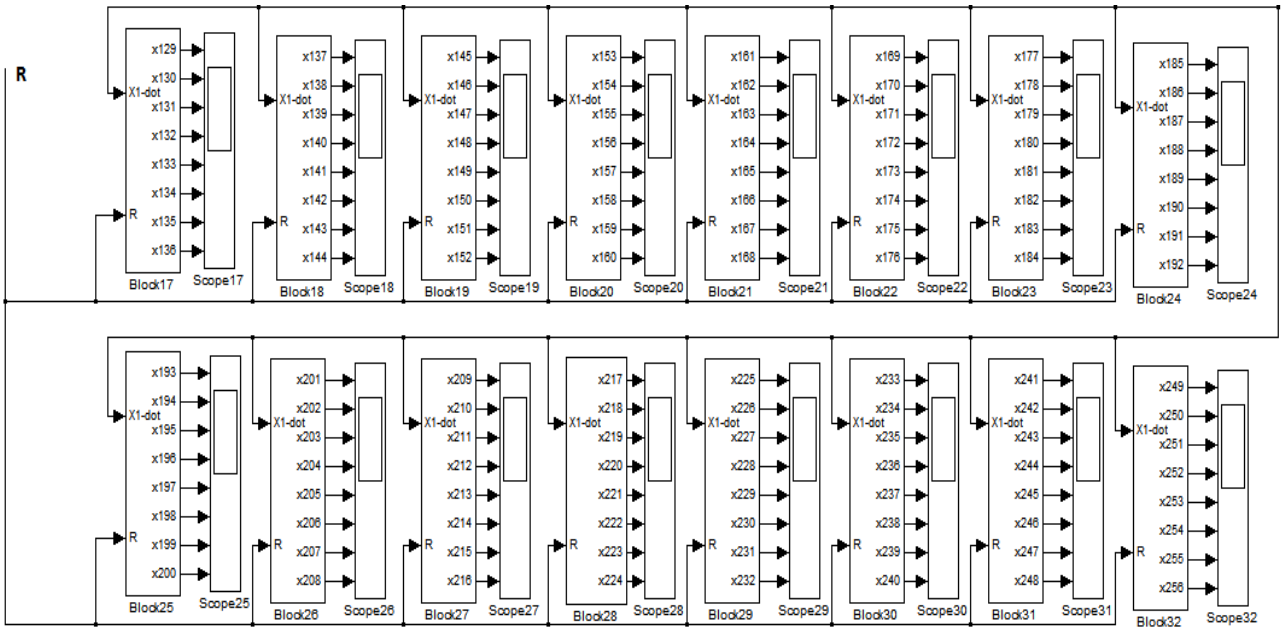

Figure 3-9 *Netware Oscillator block 17-32*

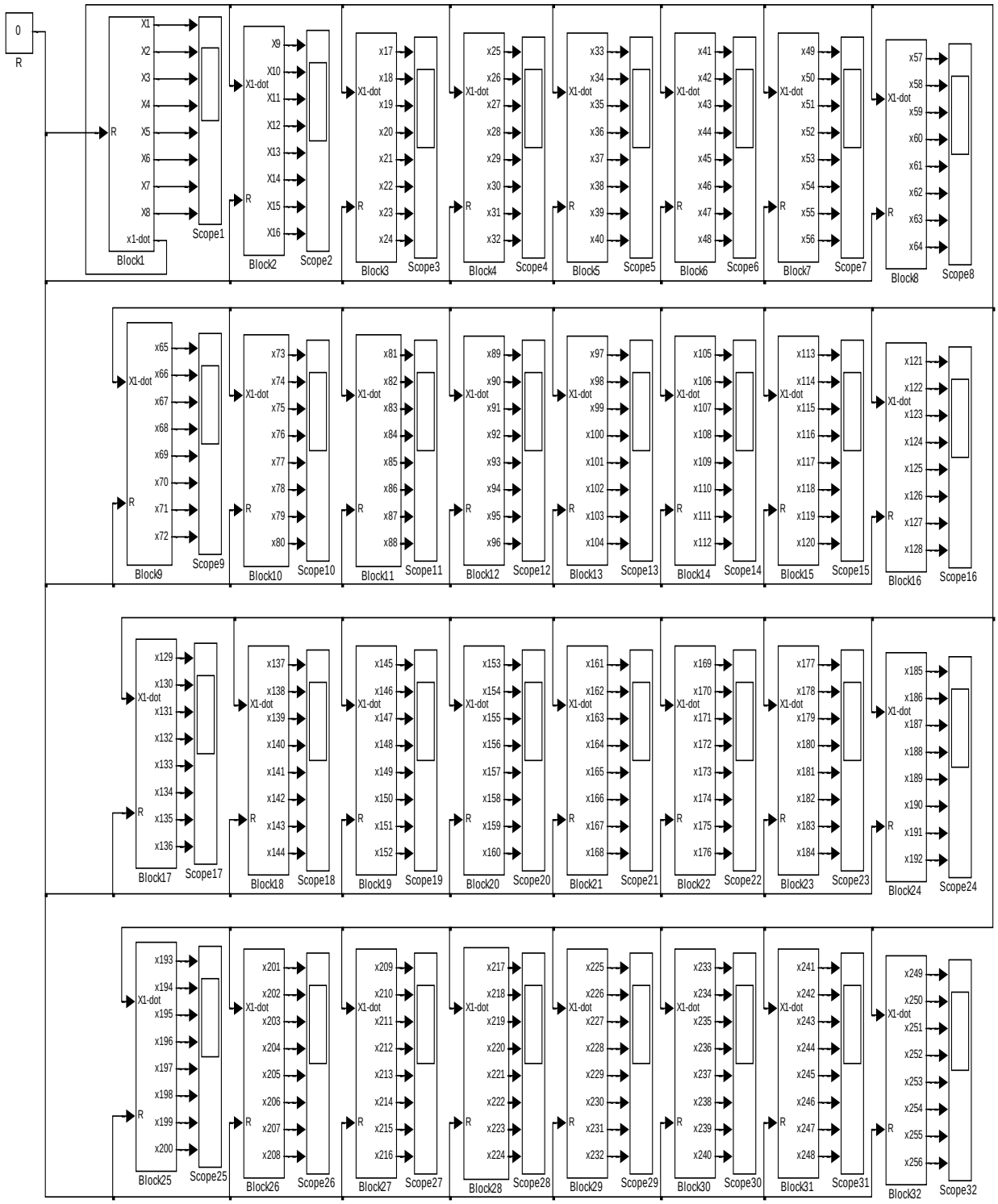

Figure 3-10 Netware oscillators all block model diagram

3.8.3 Master block interconnection:

The ***master oscillator*** provides two outputs port (**X1**) and (**X1-dot**) as in figure (3.14), the (7) ***Slave oscillators*** are connected to the master oscillator through (coupling sub system) block that provide unidirectional coupling configuration. The ***coupling sub system block*** connect to each slaves oscillator block as seen in figure (2.14) so the coupling subsystem figure(3.19) accepts three inputs this three input explain as follow :

1. The coupling factor (**R**): share and connected to all coupling sub systems.
2. **X1-dot** of master oscillator: share and connected to all coupling sub systems.
3. $\mathbf{X_n}$**-dot** of slave $_{\mathbf{n}}$: **n** is the number of slave oscillators.(1 up to 255).

So the coupling sub system provide one output that connected to each slave oscillators as coupling with the master oscillator named in block (**couple**).

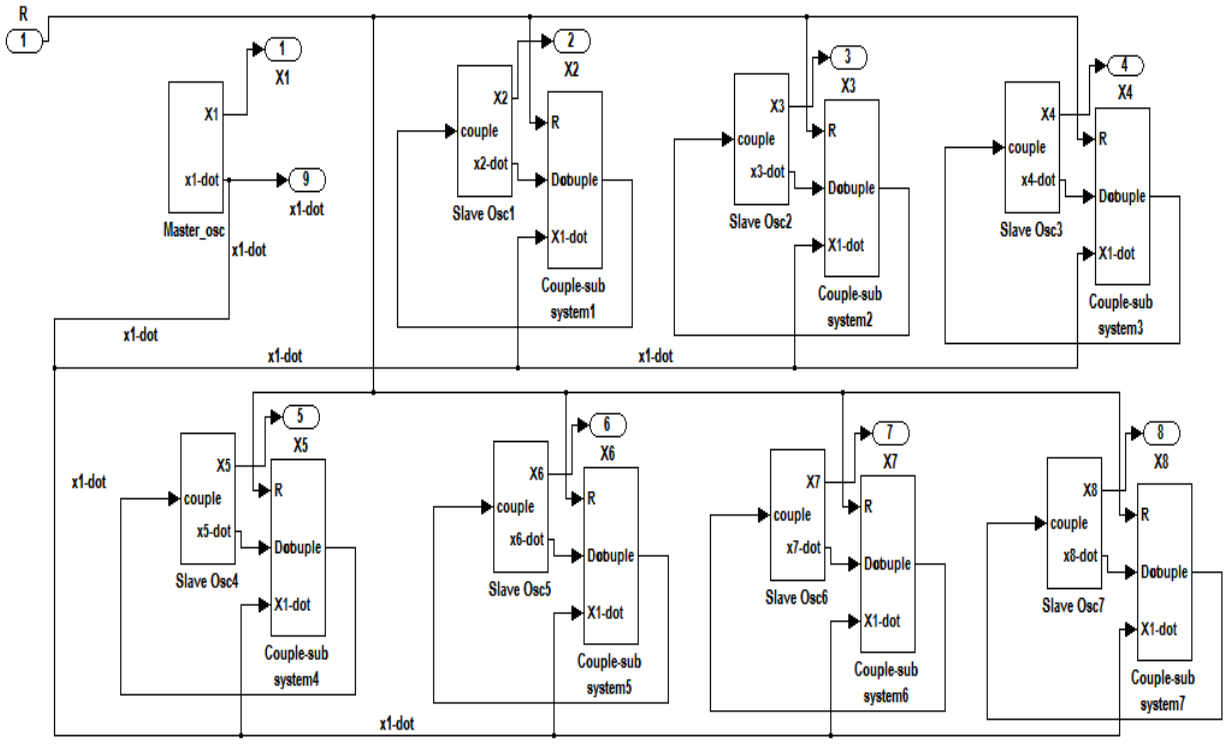

Figure 3-11 Block 1 internal structure diagram

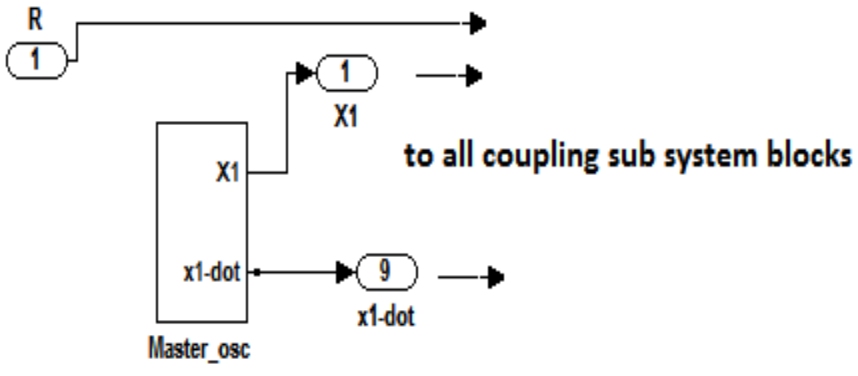

Figure 3-12 Master oscillator block connection Points

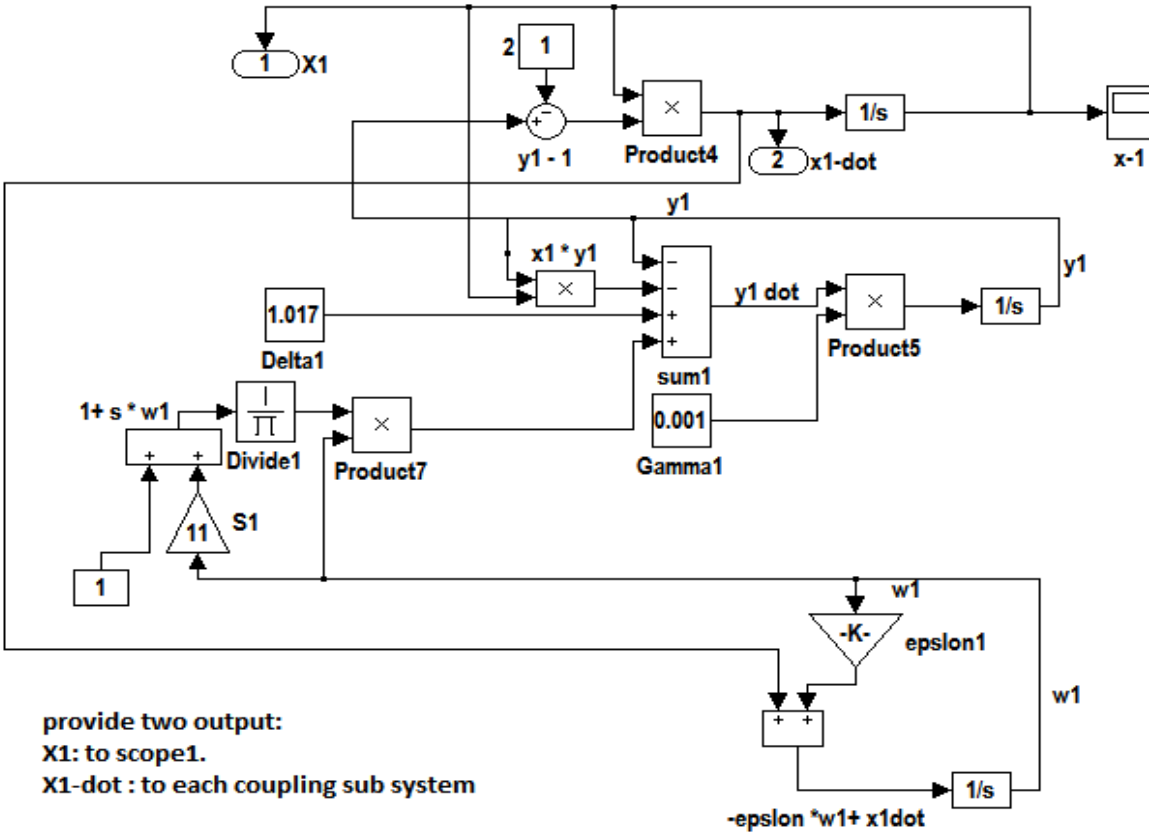

Figure 3-13 Master Oscillator internal components

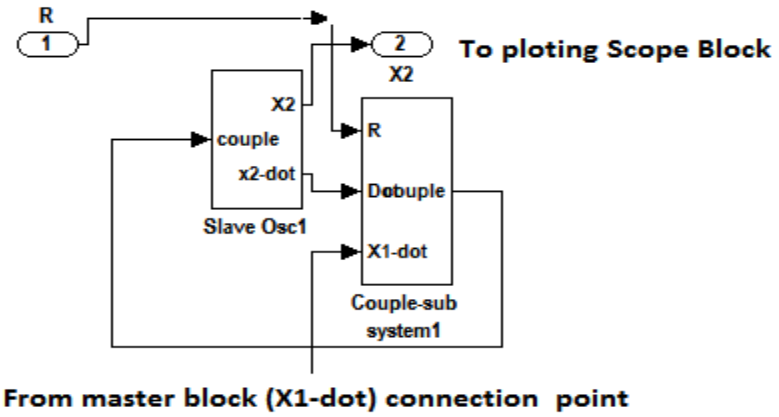

Figure 3-14 slave oscillator block connection Points

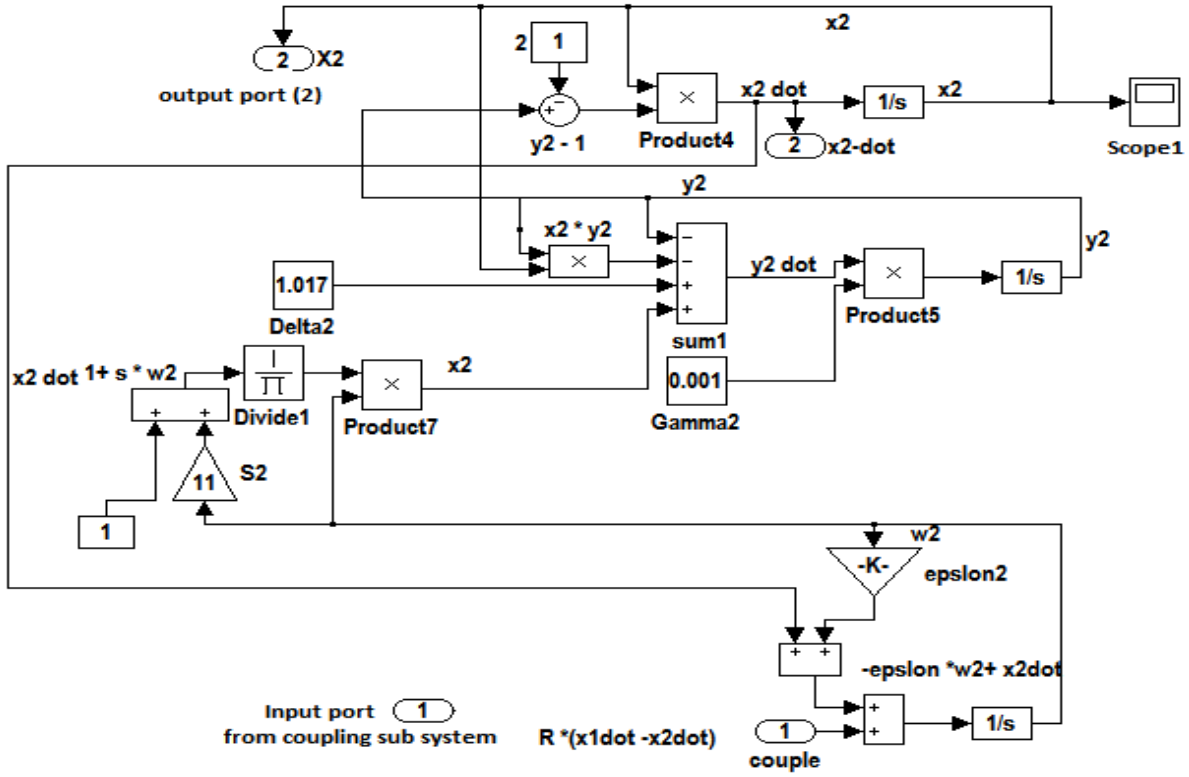

Figure 3-15 Master Oscillator internal components

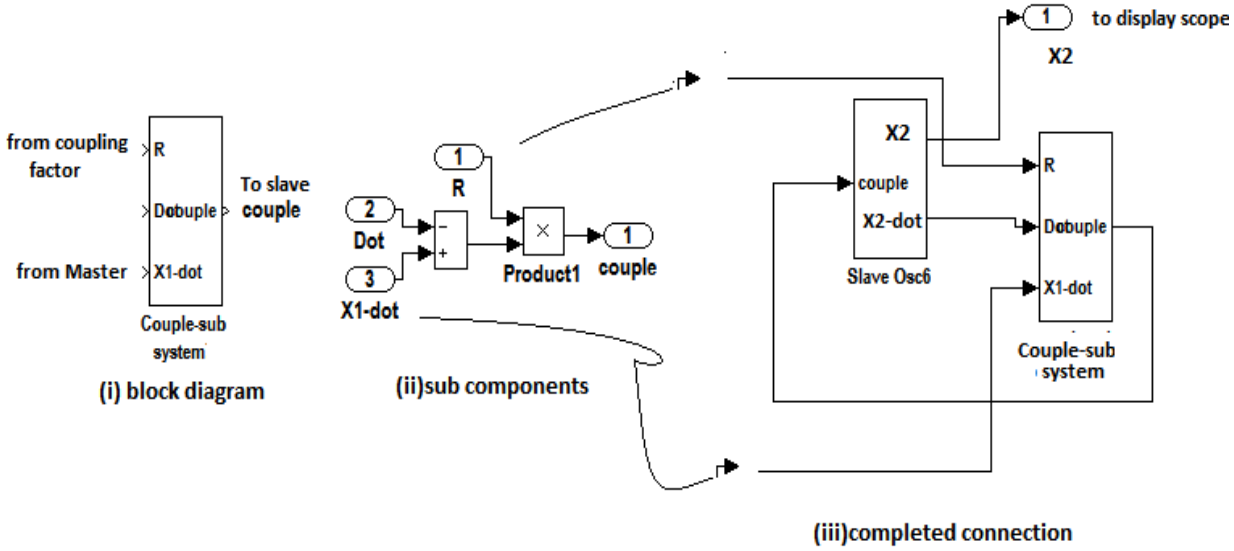

Figure 3-16 Coupling Sub System Details

4 Chapter – Four: Results and Discussion

4.1 Introduction:

The selected operation values and the other control parameters enables OEFSL simulation model and adapts its operation to simulate semiconductor laser with optoelectronic feedback actual physical system.

The simulation model dynamics explain due to the model results also the effects of bias current and feedback strength also have been demonstrated.

Results analysis based on the time series generated and the chaos regime through the model dynamics. The analysis concerns the study of the system attractors, the time series and the indicator of synchronization behavior.

4.2 The dynamics of semiconductor laser with optoelectronic feedback:

In this section system behavior and response demonstrated to explain the semiconductor laser with optoelectronics feedback.

The simulation model is running in different running modes as mention in chapter (3) section (3.6) then the dynamics of the system clear describe according to these different forms of result. The selected parameters and operation conditions values associated to each running modes mention as the table value for each case. The procedure steps for model run and results taken also are explained. The OEFSL model system structure implementing as a levels approach starting from the (single oscillator level), (two oscillators coupled level) and (Netware oscillator's level) so the result takes in each of these levels. The model parameters that use during running modes can be listed as follow:

- γ :The population inversion relaxation rate, at the model(Gama).
- δ_0 : Bias current, at the model (delta).
- ε : Feedback strength, at the model (epsilon).
- Initial states.(x_0, y_0, w_0).
- Simulation Time Interval.

4.2.1 Procedure and steps:

i. Single oscillator:

The operation and setting values defined by the parameters γ, δ_0, ε, initial condition and simulation time interval are selected as in table (4.1). The model system toggle between the steady state and the chaotic spiking the system passes through a period and period doubled and chaotic. The time series and system attractors illustrate this transition and dynamics as in results forms.

Table 4-1 Single oscillator operation value

Parameters	**Time (second)**	**Pop-inverse Gama (γ)**	**Bias current Delta(δ_0)**	**Feedback strength(ε)**	**S**	**Initial state**		
						X0	**Y0**	**W0**
Values	50000 - 600000	1*10-12	1.015;1017	0	11	0.022	1	0.005

The procedure running mode use the operation the value in table(4.1) as fixed values then vary the *feedback strength*(ε) and get model results as seen below:

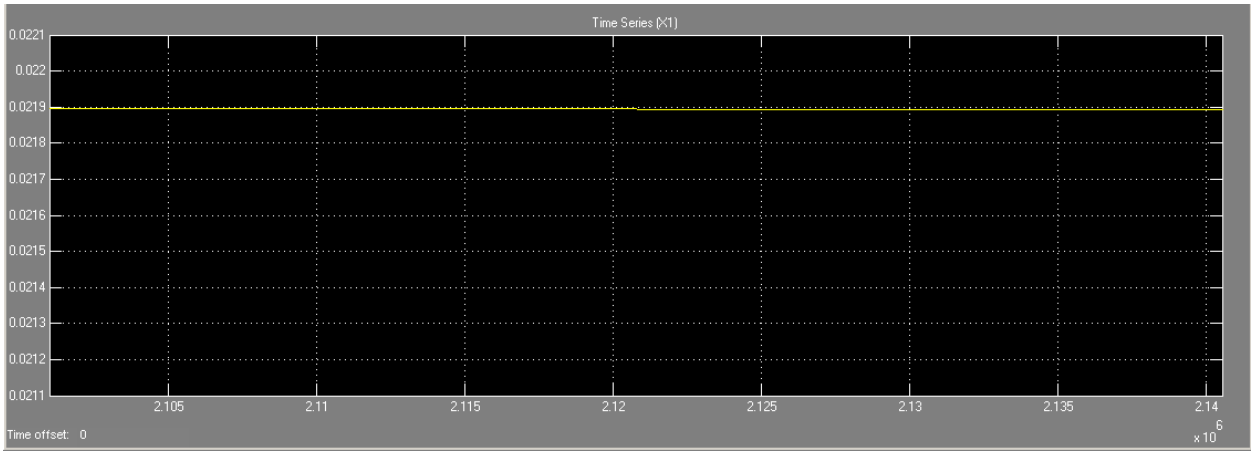

Figure 4-1- time series (x1) when the *feedback strength* (**ε**) =0, **δ0**=1.015

The time series in (figure 4-1(a)) describe the steady state (no oscillation)

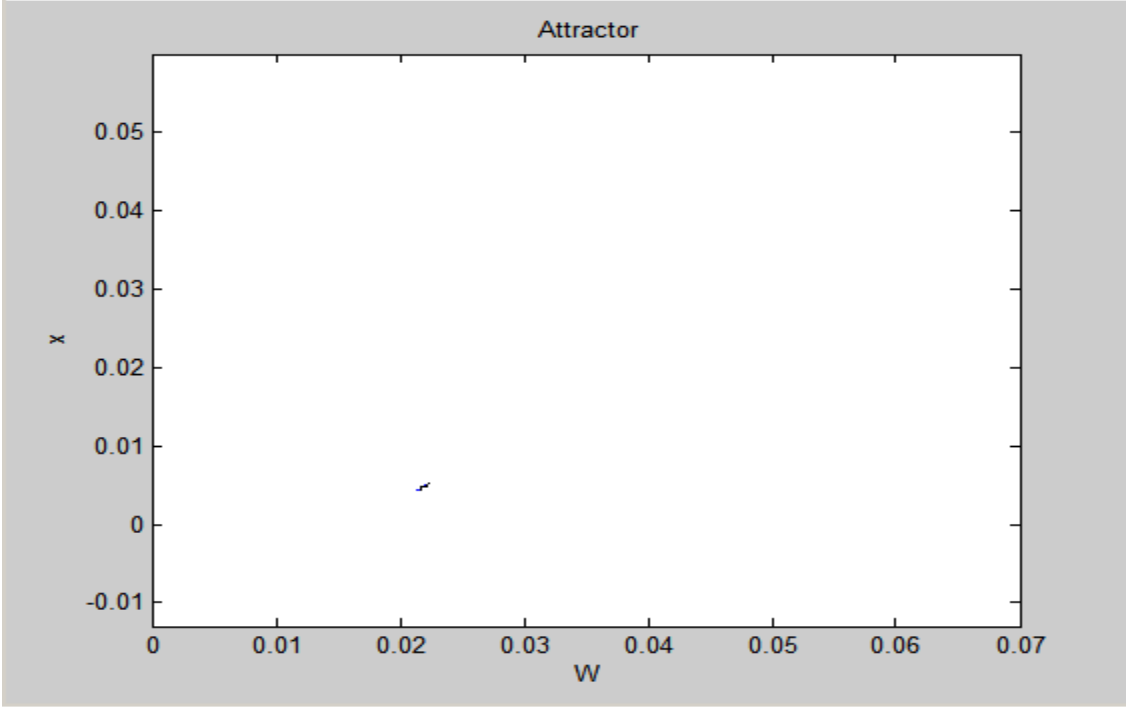

Figure 4-2 : (2- D attractor when the feedback strength (ε) =0, δ0=1.015)

The time series in (figure 4-1(b)) describe the steady state (no oscillation)

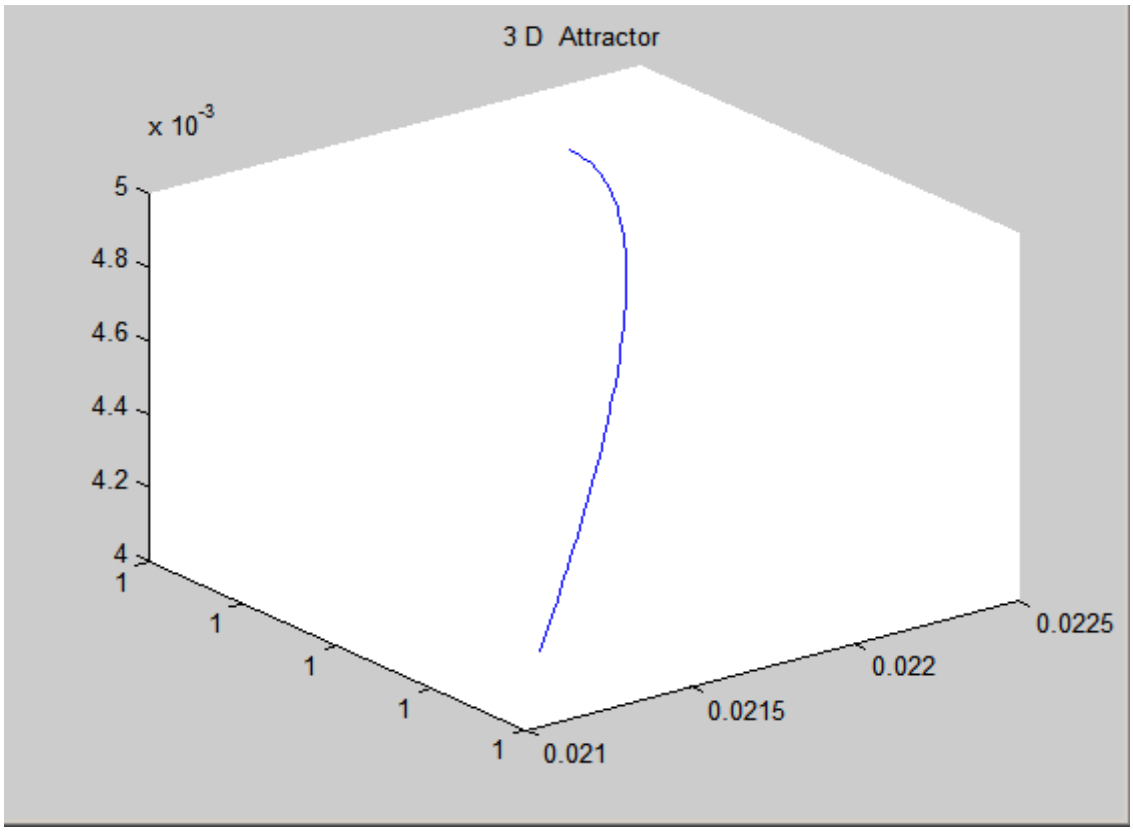

Figure 4-3 : 3- D attractor when the feedback strength (ε) =0, δ0=1.015

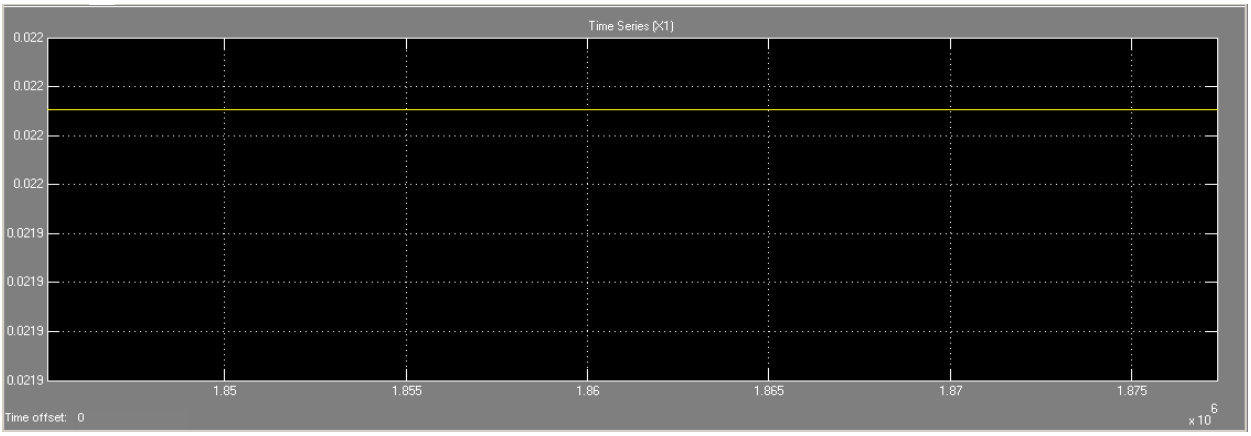

Figure 4-4 : Time series (x1) when the feedback strength (ε) =0, δ0=1.017

The time series in (figure 4-1(d)) describe the steady state (no oscillation)

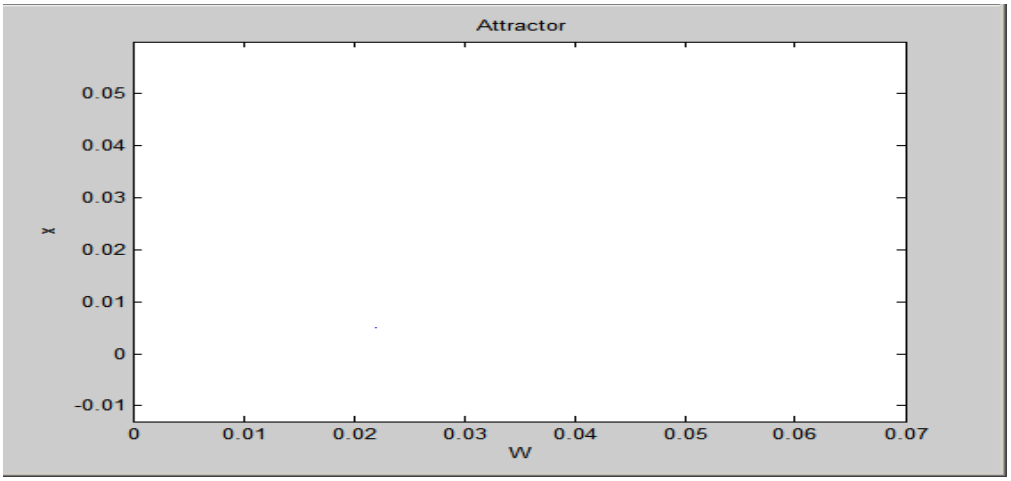

Figure 4-5 : 2-D attractor when the feedback strength (ε) =0, δ0=1.017

2-D attractor in (figure 4-5) describe the steady state (no oscillation)

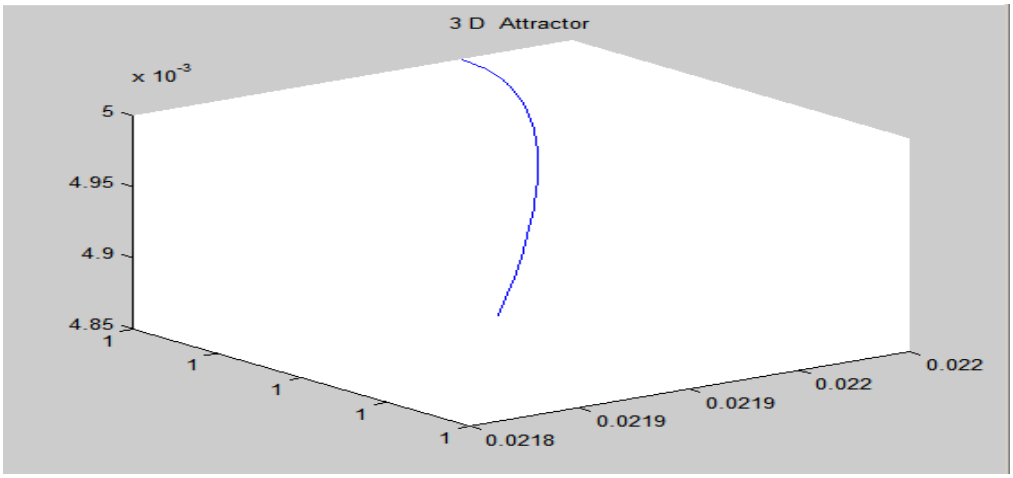

Figure 4-6 : 3-D attractor when the feedback strength (ε) =0, δ0=1.017

Table 4-2 Single oscillator operation value

Parameters	**Time (second)**	**Pop-inverse Gama (γ)**	**Bias current Delta(δ_0)**	**Feedback strength(ε)**	**S**	**Initial state**		
						X0	**Y0**	**W0**
Values	50000 - 1200000	1*10-3	1.015	-0.5e-5 ; -1.5e-5	11	0.022	1	0.005

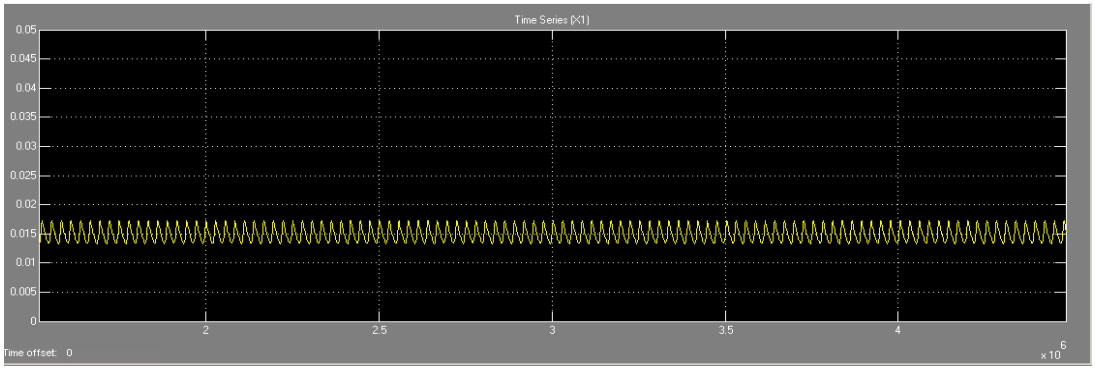

Figure 4-7 : Time series (x1) when the *feedback strength* (**ε**) = ($-0.5*10^{-5}$)

The time series in (figure 4-2(a)) describe the periodic state (oscillation) when (**ε**) increased

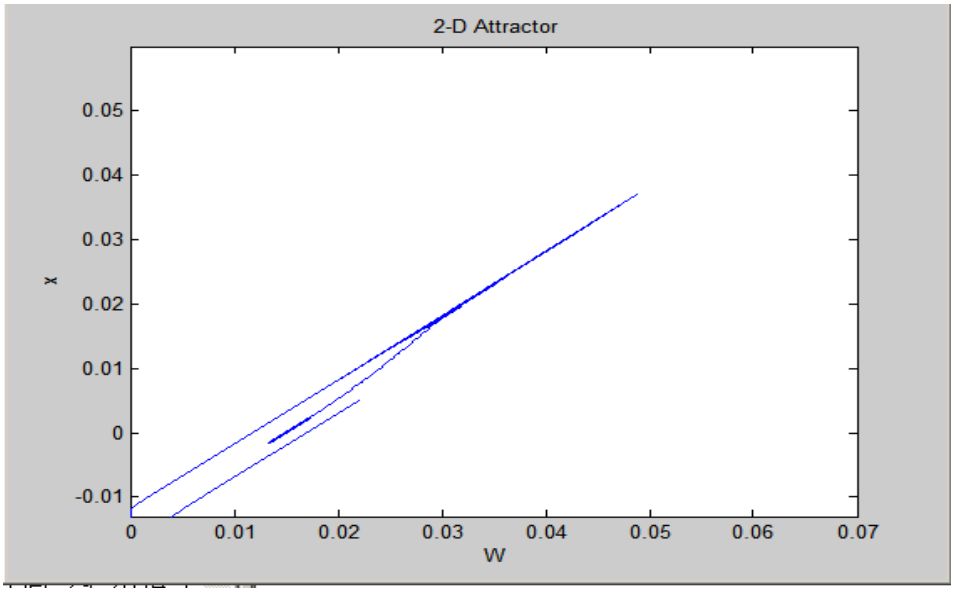

Figure 4-8 : 2-D attractor when the *feedback strength* (**ε**) = ($-0.5*10^{-5}$)

The time series in (figure 4-2(b)) describe the periodic state (oscillation) when (**ε**) increased

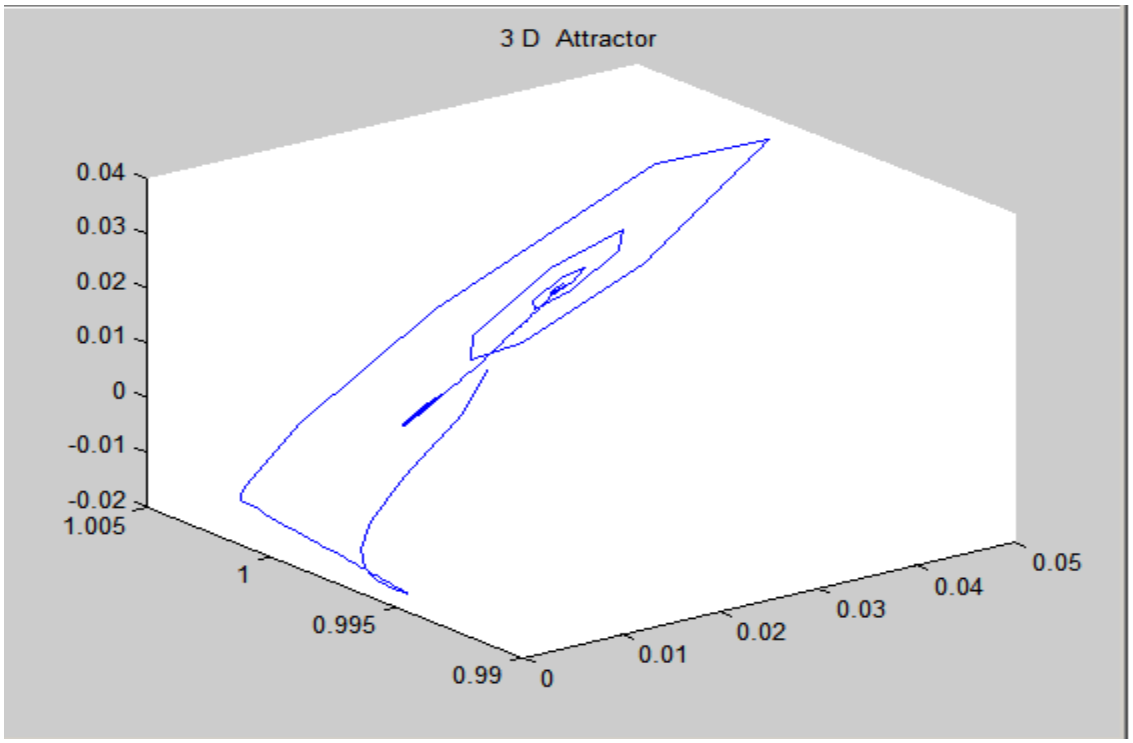

Figure 4-9 : 2-D attractor when the feedback strength (ε) = (-0.5*10-5)

The time series in (figure 4-2(c)) describe the periodic state (oscillation) when (**ε**) increased

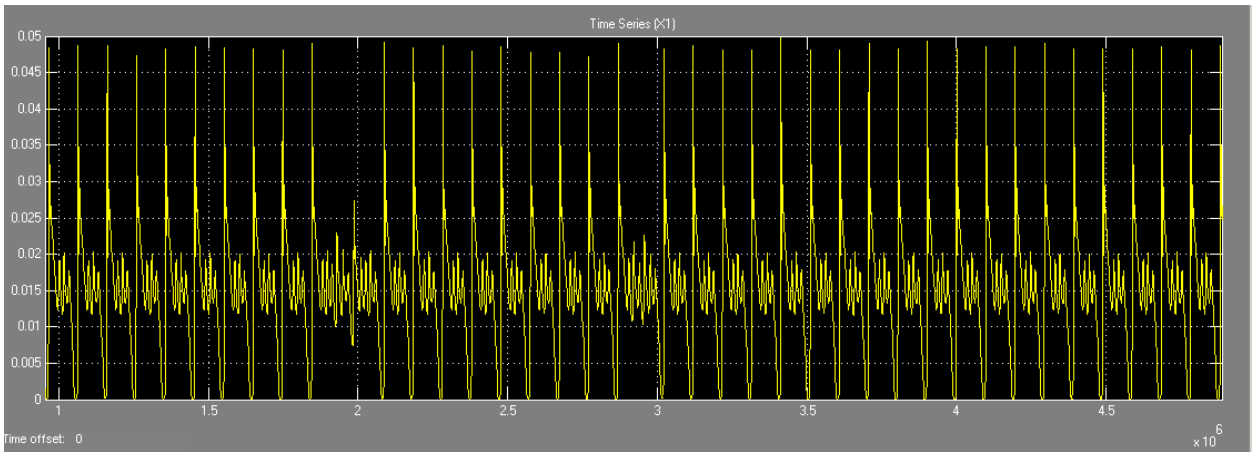

Figure 4-10 : Time series when the feedback strength (ε) = (-1.5*10-5)

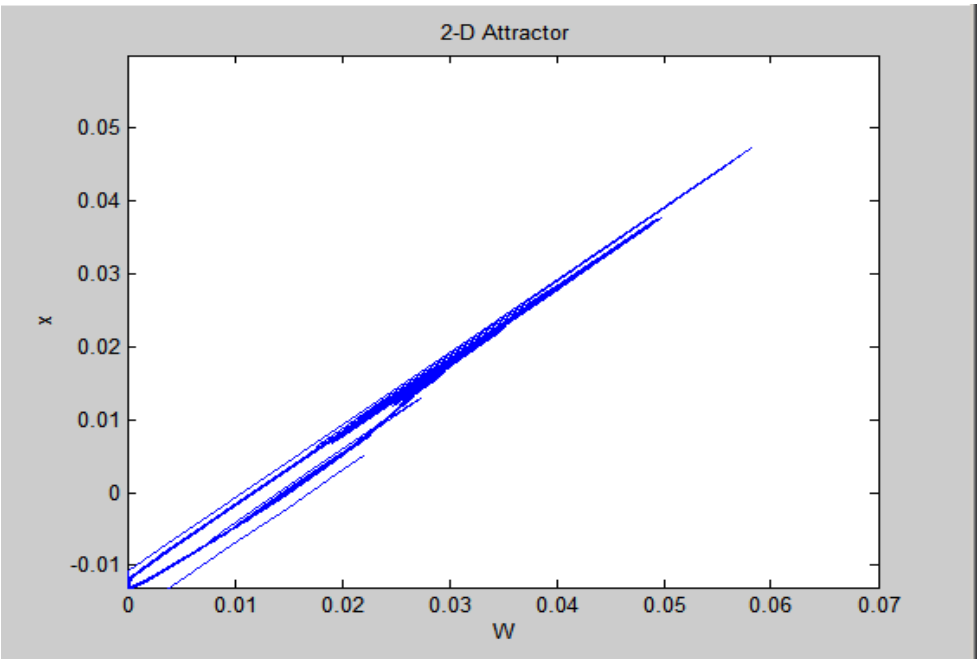

Figure 4-11 : 2-D attractor when the feedback strength (ε) = (-1.5*10-5)

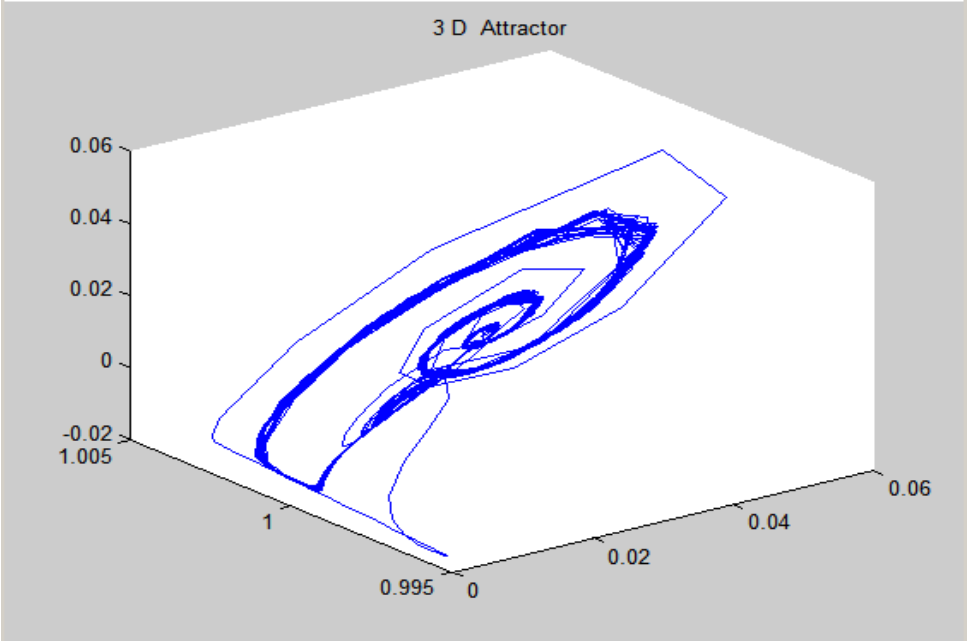

Figure 4-12 : 3-D attractor when the feedback strength (ε) = (-1.5*10-5)

Table 4-3 Single oscillator operation value

Parameters	Time (second)	Pop-inverse Gama (γ)	Bias current Delta(δ_0)	Feedback strength(ε)	S	Initial state		
						X0	Y0	W0
Values	50000 - 600000	2*10-9	1.017	$3*10^{-5}$	11	0.022	1	0.005

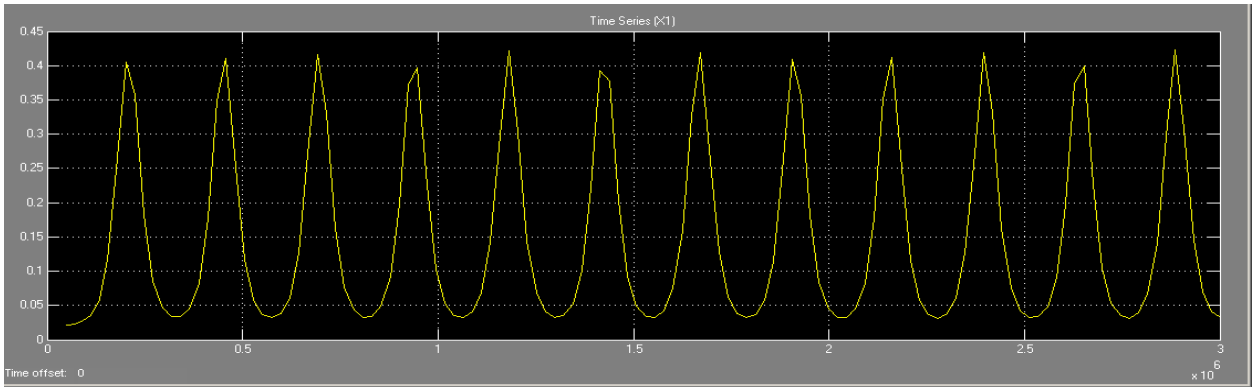

Figure 4-13 : Time series when the *feedback strength* (ε) increase to = $3*10^{-5}$

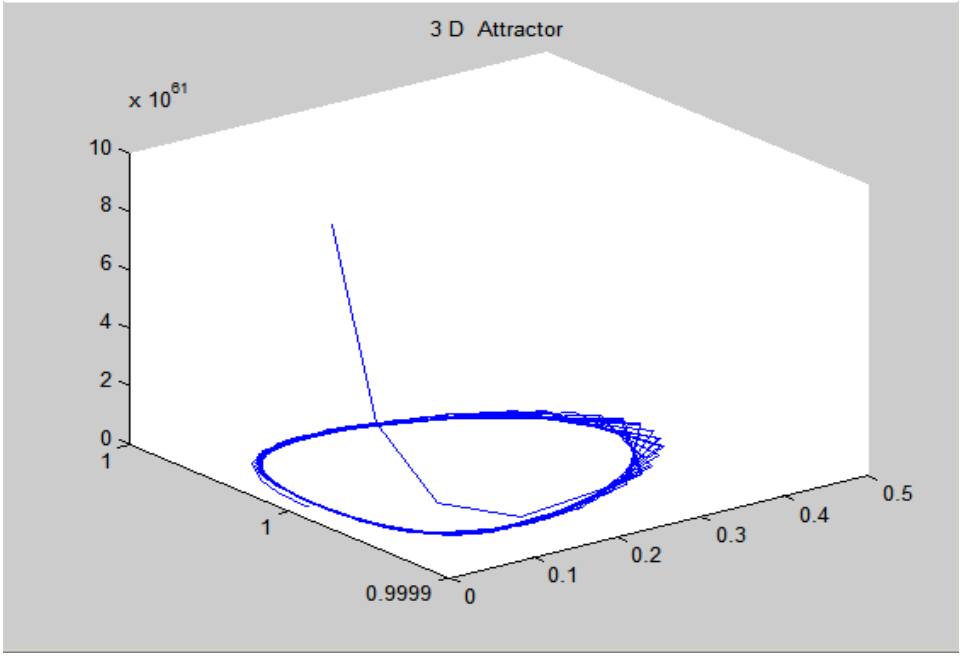

Figure 4-14 : 3-D attractor the feedback strength (ε) increase to = 3*10-5

Table 4-4 Single oscillator operation value

Parameters	**Time (second)**	**Pop-inverse Gama (γ)**	**Bias current Delta(δ_0)**	**Feedback strength(ε)**	**S**	**Initial state**		
						X0	**Y0**	**W0**
Values	50000 - 1200000	1*10-3	1.03,1.04,1.06	-2e-5	11	0.022	1	0.005

The procedure running mode use the operation the value in table(4.4) as fixed values then vary the bias current (δ_0) and get model results as seen below:

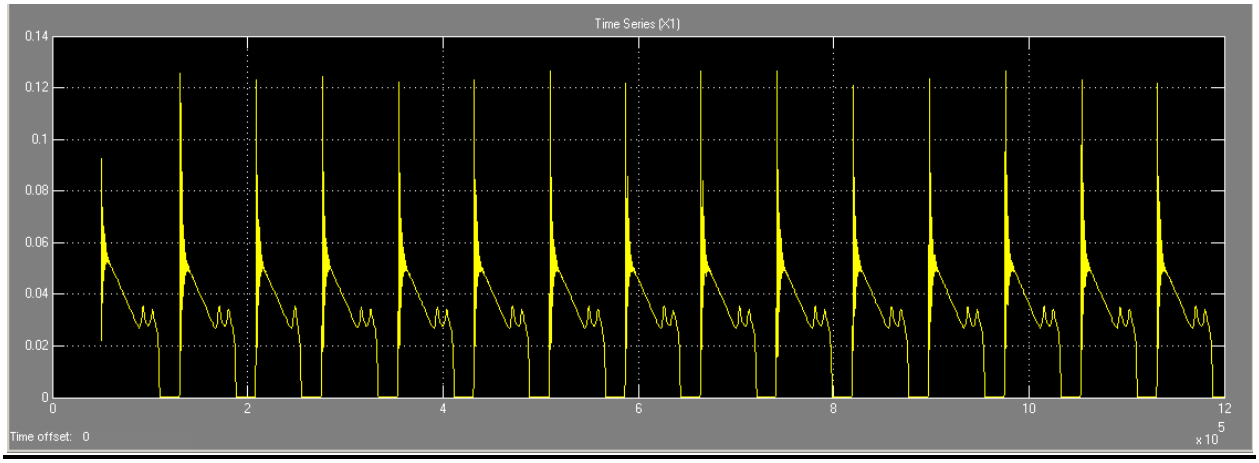

Figure 4-15 : Time series (x1) when the bias current (δ0) =1.03

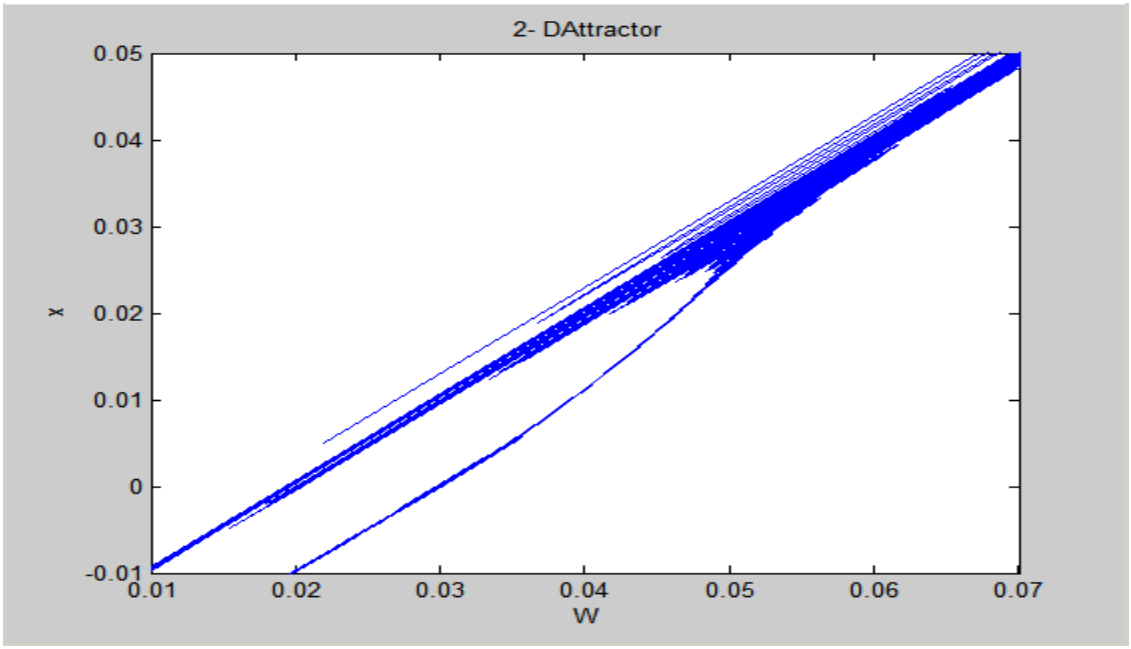

Figure 4-16 : 2-D attractor when the bias current (δ0) =1.03

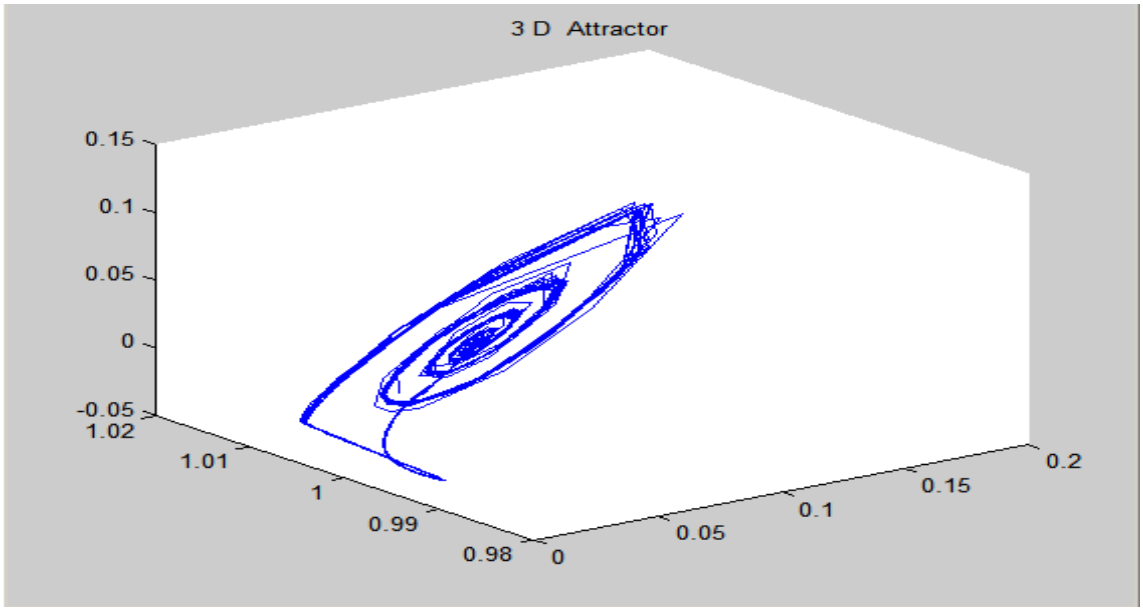

Figure 4-17 : 3-D attractor when the bias current (δ0) =1.03

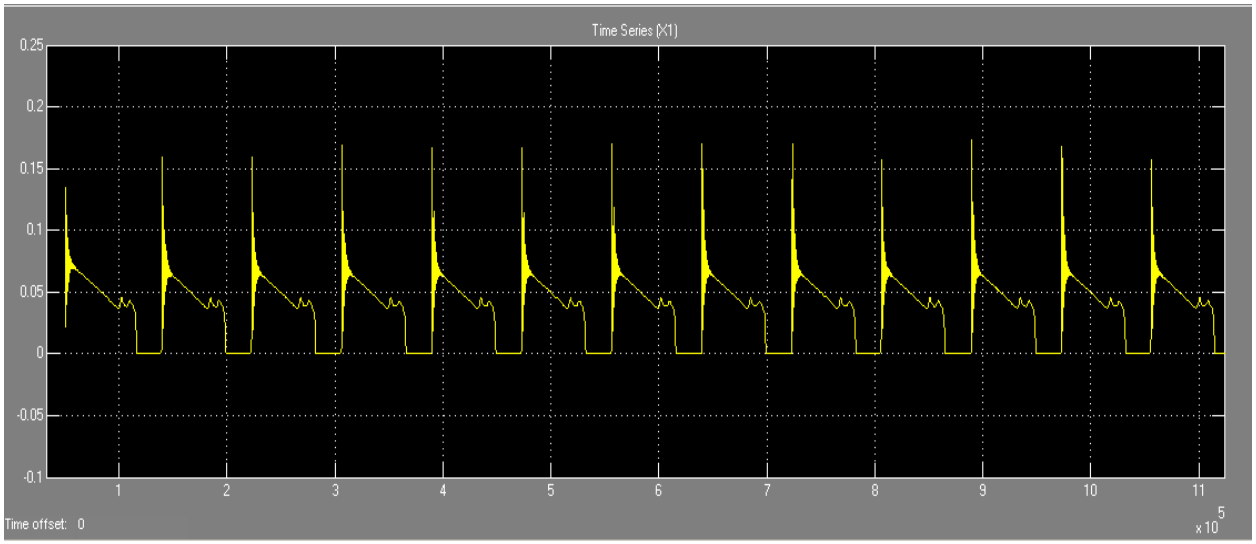

Figure 4-18 : Time series (x1) when the bias current (δ0) =1.04

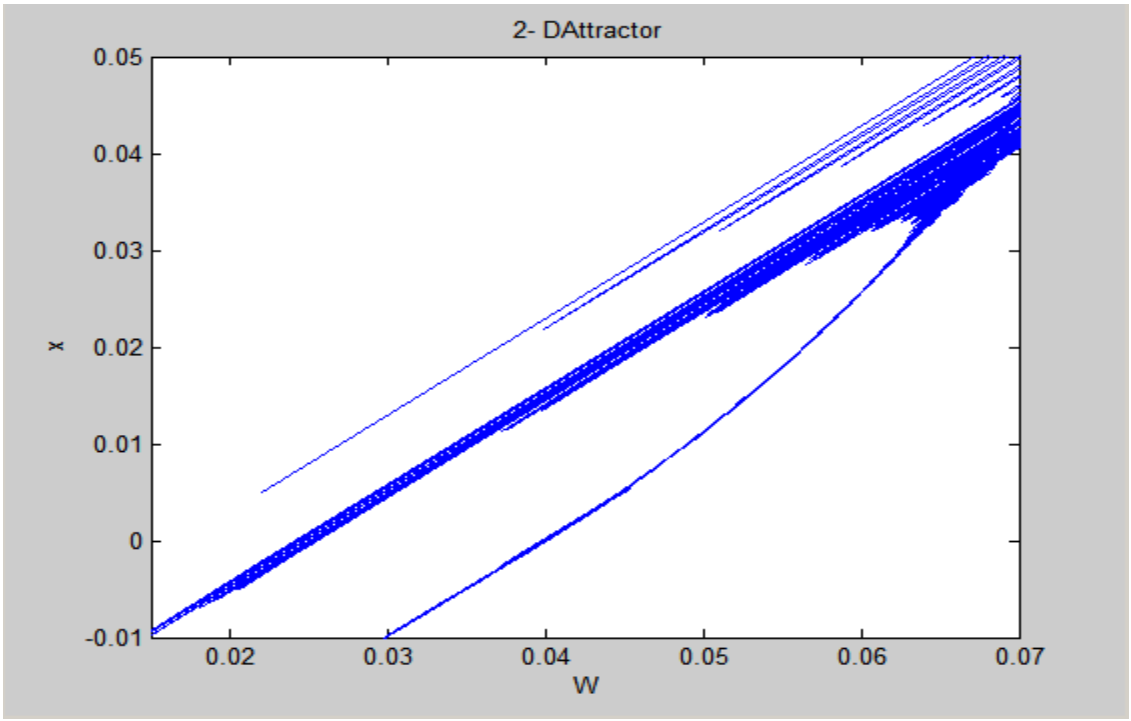

Figure 4-19 : 2-D attractor when the bias current (δ0) =1.04

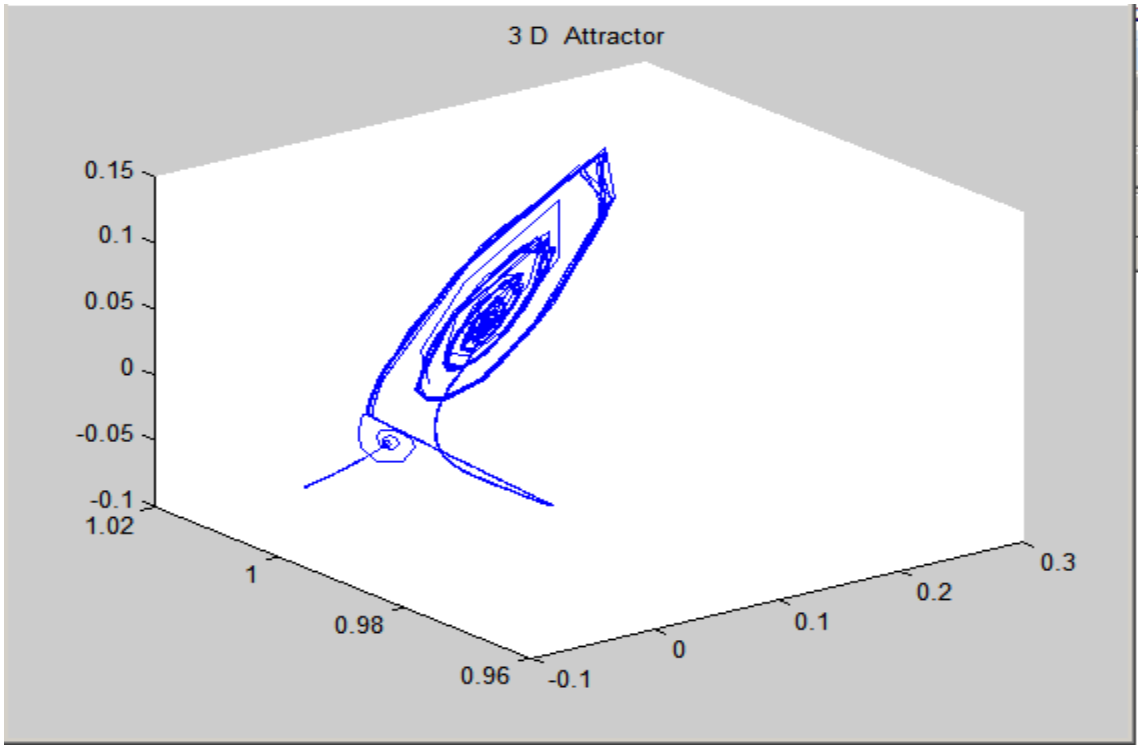

Figure 4-20 : 3-D attractor when the bias current (δ0) =1.04

4.3 Single Oscillator result discussion:

Therefore due to the model results as show in result forms figure (4.1) up to figure (4.4), the system model approves and matches the theoretical concepts of the chaos generation and SL with OEFD in contact of the following dynamics features due to the model parameters and setting:

- **i.** Steady state.
- **ii.** Periodic state
- **iii.** Chaotic state

a) The effect of the feedback strength (ε) in chaos generation when the bias current (δ0) is fixed as in table (4.1) so:

i. The steady state appears when (ε=0) as seen in figure (4.1- a, d).

ii. The periodic state with low amplitude appears when (ε) increases to (-0.5*10-5) as seen in figure (4.2-a).

iii. The chaotic state appears with high and low spikes when (ε) increases to (1.5*10-5) as seen in figure (4.2-d).

iv. So the feedback strength (ε) cause the model to be transition from steady state to periodic state and chaotic stat respectively when (ε) increased and other parameters not change .

b) The effects of the bias current(δ0) in chaos generation and model dynamics seen as results form (4.4) that base on table(4.4) when feedback strength (ε)

Fixed to (-2*10-5) and bias current (δ0) changes to (1.03) and (1.04) in this case as seen in results forms in figure changes bias current to (1.03) resulting regular chaotic clearly when more increase to bias currents cause the generated chaotic spike to be smooth and regular as in figure(4.4- d)

ii. Unidirectional Coupling Configuration:

As mention in chapter (3) section (3.6.1) and (3.6.2) the model had been setting according to the selected values and then the mode of operation also be determine as follow:

Model running modes are:

1. Free Running Mode (FRM).

The Selected operation value for both the master and slave oscillator mention in table (5.5) and the free running mode (FRM) determine by the coupling factor (R) as mention in chapter (3)table (table 3.1) .

Table 4-5 Single oscillator operation value

Parameters	**Time In (second)**	**Parameters**	**Gama**	**Delta**	**Epsilon**	**S**	**Initial state**		
							X0	**Y0**	**W0**
Master Osc	**0 - 3000000**	**Master Osc**	**0.001**	**1.017**	**-2e-5**	**11**	**0.022**	**1**	**0.005**
Slave Osc		**Slave Osc**	**0.001**	**1.017**	**-2e-5**	**11**	**0.022100**	**1**	**0.0051**

The two oscillators are setting as in table (4.5) and the coupling factor set to (0) to select free running mode as model design and then results appear as follow:

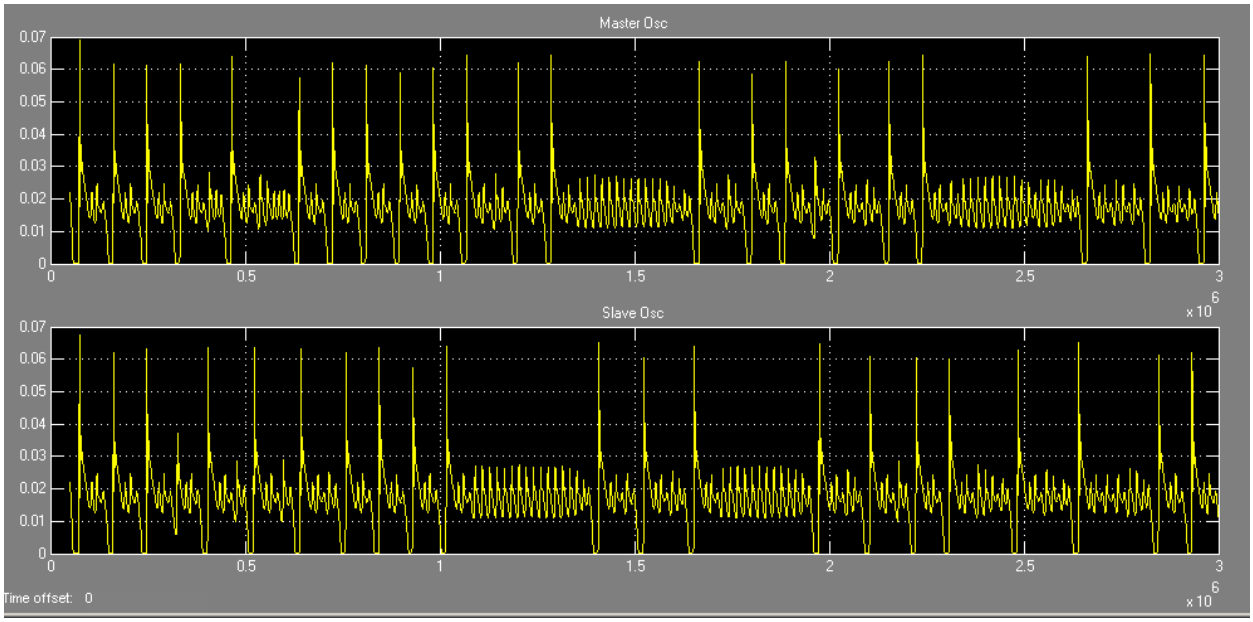

Figure 4-21 Time series for the master (upper) and slave (lower) oscillator

In free running mode when (R=0)

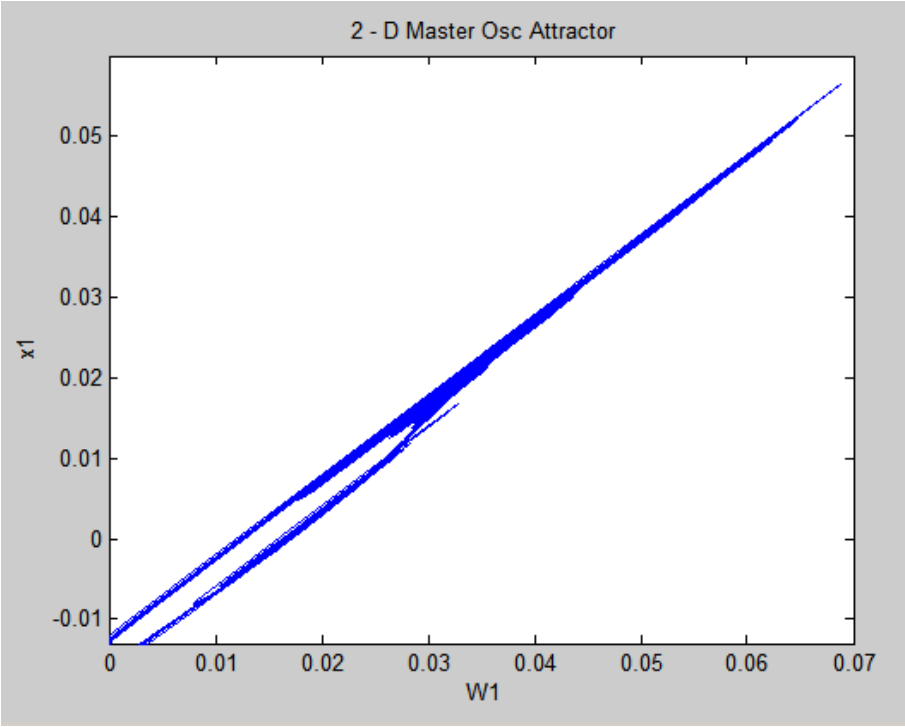

Figure 4-22 : 2-D master oscillator attractor in Free running mode when (R=0)

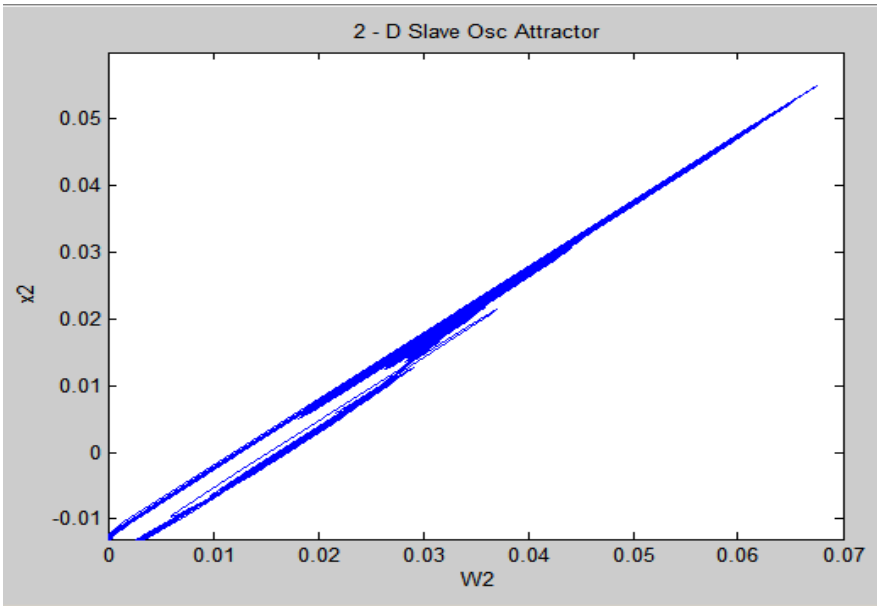

Figure 4-23 : 2-D slave oscillator attractor in Free running mode when (R=0)

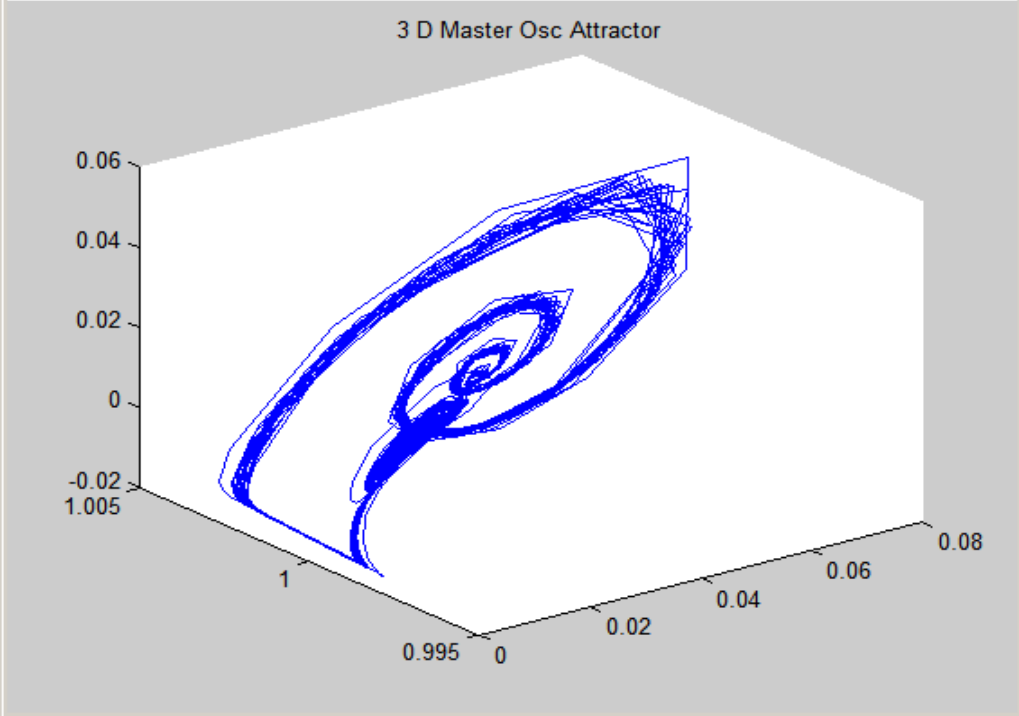

Figure 4-24 : 3-D master oscillator attractor in Free running mode when (R=0)

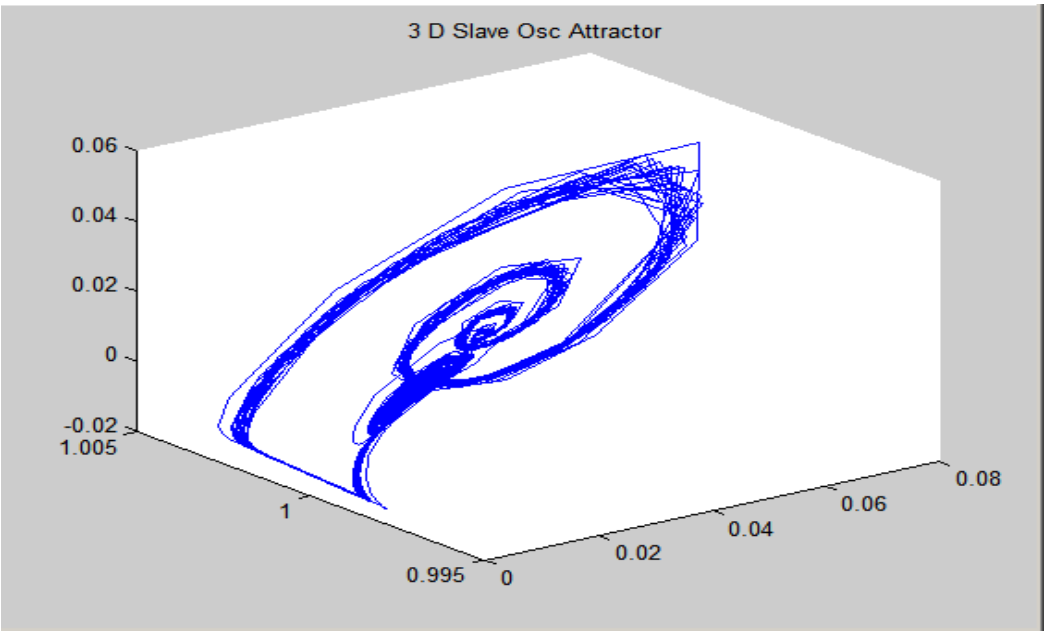

Figure 4-25 : 3-D slave oscillator attractor in Free running mode when (R=0)

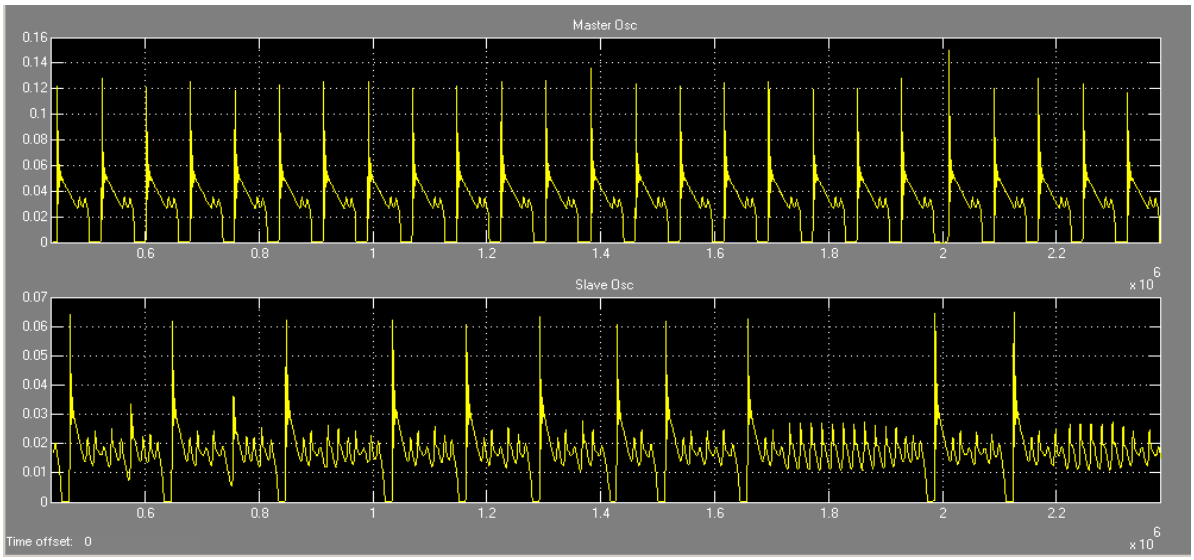

Figure 4-26 : Time series for the master (upper) and slave (lower) oscillator

In (FRM), when (R=0) Master Osc **(*δ0*)** change to (1.03)

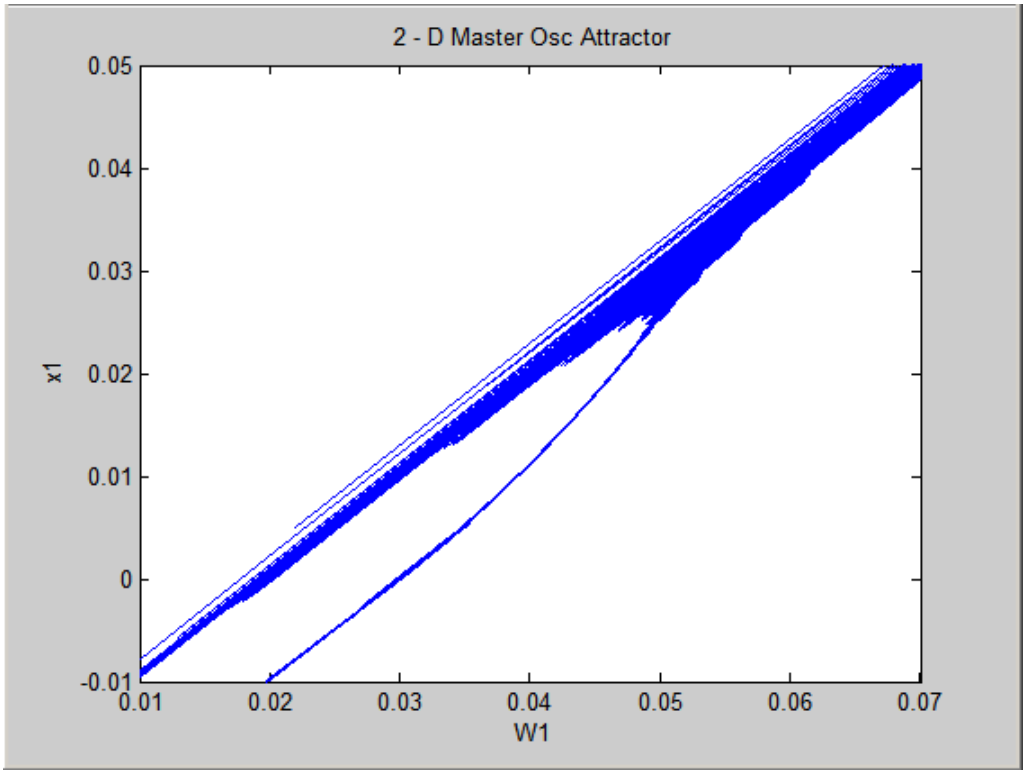

Figure 4-27 : 2-D master oscillator attractor in (FRM) when (R=0)

And master Osc **(δ_0)** change to (1.03)

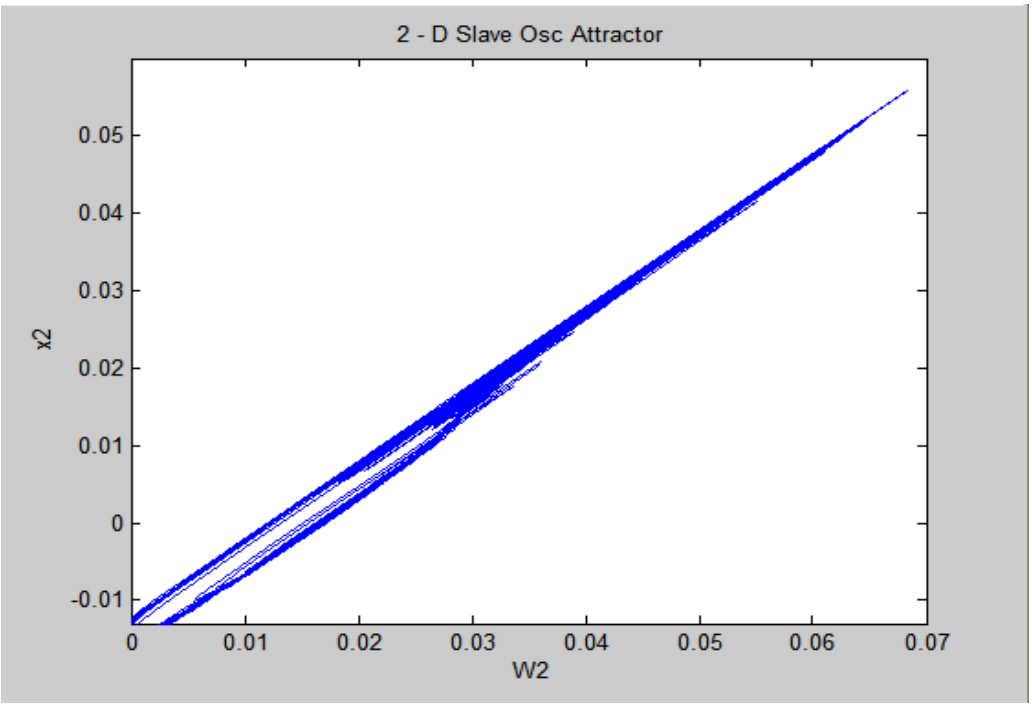

Figure 4-28 : 2-D master oscillator attractor in (FRM) when (R=0)

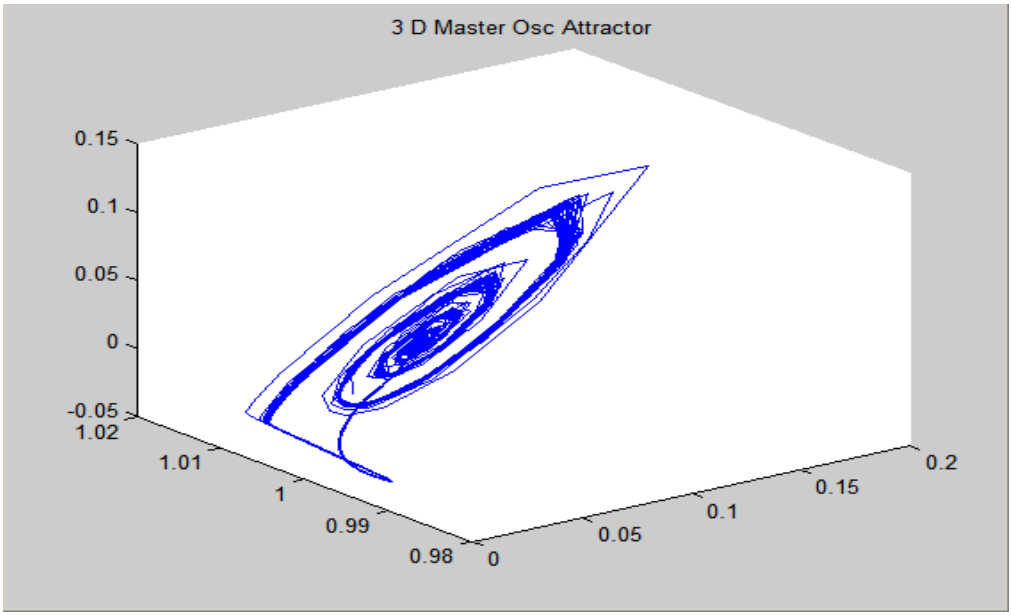

Figure 4-29 : 3-D master oscillator attractor in (FRM) when (R=0) and Master Osc **(δ_0)** change to (1.03)

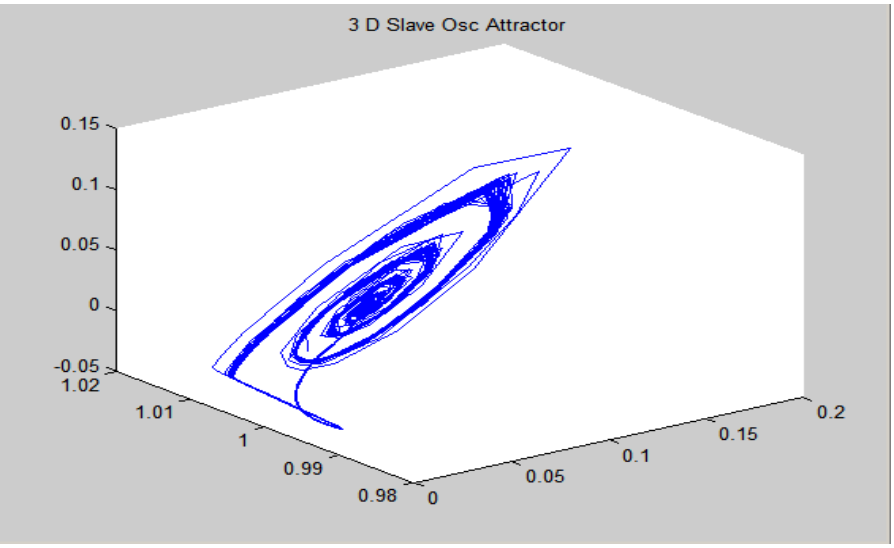

Figure 4-30 : 3-D slave oscillator attractor in (FRM) when (R=0)

2. Coupling Running Mode (CRM).

Now the model is running with same values as in (FRM) as mention in table (4.1) up to table (4.5) respectively except the coupling factor value that changes from (R=0) to (R not equal 0) so in this condition the model runs in coupling running mode and the master oscillator drive the slave oscillator as in the following result forms.

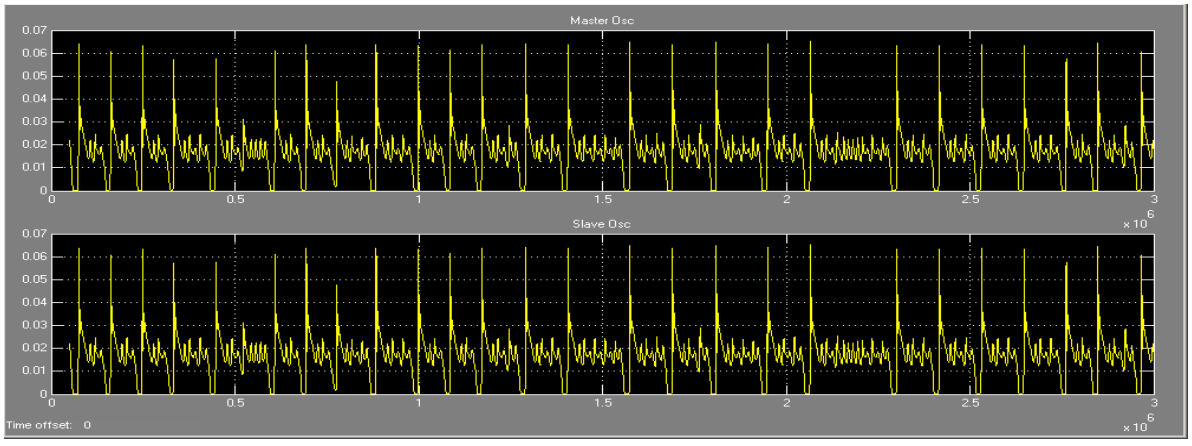

Figure 4-31 : Time series for the master (upper) and slave (lower) oscillator

In (CRM), when (R=0.02)

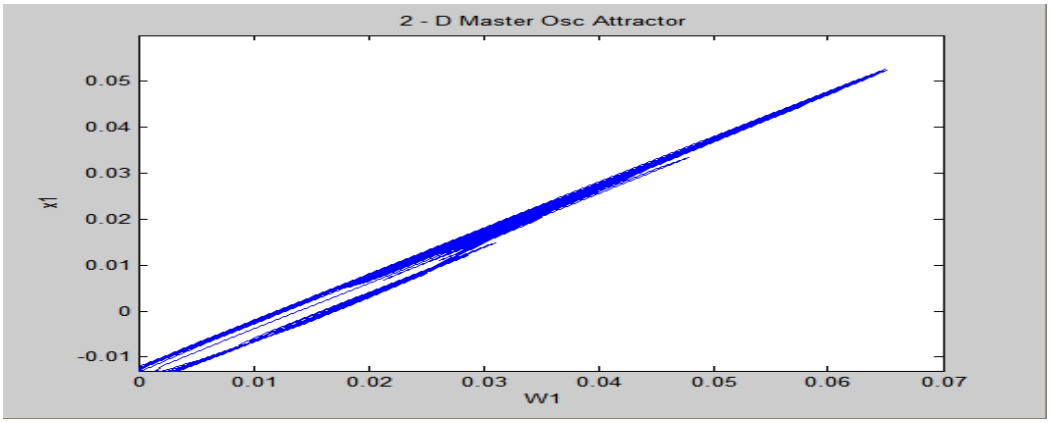

Figure 4-32 : 2-D master oscillator attractor in (CRM) when (R=0.02)

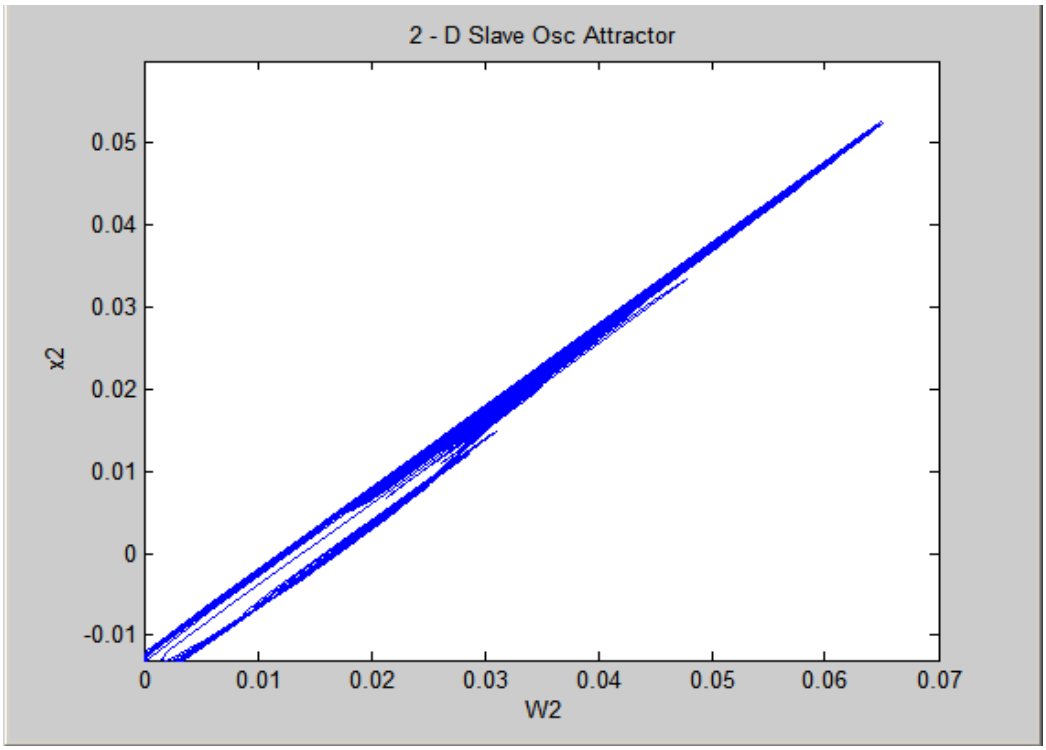

Figure 4-33 : 2-D slave oscillator attractor in (CRM) when (R=0.02)

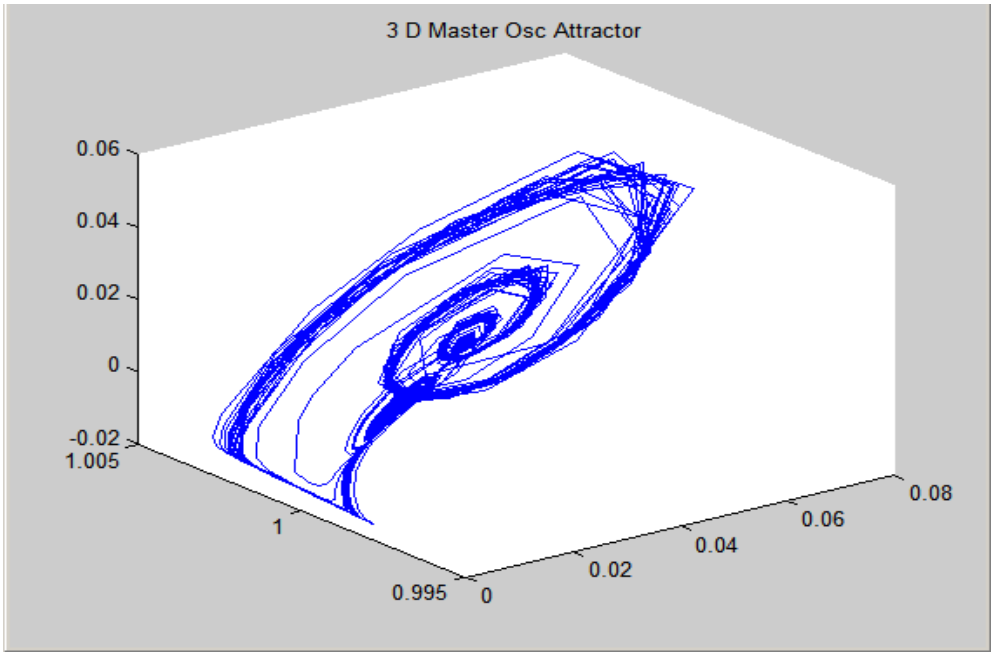

Figure 4-34 : 3-D master oscillator attractor in (CRM) when (R=0.02)

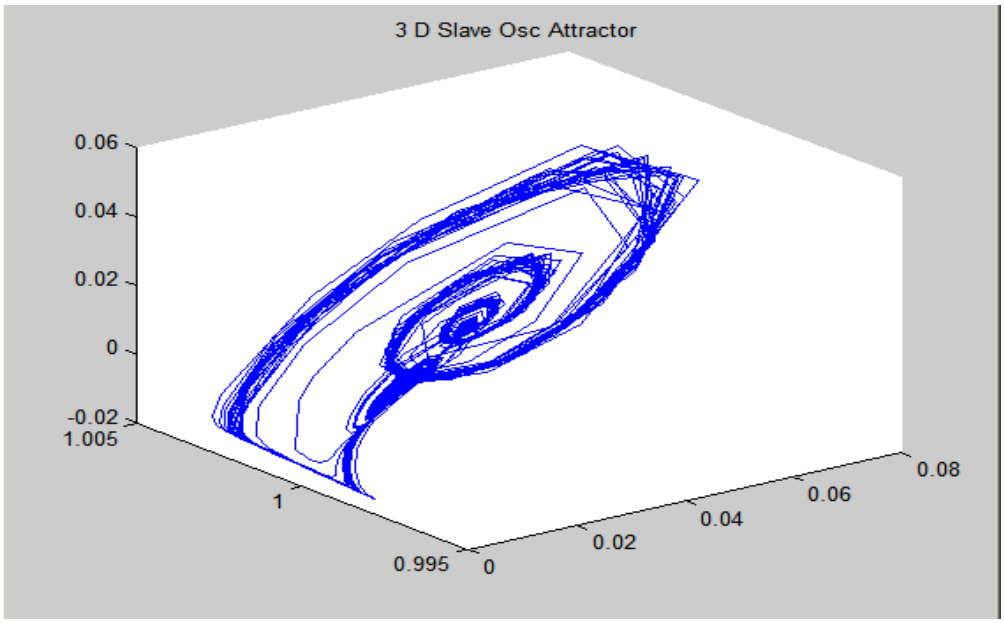

Figure 4-35 : 3-D slaver oscillator attractor in (CRM) when (R=0.02)

Increasing the master Osc bias current (δ_0) to (1.03) and other value not change as in table (4.5) and run the model in (CRM) :

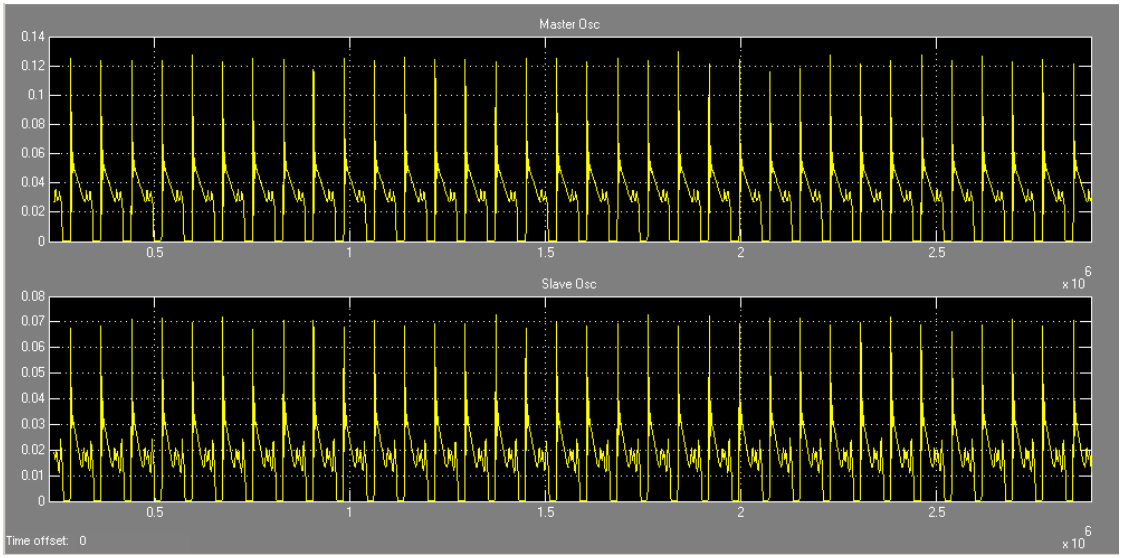

Figure 4-36 : Time series for the master (upper) and slave (lower) oscillator

In (CRM), when (R=0.02) Master Osc & (δ_0) change to (1.03)

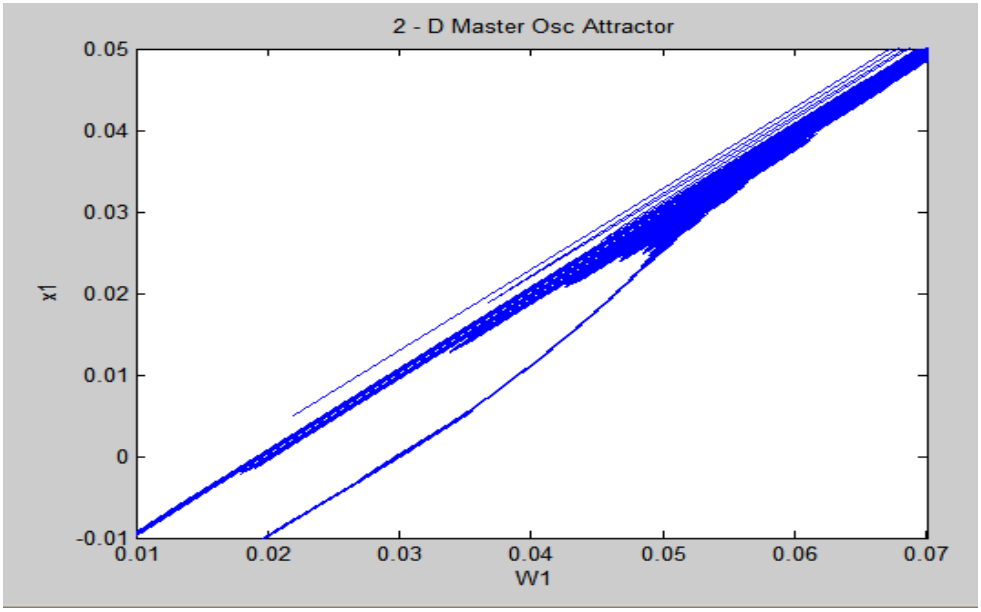

Figure 4-37 : 2-D master oscillator attractor in (CRM) when (R=0.02)

Master Osc (δ_0) change to (1.03)

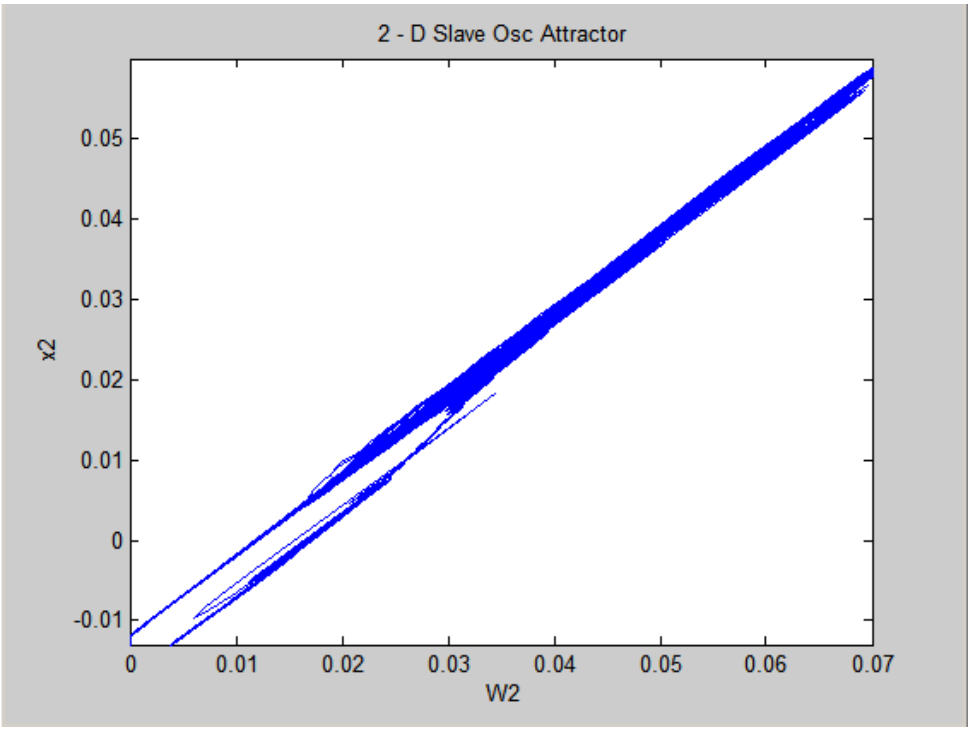

Figure 4-38 : 2-D slave oscillator attractor in (CRM) when (R=0.02)

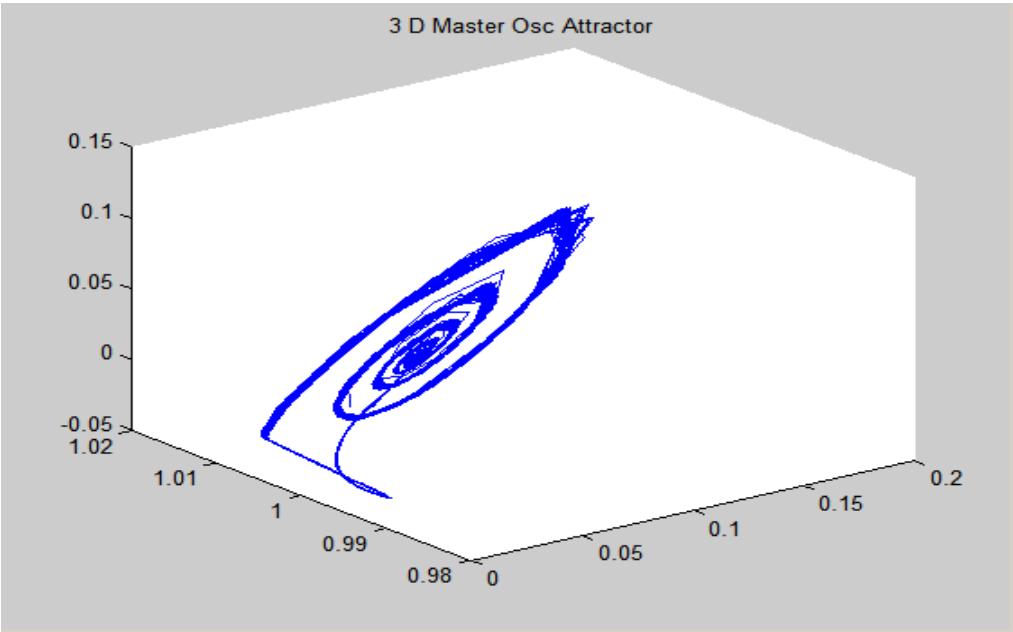

Figure 4-39 : 3-D master oscillator attractor in (CRM) when (R=0.02)

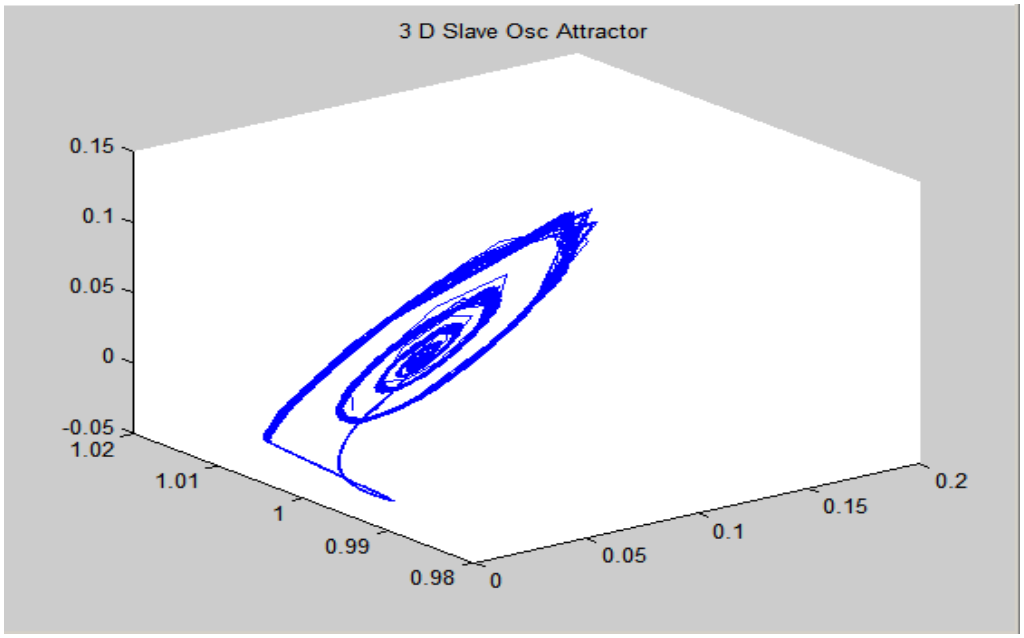

Figure 4-40 : 3-D slave oscillator attractor in (CRM) when (R=0.02)

Increasing coupling factor to (0.2) and repeating (CRM) and get results as follow:

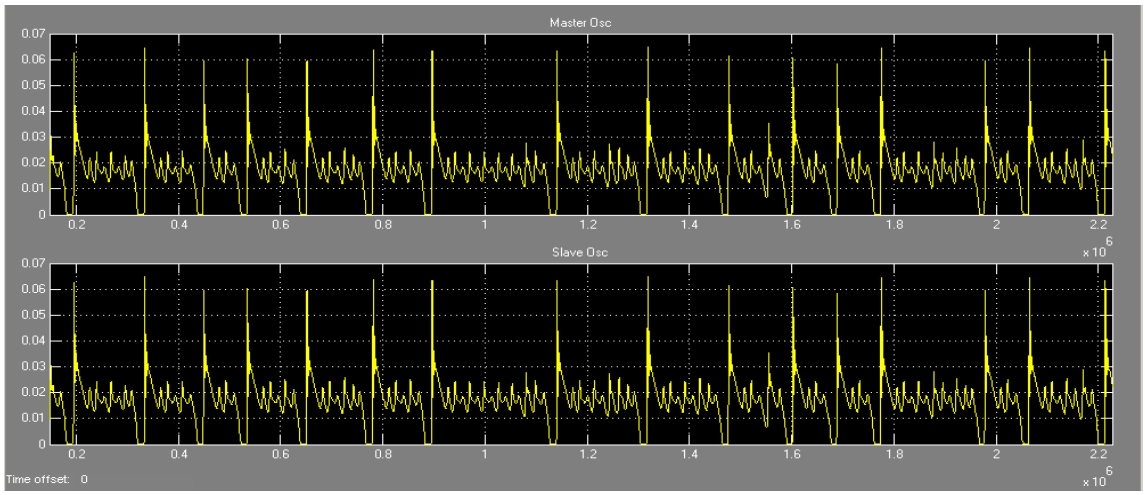

Figure 4-41 : Ttime series for the master (upper) and slave (lower) oscillator

In (CRM), when (R=0. 2) Master Osc (δ_0) change to (1.03)

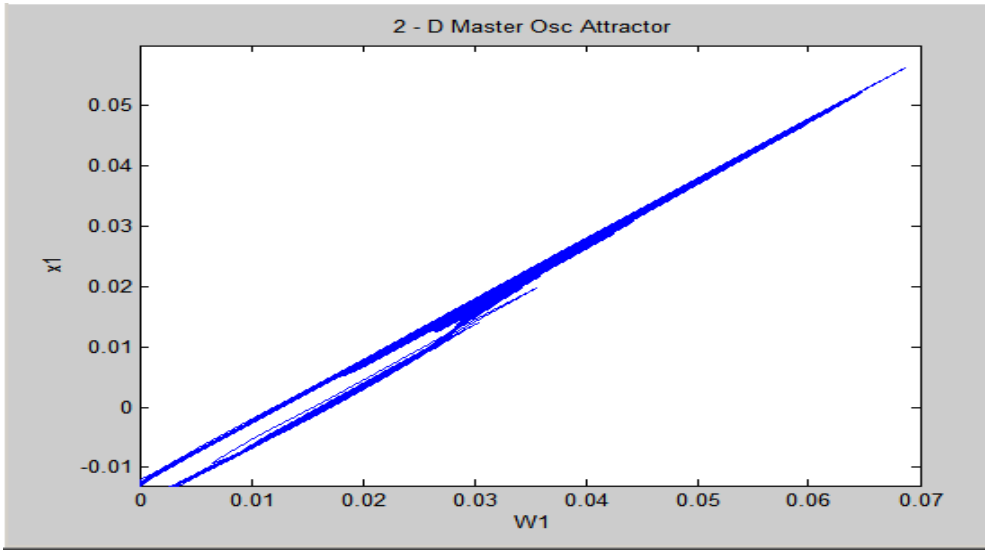

Figure 4-42 : 2-D master oscillator attractor in (CRM) when (R=0.2)

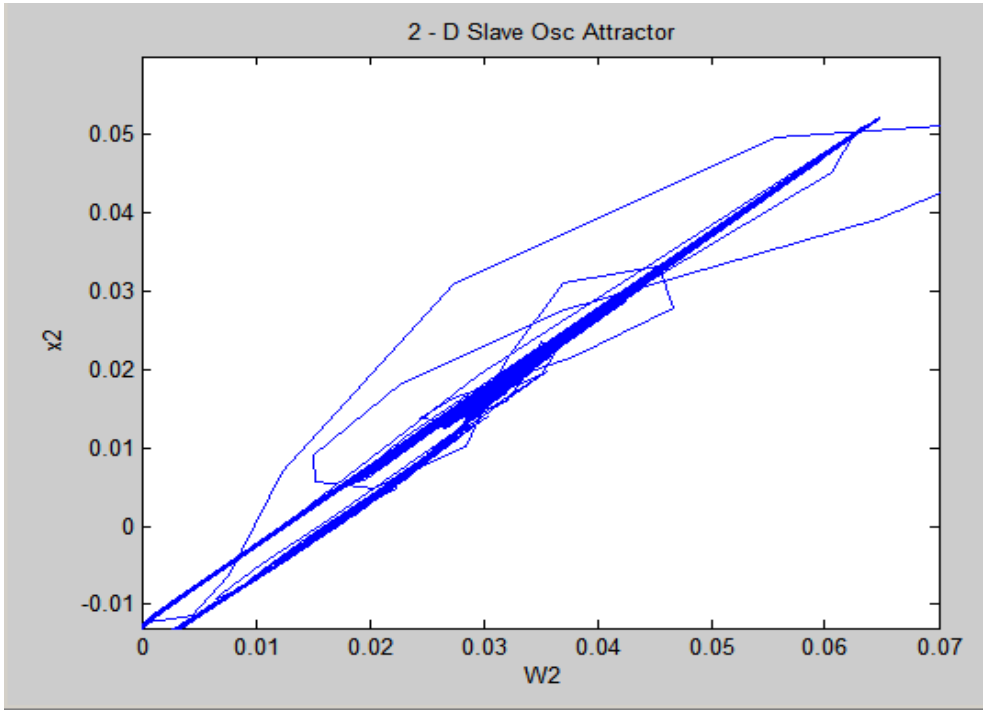

Figure 4-43 : 2-D Slave oscillator attractor in (CRM) when (R=0.2)

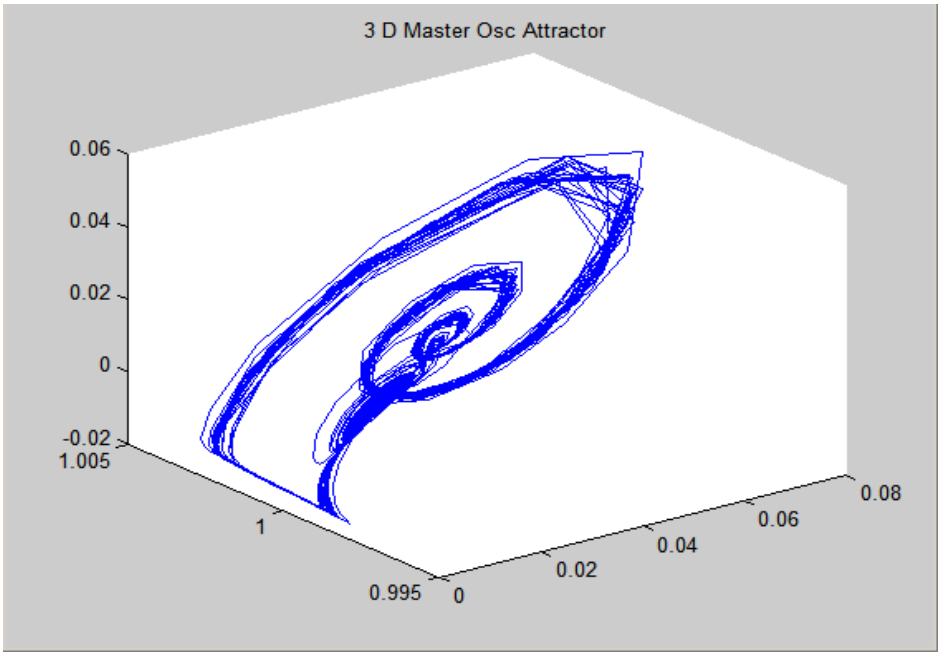

Figure 4-44 : 3-D master oscillator attractor in (CRM) when (R=0.2)

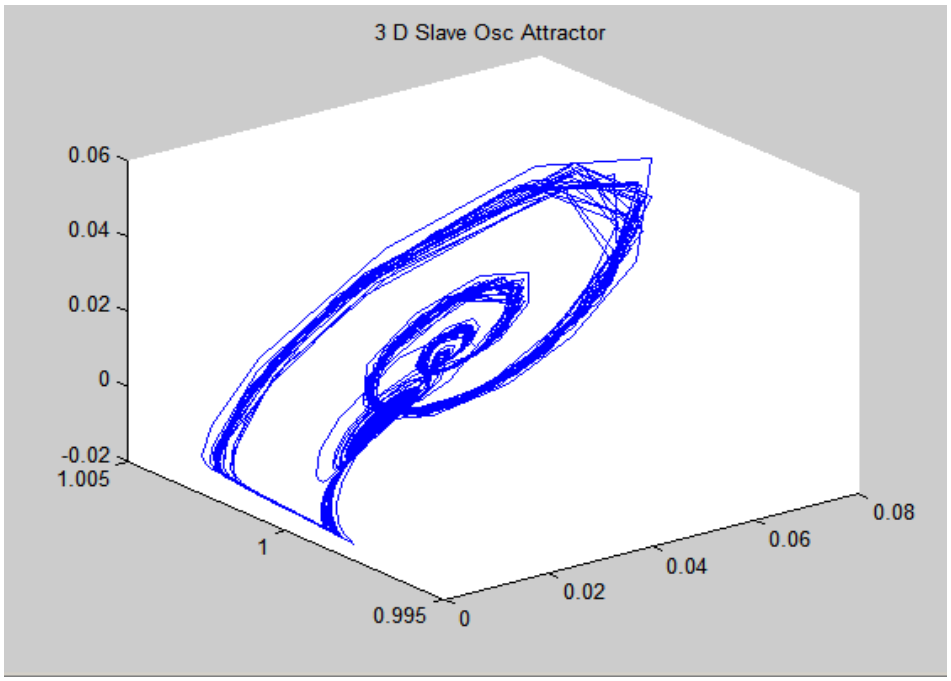

Figure 4-45 : 3-D Slave oscillator attractor in (CRM) when (R=0.2)

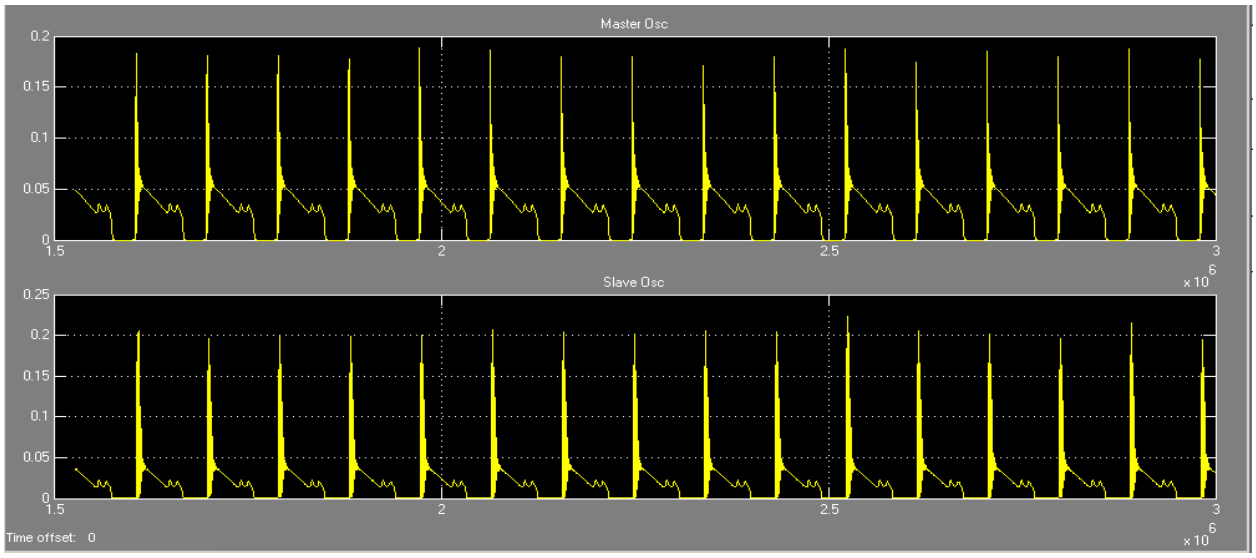

Figure 4-46 : Time series for the master (upper) and slave (lower) oscillator

In free running mode when (R=1). (alfa=1.03)

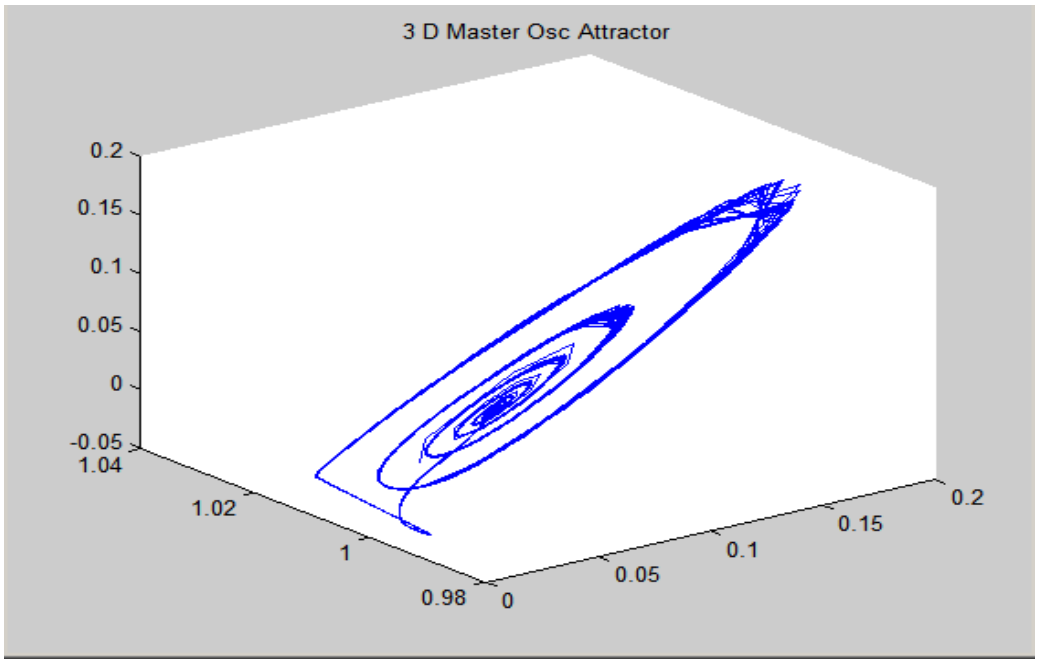

Figure 4-47 : 2-D slave oscillator attractor in (CRM) when (R=1)

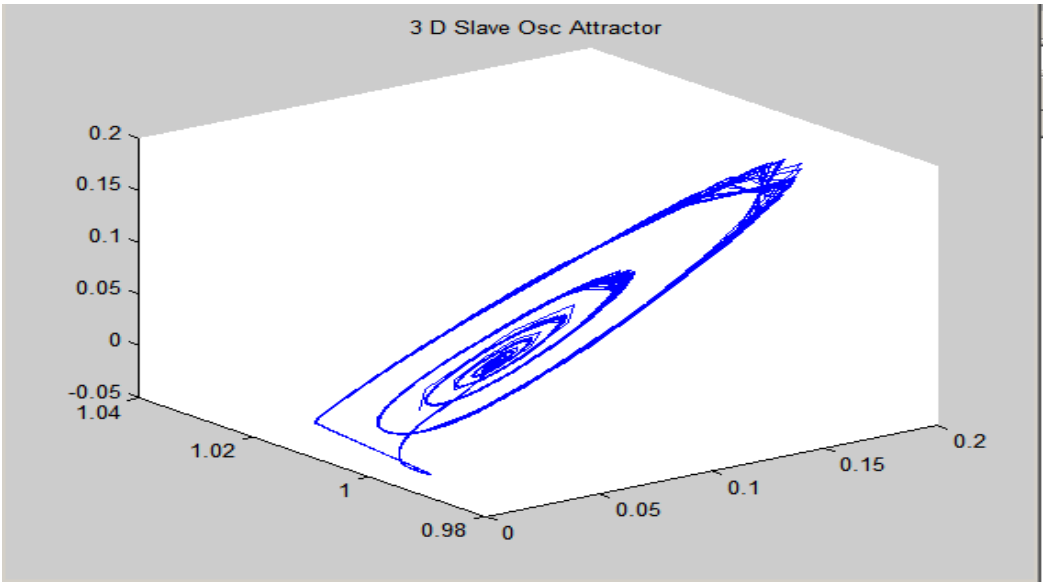

Figure 4-48 : 3-D slave oscillator attractor in (CRM) when (R=1)

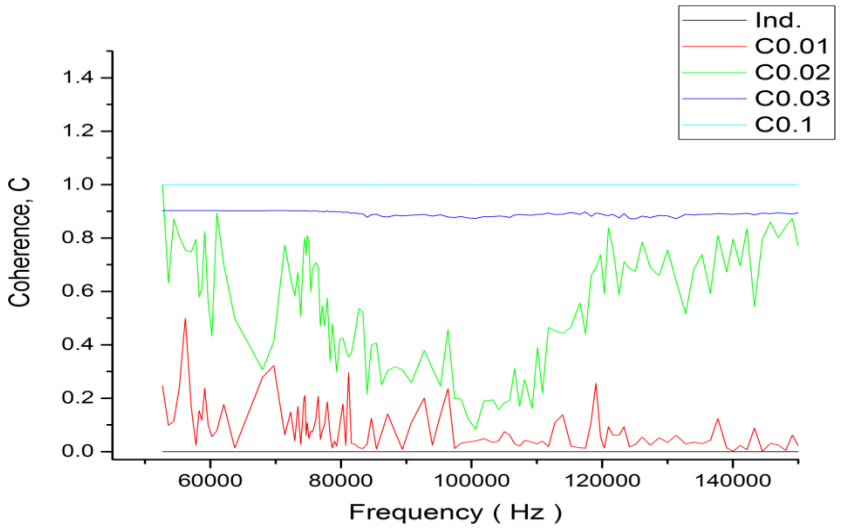

Figure 4-49 : Coherence Vs Coupling factor

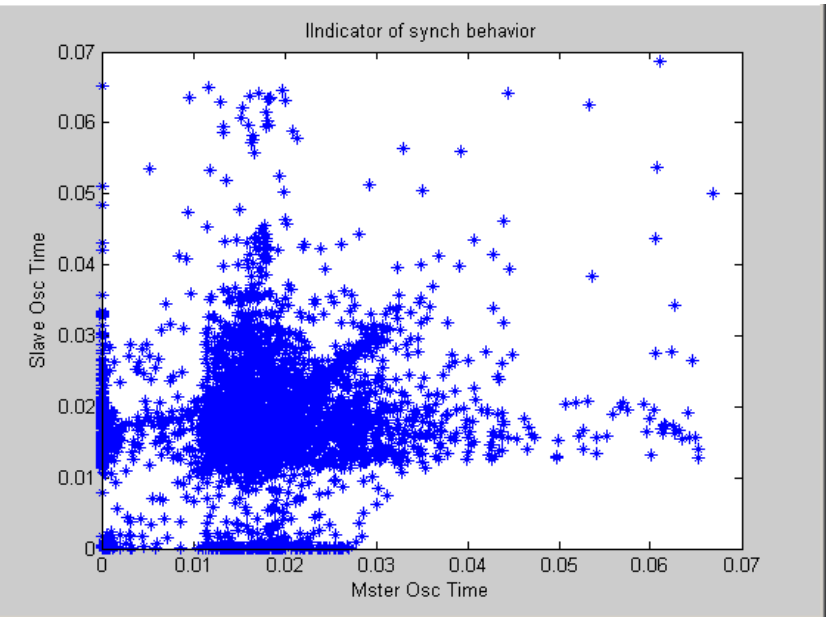

Figure 4-50 Indicator of Synch-behavior When(R=0)

No synchronization between master and slave laser

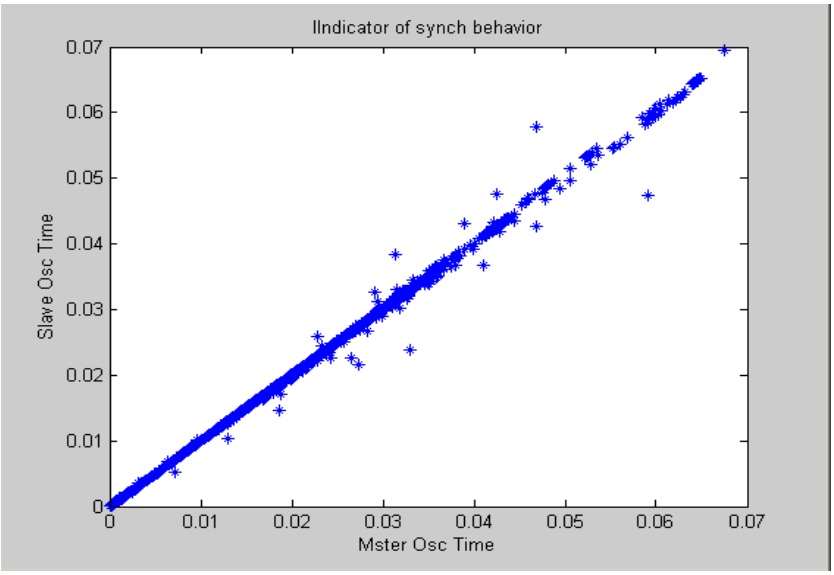

Figure 4-51 Indicator of Synch-behavior When(R=0.03)

Indicate synchronization between master and slave laser

iii. Netware Oscillator:

Interacting chaotic oscillators are of interest in many areas of physics, biology, and engineering. In the biological sciences, for instance, one of the challenging problems is to understand how a group of cells or functional units, each displaying complicated nonlinear dynamic phenomena, can interact with one another to produce a coherent response on a higher organizational level(Mosekilde et al., 2002).

The model of the Netware oscillators operation mode is symmetrical to the unidirectional coupling configuration that base on the coupling techniques and the initial condition for each of the individual oscillator that be arrange and coupled as a NetWare structure .

The key points in Netware oscillator model design is the sensitivity to initial conditions from this facts all other operation values and parameters are symmetrical between oscillators and the initial conditions for each individual oscillator are different as mention in table (4.6).

(i) Netware free running mode(NFRM):

In this mode run the NetWare oscillator according to the operation parameters and the initial condition (table 5.6) and the coupling factor (R=0) and get model results s follow:

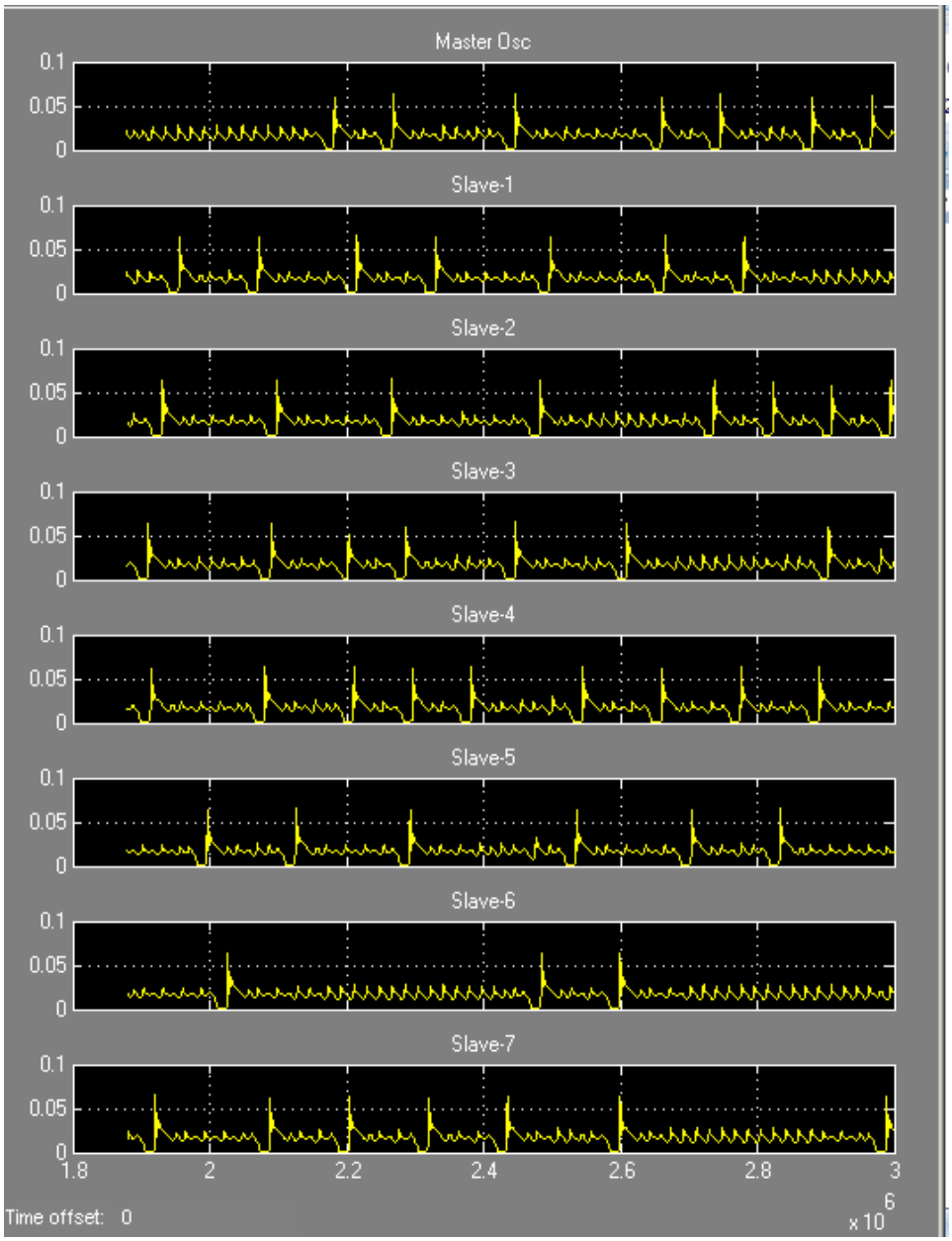

Figure 4-52 Scope-1 (Master and slave1- up to slave-7)

(NFRM) when (R=0) – No sync between oscillators

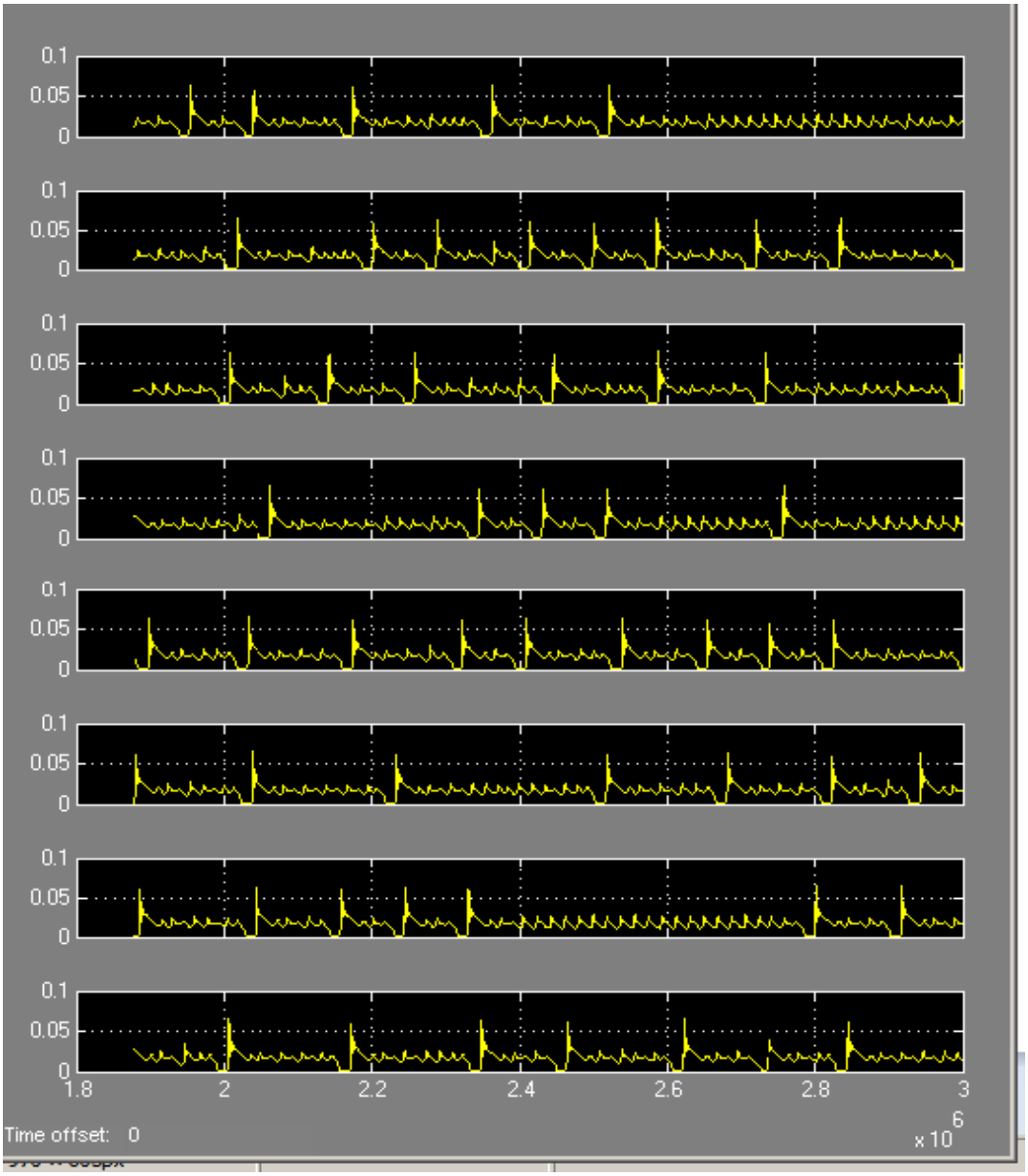

Figure 4-53 Scope-32 (slave- 248 up to slave- 255)

(NFRM) when (R=0) – No sync between oscillators

(ii) Netware coupling running mode(NCRM):

Also this mode of operation is symmetrical to the (NFRM) except the coupling factor value that change to (0.2, 1, 1.2) and then get model results respectively as follow:

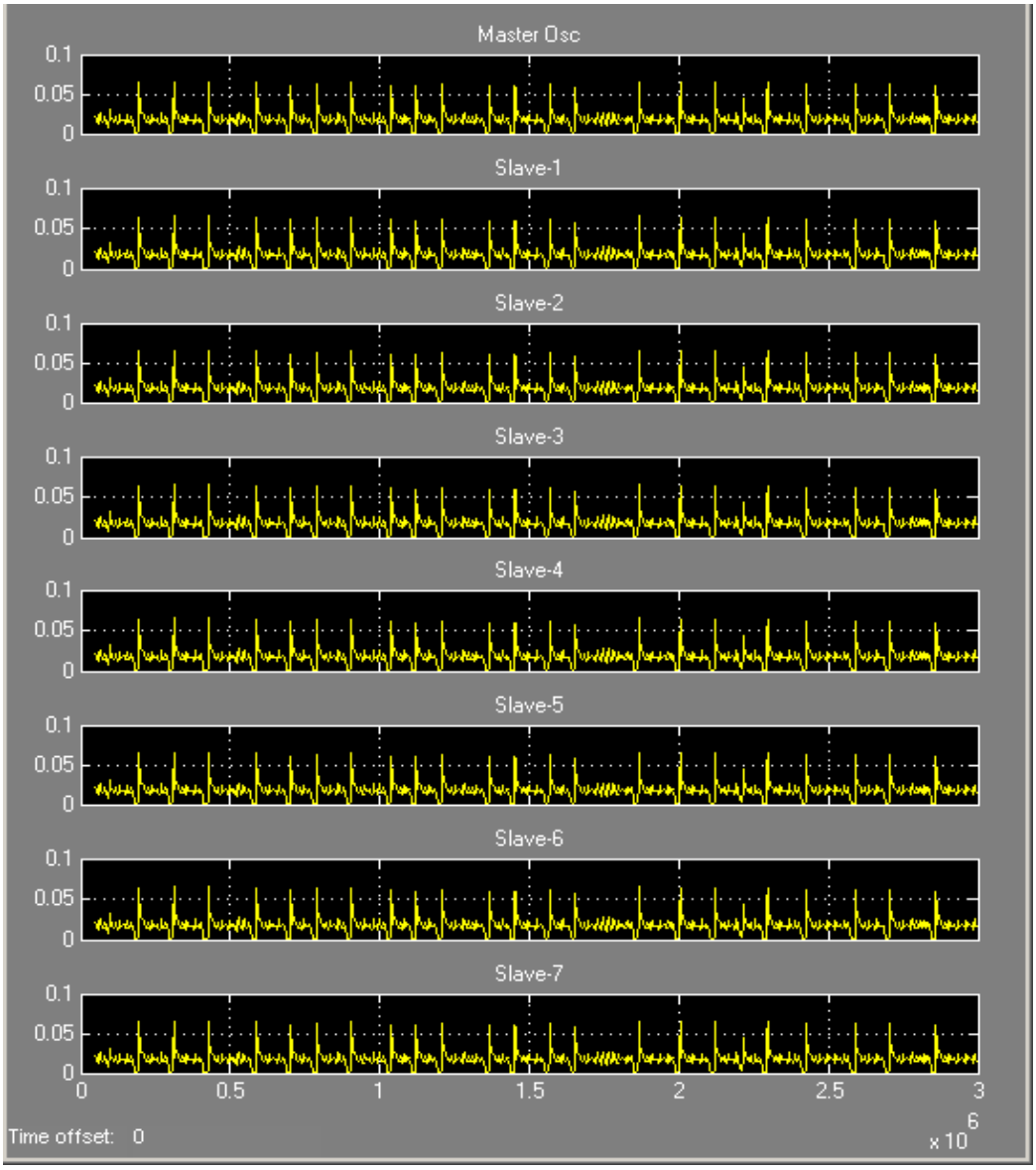

Figure 4-54 : Scope-1 (Master and slave1- up to slave-7)

(NFRM) when (R=0.5) – full sync between oscillators

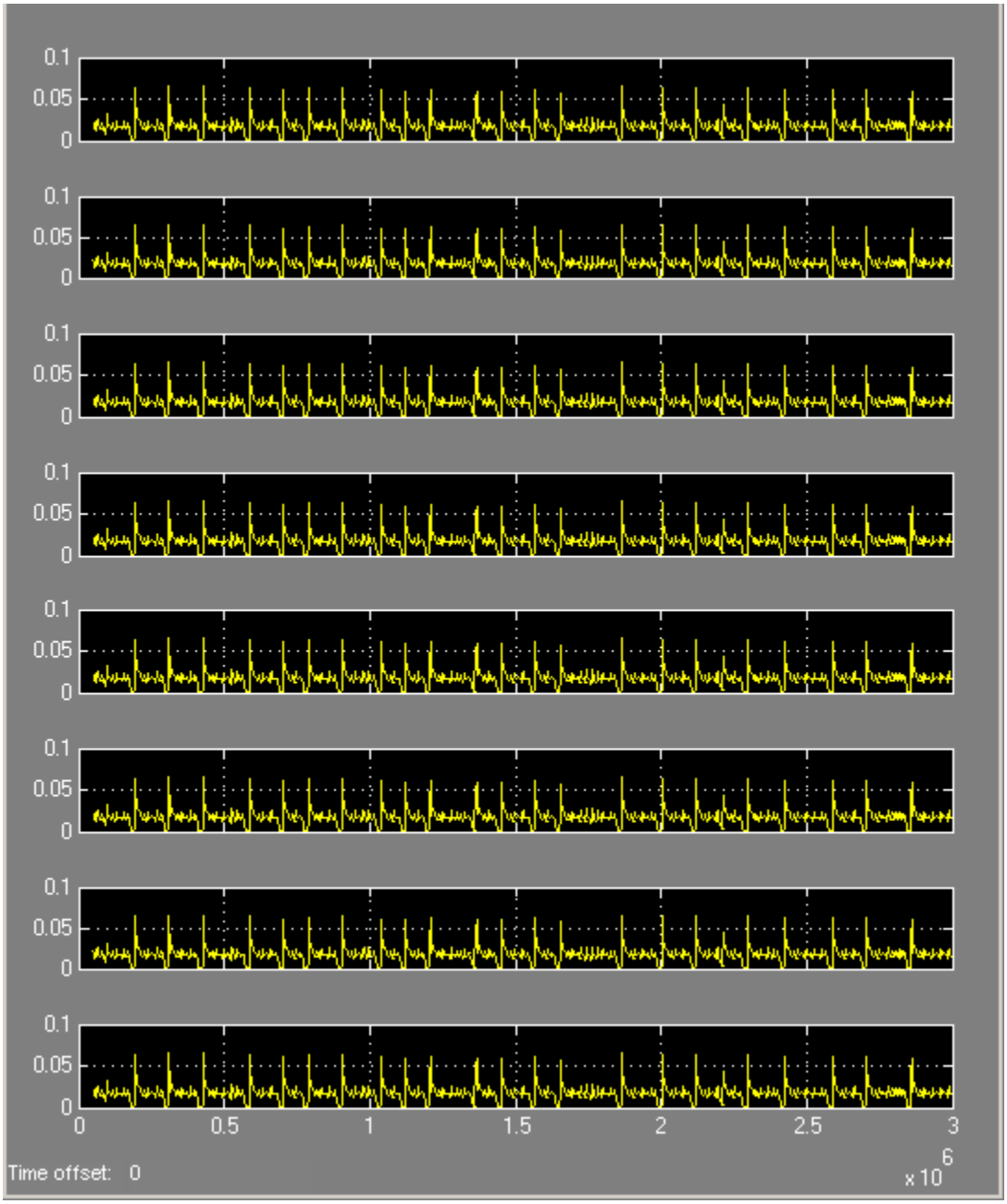

Figure 4-55 : Scope-32 (slave- 248 up to slave- 255)

(NFRM) when (R=0.5) – full sync between oscillators

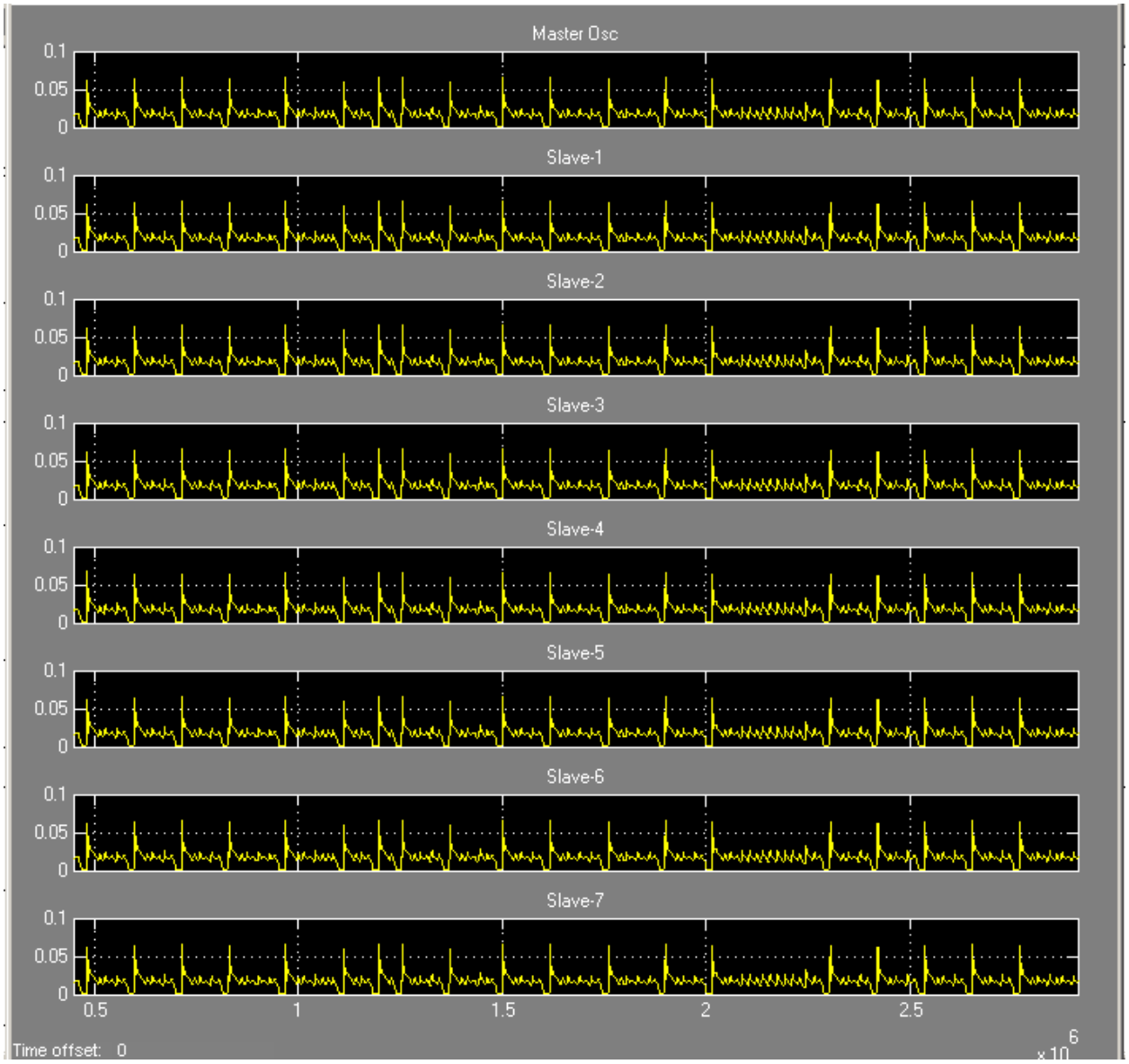

Figure 4-56 : Scope-1 (master and slave- 1 up to slave- 7)

(NFRM) when (R=0.2) – full sync between oscillators

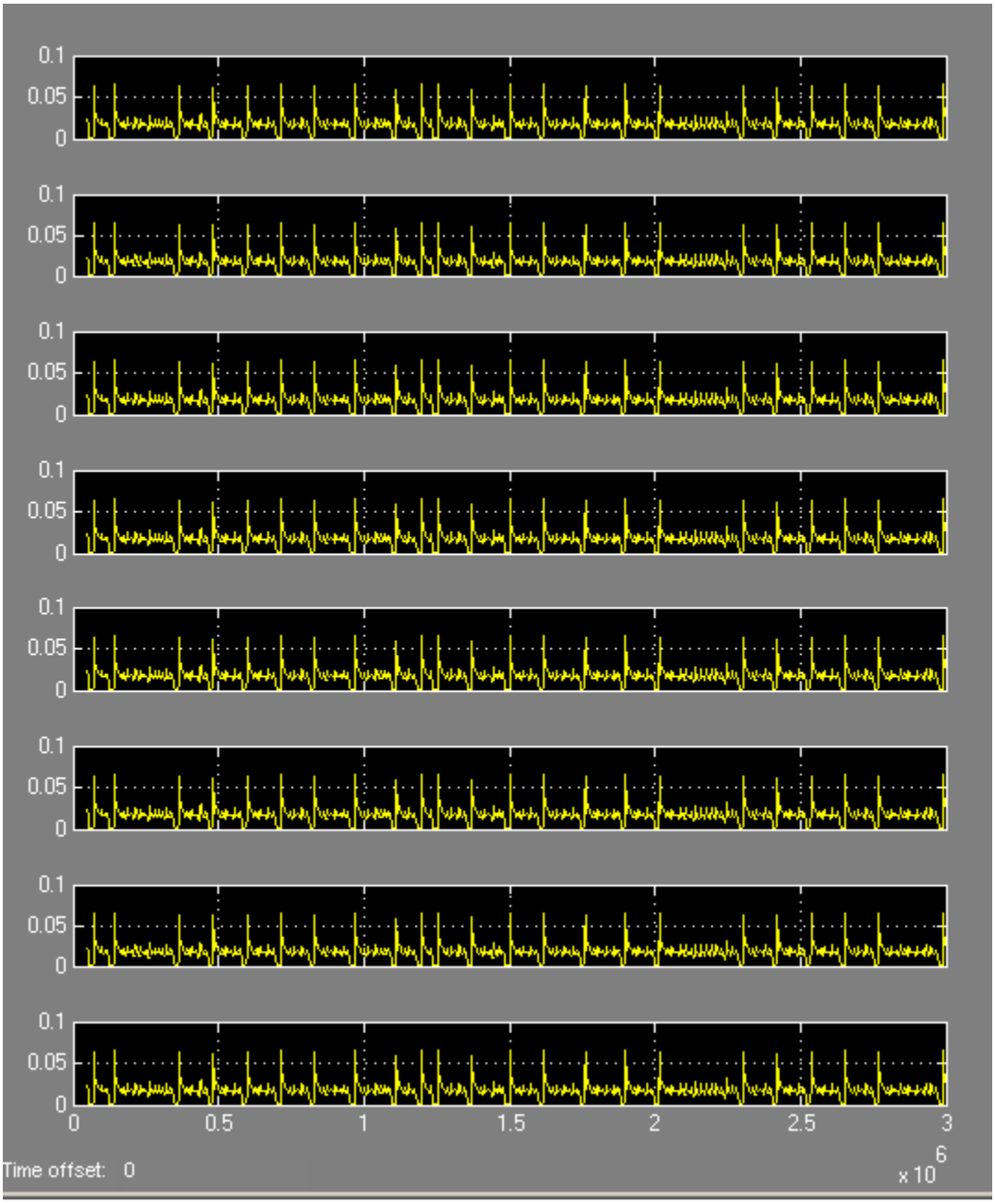

Figure 4-57 : Scope-32 (slave- 248 up to slave- 255)

(NFRM) when (R=0.2) – full sync between oscillators

Table 4-6 all NetWare oscillator initial conditions

Block-1	**Initial (x0)**	**Block-2**	**Initial (x0)**	**Block-3**	**Initial (x0)**	**Block-4**	**Initial (x0)**
Master	0.022	Slave-8	0.02208	Slave-16	0.022016	Slave-24	0.022024
Slave-1	0.02201	Slave-9	0.02209	Slave-17	0.022017	Slave-25	0.022025
Slave-2	0.02202	Slave-10	0.022010	Slave-18	0.022018	Slave-26	0.022026
Slave-3	0.02203	Slave-11	0.022011	Slave-19	0.022019	Slave-27	0.022027
Slave-4	0.02204	Slave-12	0.022012	Slave-20	0.022020	Slave-28	0.022028
Slave-5	0.02205	Slave-13	0.022013	Slave-21	0.022021	Slave-29	0.022029
Slave-6	0.02206	Slave-14	0.022014	Slave-22	0.022022	Slave-30	0.022030
Slave-7	0.02207	Slave-15	0.022015	Slave-23	0.022023	Slave-31	0.022031
Block-5	**Initial (x0)**	**Block-6**	**Initial (x0)**	**Block-7**	**Initial (x0)**	**Block-8**	**Initial (x0)**
Slave-32	0.022032	Slave-40	0.022040	Slave-48	0.022048	Slave-56	0.022056
Slave-33	0.022033	Slave-41	0.022041	Slave-49	0.022049	Slave-57	0.022057
Slave-34	0.022034	Slave-42	0.022042	Slave-50	0.022050	Slave-58	0.022058
Slave-35	0.022035	Slave-43	0.022043	Slave-51	0.022051	Slave-59	0.022059
Slave-36	0.022036	Slave-44	0.022044	Slave-52	0.022052	Slave-60	0.022060
Slave-37	0.022037	Slave-45	0.022045	Slave-53	0.022053	Slave-61	0.022061
Slave-38	0.022038	Slave-46	0.022046	Slave-54	0.022054	Slave-62	0.022062
Slave-39	0.022039	Slave-47	0.022047	Slave-55	0.022055	Slave-63	0.022063
Block-9	**Initial (x0)**	**Block-10**	**Initial (x0)**	**Block-11**	**Initial (x0)**	**Block-12**	**Initial (x0)**
Slave-64	0.022064	Slave-72	0.022072	Slave-80	0.022080	Slave-88	0.022088
Slave-65	0.022065	Slave-73	0.022073	Slave-81	0.022081	Slave-89	0.022089
Slave-66	0.022066	Slave-74	0.022074	Slave-82	0.022082	Slave-90	0.022090
Slave-67	0.022067	Slave-75	0.022075	Slave-83	0.022083	Slave-91	0.022091
Slave-68	0.022068	Slave-76	0.022076	Slave-84	0.022084	Slave-92	0.022092
Slave-69	0.022069	Slave-77	0.022077	Slave-85	0.022085	Slave-93	0.022093
Slave-70	0.022070	Slave-78	0.022078	Slave-86	0.022086	Slave-94	0.022094
Slave-71	0.022071	Slave-79	0.022079	Slave-87	0.022087	Slave-95	0.022095
Block-13	**Initial (x0)**	**Block-14**	**Initial (x0)**	**Block-15**	**Initial (x0)**	**Block-16**	**Initial (x0)**
Slave-96	0.022096	Slave-104	0.022104	Slave-112	0.022112	Slave-120	0.022120
Slave-97	0.022097	Slave-105	0.022105	Slave-113	0.022113	Slave-121	0.022121
Slave-98	0.022098	Slave-106	0.022106	Slave-114	0.022114	Slave-122	0.022122
Slave-99	0.022099	Slave-107	0.022107	Slave-115	0.022115	Slave-123	0.022123
Slave-100	0.022100	Slave-108	0.022108	Slave-116	0.022116	Slave-124	0.022124
Slave-101	0.022101	Slave-109	0.022109	Slave-117	0.022117	Slave-125	0.022125
Slave-102	0.022102	Slave-110	0.022110	Slave-118	0.022118	Slave-126	0.022126
Slave-103	0.022103	Slave-111	0.022111	Slave-119	0.022119	Slave-127	0.022127
Block-17	**Initial (x0)**	**Block-18**	**Initial (x0)**	**Block-19**	**Initial (x0)**	**Block-20**	**Initial (x0)**
Slave-128	0.022128	Slave-136	0.022136	Slave-144	0.022144	Slave-152	0.022152

Slave-129	0.022129	Slave-137	0.022137	Slave-145	0.022145	Slave-153	0.022153
Slave-130	0.022130	Slave-138	0.022138	Slave-146	0.022146	Slave-154	0.022154
Slave-131	0.022131	Slave-139	0.022139	Slave-147	0.022147	Slave-155	0.022155
Slave-132	0.022132	Slave-140	0.022140	Slave-148	0.022148	Slave-156	0.022156
Slave-133	0.022133	Slave-141	0.022141	Slave-149	0.022149	Slave-157	0.022157
Slave-134	0.022134	Slave-142	0.022142	Slave-150	0.022150	Slave-158	0.022158
Slave-135	0.022135	Slave-143	0.022143	Slave-151	0.022151	Slave-159	0.022159
Block-21	**Initial (x0)**	**Block-22**	**Initial (x0)**	**Block-23**	**Initial (x0)**	**Block-24**	**Initial (x0)**
Slave-160	0.022160	Slave-168	0.022168	Slave-176	0.022176	Slave-184	0.022184
Slave-161	0.022161	Slave-169	0.022169	Slave-177	0.022177	Slave-185	0.022185
Slave-162	0.022162	Slave-170	0.022170	Slave-178	0.022178	Slave-186	0.022186
Slave-163	0.022163	Slave-171	0.022171	Slave-179	0.022179	Slave-187	0.022187
Slave-164	0.022164	Slave-172	0.022172	Slave-180	0.022180	Slave-188	0.022188
Slave-165	0.022165	Slave-173	0.022173	Slave-181	0.022181	Slave-189	0.022189
Slave-166	0.022166	Slave-174	0.022174	Slave-182	0.022182	Slave-190	0.022190
Slave-167	0.022167	Slave-175	0.022175	Slave-183	0.022183	Slave-191	0.022191
Block-25	**Initial (x0)**	**Block-26**	**Initial (x0)**	**Block-27**	**Initial (x0)**	**Block-28**	**Initial (x0)**
Slave-192	0.022192	Slave-200	0.022200	Slave-208	0.022208	Slave-216	0.022216
Slave-193	0.022193	Slave-201	0.022201	Slave-209	0.022209	Slave-217	0.022217
Slave-194	0.022194	Slave-202	0.022202	Slave-210	0.022210	Slave-218	0.022218
Slave-195	0.022195	Slave-203	0.022203	Slave-211	0.022211	Slave-219	0.022219
Slave-196	0.022196	Slave-204	0.022204	Slave-212	0.022212	Slave-220	0.022220
Slave-197	0.022197	Slave-205	0.022205	Slave-213	0.022213	Slave-221	0.022221
Slave-198	0.022198	Slave-206	0.022206	Slave-214	0.022214	Slave-222	0.022222
Slave-199	0.022199	Slave-207	0.022207	Slave-215	0.022215	Slave-223	0.022223
Block-29	**Initial (x0)**	**Block-30**	**Initial (x0)**	**Block-31**	**Initial (x0)**	**Block-32**	**Initial (x0)**
Slave-224	0.022224	Slave-232	0.022232	Slave-240	0.022240	Slave-248	0.022248
Slave-225	0.022225	Slave-233	0.022233	Slave-241	0.022241	Slave-249	0.022249
Slave-226	0.022226	Slave-234	0.022234	Slave-242	0.022242	Slave-250	0.022250
Slave-227	0.022227	Slave-235	0.022235	Slave-243	0.022243	Slave-251	0.022251
Slave-228	0.022228	Slave-236	0.022236	Slave-244	0.022244	Slave-252	0.022252
Slave-229	0.022229	Slave-237	0.022237	Slave-245	0.022245	Slave-253	0.022253
Slave-230	0.022230	Slave-238	0.022238	Slave-246	0.022246	Slave-254	0.022254
Slave-231	0.022231	Slave-239	0.022239	Slave-247	0.022247	Slave-255	0.022255

4.4 Conclusions:

In conclusions, the chaotic spiking in semiconductor laser with an optical feedback is numerically demonstrated. It has been shown that the time scale of these dynamics is fully determined by the feedback loop and their erratic though deterministic. Several aspects of the dynamic response of chaotic system to different values of feedback strength and bias current are studied, the optoelectronic feedback strength effect on chaotic behavior, when the feedback strength is high the chaotic signal has large amplitude and it decrease with the decreasing of the feedback strength.

The attractors show that the attenuation value could control the chaotic amplitude. The chaotic behavior could be studied in terms of attractor corresponding to time series. The system could be controlled by these parameters.

Finally, in this work we presented numerical result on synchronization in chaotic optoelectronic network.

We give numerical evidence showing that the coupling between master-slave oscillators plays a crucial rule in synchronization mechanism, which start from different conditions, leads eventually to their perfect synchronization in time scale. The investigation of transition between non synchronization and synchronization states in 256 laser oscillations is done by means of Simulink- MATLAB environment.

The correlation of chaotic intensities of different oscillators and the coherence of time scales are considered as a synchronization control parameters in optoelectronic networks.

4.5 Future Work:

- Bursting control in semiconductor lasers with optical feedback.
- The synchronization of matrix configuration (i.e. N*N oscillators) of chaotic laser output with optical feedback.
- Trying to apply noise –induced phenomena especially synchronization on a real communication systems.
- The investigation of the stochastic and coherence resonance in optical feedback.

References:

ABDALAH, S., AL NAIMEE, K., MEUCCI, R., AL MUSLET, N. & ARECCHI, F. 2010. Experimental Evidence of Slow Spiking Rate in a Semiconductor Laser by Electro-optical Feedback: Generation and Control. *Applied Physics Research,* 2**,** 170.

ABDALAH, S. F., ARECCHI, F. T., MARINO, F., AL NAIMEE, K., CISZAK, M. & MEUCCI, R. 2011. *Optoelectronic feedback in semiconductor light sources: optimization of network components for synchronization*, INTECH Open Access Publisher.

AL NAIMEE, K., MARINO, F., CISZAK, M., ABDALAH, S., MEUCCI, R. & ARECCHI, F. 2010. Excitability of periodic and chaotic attractors in semiconductor lasers with optoelectronic feedback. *The European Physical Journal D,* 58**,** 187-189.

AL NAIMEE, K., MARINO, F., CISZAK, M., MEUCCI, R. & ARECCHI, F. T. 2009. Chaotic spiking and incomplete homoclinic scenarios in semiconductor lasers with optoelectronic feedback. *New Journal of Physics,* 11**,** 073022.

ARGYRIS, A., KANAKIDIS, D., BOGRIS, A. & SYVRIDIS, D. 2005. Spectral synchronization in chaotic optical communication systems. *Quantum Electronics, IEEE Journal of,* 41**,** 892-897.

BAKER, G. L. & GOLLUB, J. P. 1996. *Chaotic dynamics: an introduction*, Cambridge University Press.

CHAN, S.-C. & LIU, J.-M. 2005. Microwave frequency division and multiplication using an optically injected semiconductor laser. *Quantum Electronics, IEEE Journal of,* 41**,** 1142-1147.

CHEMBO KOUOMOU, Y. 2006. Nonlinear Dynamics of Semiconductor Laser Systems with Feedback: Applications to Optical Chaos Cryptography, Radar Frequency Generation, and Transverse Mode Control.

CHEN, H. & LIU, J. 2000. Open-loop chaotic synchronization of injection-locked semiconductor lasers with gigahertz range modulation. *Quantum Electronics, IEEE Journal of,* 36**,** 27-34.

CUOMO, K. M. & OPPENHEIM, A. V. 1993. Circuit implementation of synchronized chaos with applications to communications. *Physical Rev. Letter,* vol. 71**,** pp. 65-68.

DANFORTH, C. M. 2013. Chaos in an atmosphere hanging on a wall. *Mathematics of Planet Earth*.

DECUSATIS, C. 2002. *Fiber Optic Data Communication: Technology Advances and Futures*, Academic press.

DING, M. & OTT, E. 1994. Enhancing synchronism of chaotic systems. *Physical Review E,* 49**,** R945.

FISCHER, I., LIU, Y. & DAVIS, P. 2000. Synchronization of chaotic semiconductor laser dynamics on subnanosecond time scales and its potential for chaos communication. *Physical Review A,* 62**,** 011801.

ISRAR AHMED, A. B. S. December 2015. A research on Active Control to Synchronization a New 3D Chaotic System.

LIU, J., CHEN, H. & TANG, S. 2001. Optical-communication systems based on chaos in semiconductor lasers. *Circuits and Systems I: Fundamental Theory and Applications, IEEE Transactions on*, 48**,** 1475-1483.

LORENZ & N., E. 1993. The Essence of chao. *University of Washington Press,Seattle*.

MEDIO, A. & LINES, M. 2001. *Nonlinear dynamics: A primer*, Cambridge University Press.

MOSEKILDE, E., MAISTRENKO, Y. & POSTNOV, D. 2002. *Chaotic synchronization: applications to living systems*, World Scientific.

OHTSUBO, J. 2013. Dynamics of Semiconductor Lasers with Optoelectronic Feedback and Modulation. *Semiconductor Lasers.* Springer.

OUANNAS, A. 2014. Nonlinear control method of chaos synchronization for arbitrary 2D quadratic dynamical systems in discrete-time. *Int. J. Math. Anal,* 8**,** 2611-2617.

PISARCHIK, R., M. & F.T., A. 2001. Theoretical and experimental study of discrete behavior of Shilnikov chaos in a CO 2 laser. *Eur Phys J D* 13**,** 385-391.

ROSENBLUM, M. G., PIKOVSKY, A. S. & KURTHS, J. 1996. Phase synchronization of chaotic oscillators. *Physical review letters,* 76**,** 1804.

SILVA, C. P. 2011. Nonlinear Dynamics and Chaos: From Concept to Application. *Nonlinear Dynamics,* 2011.

SIVAPRAKASAM, S., PIERCE, I., REES, P., SPENCER, P. S., SHORE, K. A. & VALLE, A. 2001. Inverse synchronization in semiconductor laser diodes. *Physical Review A,* 64**,** 013805.

SIVAPRAKASAM, S. & SHORE, K. A. 1999. Demonstration of optical synchronization of chaotic external-cavity laser diodes. *Optics letters,* 24**,** 466-468.

SORA, AL-NAIMEE, K., MEUCCI, R., AL MUSLET, N. & ARECCHI, F. 2010. Experimental Evidence of Slow Spiking Rate in a Semiconductor Laser by Electro-optical Feedback: Generation and Control. *Applied Physics Research,* 2**,** 170.

SOUCEK, B. 1992. *Dynamic, genetic, and chaotic programming: the sixth-generation*, John Wiley & Sons, Inc.

SYVRIDIS, D. & BOGRIS, A. 2006. Secure communications links based on chaotic optical carriers. *SPIE Newsroom*, 10**,** 0486.

TRICKER, R. 2002. *Optoelectronics and fiber optic technology*, Newnes.

UCHIDA, A. 2012. *Optical communication with chaotic lasers: applications of nonlinear dynamics and synchronization*, John Wiley & Sons.

WERNDL, C. 2009. What are the new implications of chaos for unpredictability? *The British Journal for the Philosophy of Science,* 60**,** 195-220.

WIECZOREK, S., KRAUSKOPF, B. & LENSTRA, D. 2001. Sudden chaotic transitions in an optically injected semiconductor laser. *Optics letters,* 26**,** 816-818.